INVESTIGATIONS INTO GEL ELECTROPHORESIS WITH QUANTUM DOT END-LABELED DNA

A Dissertation

by

XIAOJIA CHEN

Submitted to the Office of Graduate Studies of
Texas A&M University
in partial fulfillment of the requirements for the degree of

DOCTOR OF PHILOSOPHY

August 2008

Major Subject: Chemical Engineering

INVESTIGATIONS INTO GEL ELECTROPHORESIS WITH QUANTUM DOT END-LABELED DNA

A Dissertation

by

XIAOJIA CHEN

Submitted to the Office of Graduate Studies of
Texas A&M University
in partial fulfillment of the requirements for the degree of

DOCTOR OF PHILOSOPHY

Approved by:

Chair of Committee,	Victor M. Ugaz
Committee Members,	Yue Kuo
	Zhengdong Cheng
	Gyula Vigh
Head of Department,	Michael Pishko

August 2008

Major Subject: Chemical Engineering

ABSTRACT

Investigations into Gel Electrophoresis with Quantum Dot End-Labeled DNA. (August 2008)

Xiaojia Chen, B.S., Sichuan University

Chair of Advisory Committee: Dr. Victor M. Ugaz

Invented in the 1950s, gel electrophoresis has now become a routine analytical method to verify the size of nucleic acids and proteins in molecular biology labs. Conventional gel electrophoresis can successfully separate DNA fragments from several base pairs to a few tens of kilo base pairs, beyond which a point is reached that DNA molecules cannot be resolved due to the size independent mobility. In this case, pulsed field gel electrophoresis (PFGE) was introduced to extend the range of DNA fragment sizes that can be effectively separated. But despite the incredible success of PFGE techniques, some important drawbacks remain. First, separation time is extremely long, ranging from several hours to a few days. Second, detection methods still rely on staining the gel after the run. Real time observation and study of band migration behavior is impossible due to the large size of the PFGE device. Finally, many commercial PFGE instruments are relatively expensive, a factor that can limit their accessibility both for routine analytical and preparative use as well as for performing fundamental studies.

In this research, a miniaturized PFGE device was constructed with dimension 2cm x 2.6cm, capable of separating DNA fragments ranging from 2.5kb to 32kb within three hours using low voltage. The separation process can be observed in real time under a fluorescence microscope mounted with a cooled CCD camera. Resolution and mobility of the sample were measured to test the efficiency of the device. We also explored manipulating DNA fragments by end labeling DNA molecules with quantum dot nanocrystals. The quantum dot-DNA conjugates can be further modified through binding interactions with biotinylated single-stranded DNA primers. Single molecule visualization was performed during gel electrophoresis and the extension length, entanglement probability and reorientation time of different conjugates were measured to study their effect on DNA migration through the gel. Finally, electrophoresis of DNA conjugates was performed in the miniaturized PFGE device, and shaper bands were observed compared with the non end-labeled sample. Furthermore, by end-labeling DNA with quantum dots, the migration distance of shorter fragments is reduced, providing the possibility of separating a wider range of DNA fragment sizes on the same gel to achieve further device miniaturization.

DEDICATION

I dedicate this dissertation to my dear parents, my beloved husband, and my wonderful friends. Without their love and support this would not have been possible.

ACKNOWLEDGEMENTS

I would like to express my true gratitude to my advisor, Dr. Victor M. Ugaz, who, during these years, unselfishly passed his knowledge on to me and provided me valuable advice and support.

Many thanks to Dr. Gyula Vigh, Dr. Yue Kuo, Dr. Zhengdong Cheng for agreeing to serve on my committee.

Many thanks to Dr. Bittner and his group at the Translation Genomic Research Institute for their instruction and help during my internship, which provided me not only the professional molecular biological lab skills, but also a great opportunity to experience the fusion of engineering concepts and biological practice.

Thanks also go to Dr. Mark Holtzapple. Without his help, I would never have come to Texas A&M University and later met my husband here.

I would like to thank my friends for bringing happiness to my life and helping me when I needed it.

It is impossible to adequately express my appreciation to my parents and my husband for their support and endless love.

Finally, I would like to thank the Artie McFerrin Department of Chemical Engineering for providing me a wonderful experience while I pursued my studies.

NOMENCLATURE

DNA	Deoxyribonucleic Acid
ds DNA	Double-stranded DNA
A	Adenine
T	Thymine
G	Guanine
C	Cytosine
PCR	Polymerase Chain Reaction
PFGE	Pulsed Field Gel Electrophoresis
FIGE	Field Inversion Gel Electrophoresis
CHEF	Contour-clamped Homogeneous Electric Field
RGE	Rotating Gel Electrophoresis
TAFE	Transverse Alternating Field Electrophoresis
QD	Quantum Dot
RD	Restriction Digest
λ DNA	Lambda Phage DNA
E	Electric Field Strength
t	Time

TABLE OF CONTENTS

CHAPTER Page

CHAPTER Page

LIST OF FIGURES

FIGURE Page

FIGURE Page

LIST OF TABLES

CHAPTER I

INTRODUCTION*

1. Understanding DNA

Human beings have been living on this planet for thousands of years. Being the most intelligent creature, human beings create language to communicate, word to record their minds, design and fabricate machines to make their lives easier, send out satellites to the universe to discover the culture beyond the earth….. But no matter how powerful we are, we still have limited knowledge and understanding of ourselves. DNA is one of the keys opening the door to the secret of life, because it contains all genetic information that is passing from one generation to the next and that keeps the characteristics of each species distinct from others.

DNA is short for deoxyribonucleic acid, a molecule that carries genetic information in all living organisms. It was first isolated by the Swiss physician Friedrich Miescher in 1869. However, it was not until 1953 that the veil of DNA was finally removed by James Watson and Francis Crick, and its double helix structure of DNA was released.

This dissertation follows the style of *Electrophoresis*.

* Part of the material reported in this chapter is reprinted with permission from: An inexpensive microslab gel DNA electrophoresis system with real-time fluorencence detection by Chen, X.; Ugaz, V. M., *Electrophoresis* 2006, *27*, 387-393.

DNA is composed of phosphate, sugar and bases. Alternating sugar and phosphate sequences form the backbone of DNA. DNA molecules consist of two complementary chains of nucleotides, in a shape of a double helix---like a twisted ladder. Nucleotides are the repeating units along the double helix. The two nucleotides on the complementary strands are called a base pair, and associate through hydrogen bonding. There are certain rules by which the base pairs bind to each other. For example, adenine (A) and thymine (T) are a base pair, the same as guanine (G) and cytosine (C). A DNA sequence encodes information about gene expression that forms a blueprint for producing all the proteins needed to regulated different cellular functions. The structure of DNA is demonstrated in Figure I.1.

Understanding the DNA sequence is the key deciphering the code of life, which was the goal of Human Genome Project (HGP). This thirteen years project was finally completed in April 2003, successfully obtaining the accurate and complete human genome sequence. With this enormous data in hand, researchers are able to pursue further genomic investigation on diseases early diagnose, treatment and prevention. Not only this, the HGP has greatly promoted the development of new technologies, in order to get accurate data within short time. Thus, high-throughput technologies for DNA analysis are in great demand, and will continue to be a research focus.

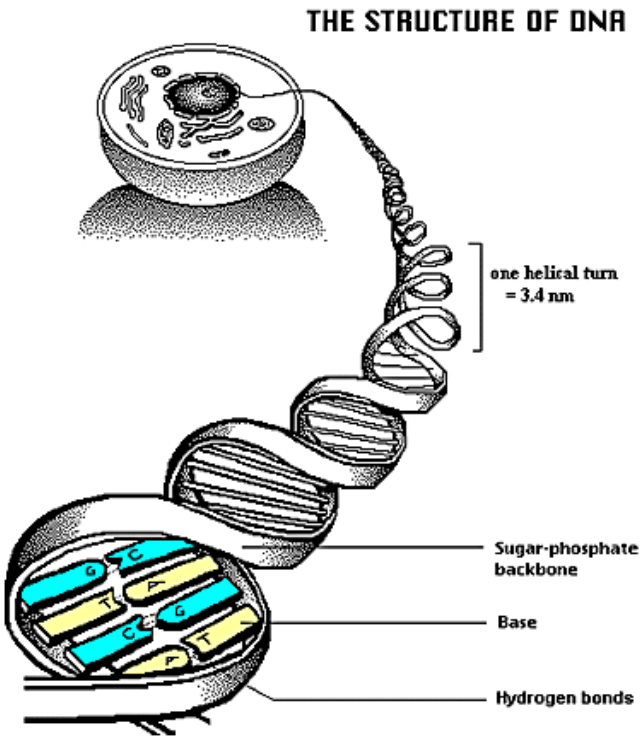

Figure I.1. The structure of DNA[1].

Among all aspects of the HGP, DNA sequencing is one of the primary research areas. It is the way to obtain the whole sequence of human genome, and allows scientists to identify individual variations. Sieving DNA fragments by size is one of the most important steps in the DNA sequencing, and must be performed with a highly degree of process accuracy and sensitivity. Yet, it is also a time consuming and labor intensive step. Therefore, the improvement of DNA separation technology is the key to increase the efficiency of DNA sequencing.

2. DNA separation technology

2.1 Electrophoresis

The term electrophoresis refers to a technique that employs an applied electric field causing charged particles or molecules to migrate through a matrix at speeds that depend on their sizes. It is one of the most widely used techniques for analysis of charged biomolecules, such as DNA and proteins. By exploiting the dependence of electrophoretic mobility on an analyte molecule's size and charge, individual species in a multi-component mixture can be distinguished by observing differences in migration velocity under an applied electric field. Electrophoresis techniques have been used for a long time and are proven to be an indispensable tool in the area of DNA analysis, with applications ranging from separation of single-stranded Sanger sequencing products, to separation of double-stranded PCR and restriction enzyme digestion products, to preparative and analytical separations of DNA fragments in the kilobase to megabase size range.

DNA can hardly be separated in free solution due to its free-draining coil behavior during free solution electrophoresis. This was first mentioned by Olivera et al. in their paper in 1964. In their discussion, the Hermans theory was adopted, which regarded DNA as a random coil polyelectrolyte. The mobility of DNA was finally simplified as [2]:

$$\mu = z / f \qquad \text{(I.1)}$$

According to this picture, each segment of DNA chain interacts with solvent independently, and the charge per unit length of DNA molecule is constant. These facts result in the size independent mobility of DNA molecules. Consequently, addition of a spongy-like gel matrix is critical in order to successfully separate DNA by size. By using the matrix, more resistance is introduced to prevent DNA molecule from migrating uniformly under the electric field.

Commonly used sieving media are polyacrylamide and agarose. Polyacrylamide is a cross-linked polymer of acrylamide. The pore size of polyacrylamide gel is determined by the concentration of acrylamide used. It is normally used to separate DNA fragments less than about 500 bp. The separation resolution provided by polyacrylamide is very high, for example, proper concentration of polyacrylamide gel can resolve DNA fragments with a single base pair difference in length. Agarose is a marine polysaccharide, which forms a thermoreversible gel. Agarose gels are crosslinked by hydrogen bonds and on the contrary to polyacrylamide gel, can form larger pores. This property makes agarose gel suitable for the separation of large DNA fragments in range from 100bp to several kilo bases.

Gel electrophoretic separations are typically performed in one of two predominant formats, slab gel or capillary, each with its own advantages and disadvantages. Slab gel electrophoresis is attractive because the hardware required is inexpensive and relatively

simple to operate, however the total time scale associated with casting and running the gel (typically on the order of hours) can be a limiting factor. Capillary electrophoresis, on the other hand, can be automated to provide rapid high-resolution separations with reduced sample volume requirements; however these systems cannot provide lane-to-lane comparison between different samples, and are more expensive and complex making them impractical for use in many laboratory and classroom settings. Consequently, there is a strong and growing need for gel electrophoresis instrumentation that combines the cost and simplicity of slab gels with the speed and reduced sample volume requirements of the capillary format.

A few research groups have made progress toward constructing inexpensive and rapid gel electrophoresis systems [3]. As early as 1972, Maurer and Dati investigated the design and operation of a micro-slab gel electrophoresis apparatus for separation of human serum proteins [4]. In their system, a vertical polyacrylamide gel was cast between standard glass microscope slides with injection wells formed using a specially constructed Teflon comb. After carefully loading a 1–5 µl sample volume into each lane, electrophoresis was performed at 60-100 V (3 mA) for 100 minutes at room temperature [5]. When the separation was completed, the gel was removed from the casting mold and post-stained to allow visualization of the separated bands. Although successful results were obtained using this system, several problems were encountered that made operation somewhat cumbersome including buffer leaks and formation of air bubbles in the gel (both during casting and during the separation run), the delicate

process of defining injection wells using the Teflon comb, difficulties in loading small sample volumes, fragility of the gels that made handling difficult during post-staining, and lack of gel imaging sensitivity [4]. Although these drawbacks hindered further progress with this apparatus, the authors recognized the potential value of such a system for performing a wide variety of biochemical and biomedical assays.

In the late 1990s, Guttman and co-workers revisited the use of a micro-slab gel format in a series of applications involving both protein [6] and DNA [3, 7, 8, 9, 10] analysis. Their separation platform consisted of a glass gel cartridge incorporating 15 ml plastic buffer reservoirs at both ends. A forced air cooling system was also included in order to counteract the effects of Joule heating during the separation run [6]. A gel matrix (2% agarose or hybrid mixtures of 2% agarose and 1% linear polyacrylamide) was cast inside the cartridge with Tris-borate-EDTA (TBE) buffer containing 50 nM of ethidium bromide to enable visualization of the separated bands [7]. A membrane-mediated sample loading technique was used in order to avoid problems associated with the traditional process of using a comb to define injection wells. This technique also allowed automated gel loading to be performed by robotically spotting 0.2–0.5 μL samples using a 32 or 96 tab membrane loader [9, 11]. Electrophoresis was performed at 750 V and 25 °C for approximately 25 minutes. A significant advance over previous work was the incorporation of real time detection of the migrating bands using a scanning laser-induced fluorescence/avalanche photodiode apparatus. Although this system allowed rapid separations to be performed with good resolution using small

sample quantities, its overall cost, particularly the detection component, was still too high to be practical for use in many applications.

2.2 DNA electrophoresis behavior

DNA separation can be generally classified into four regimes, based on the relationship between DNA fragments size and the gel pore size. Figure I.2. shows a general picture of how mobility varies with molecular size under continuous electric field electrophoresis.

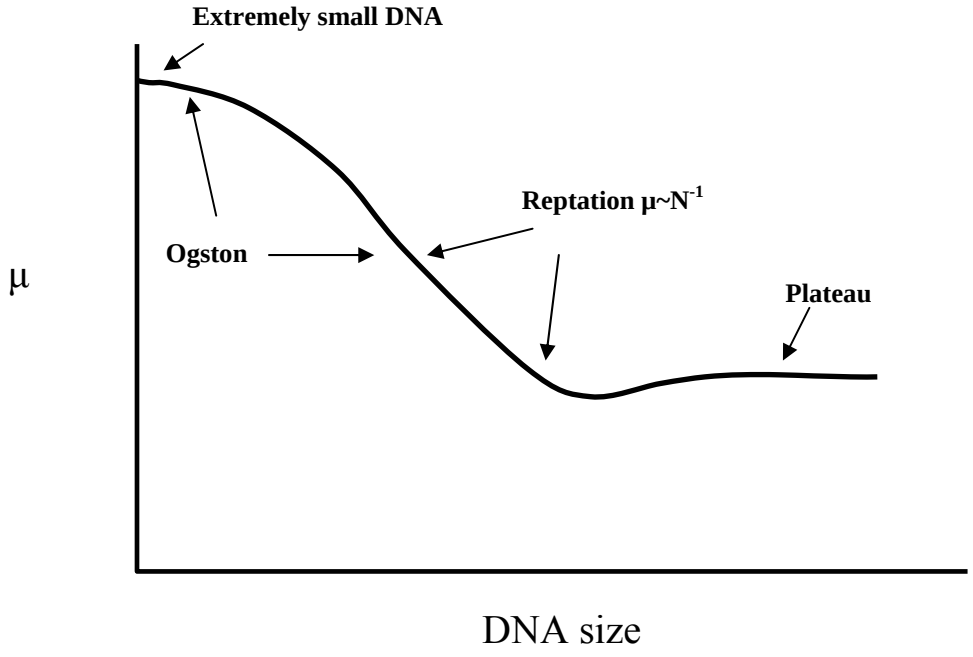

Figure I.2. Schematic log-log plot of relative mobility μ/μ_0 vs DNA molecular size.

When DNA size is extremely small, in which the contour length L is smaller than the persistence length P, the mobility of DNA fragments are independent of the size and equal to free solution mobility [12].

For DNA contour length L that is larger than the persistence length P, but radius of gyration R_g smaller than the average pore size, Ogston model is applied to describe the relationship between mobility and DNA size, which assumes DNA molecules are globular in shape. In this regime, all sizes of DNA fragments are migrating through the gel pores at the same local speed. However, smaller ones follow the almost straight path, while the larger ones have to wind through trying to find bigger pore size, which takes them longer time. This is why the smaller fragments show bands that move faster than the larger ones seen from gel image, yet it misleads to a wrong impression that the smaller fragments have higher migrating speed than the larger ones. Based on this mechanism, the size-dependent separation is achieved. The Ogston model describes the electrophoretic migration of rigid particles in a porous media, and it assumes that the scaled or reduced mobility μ^*---the ratio of the mobility in a sieving media μ and the one in the free solution μ_0---is equal to the fraction f of the volume available to the particle [13].

$$\mu^* = \mu / \mu_0 = f(C,M) \qquad \text{(I.2)}$$

here, f is the function of the gel concentration C and particle molecular size M [13].

When radius of gyration is larger than the pore size, DNA molecules have to distort their coil shape in order to move through the gel matrix. DNA threading through the gel is like snake crawling their way in thick grass [14]. This is described as “reptation in a tube”. This concept was first opened up in 1982 by Lumpkin and Zimm respectively. After that, theoretical predictions on DNA electrophoresis were developed. Later, the biased reptation model was proposed, which was more precise to perdict the movement under an external field. Even further, when molecule fluctuations were considered, biased reptation with fluctuations model was developed based on the progress of simulations and experiments. Generally, perdicted by reptation model, DNA electrophoretic mobiliy μ scales as $\mu \sim N^{-1}$ (N is the chain length). The movement of DNA in the gel can be described as ‘reptation-without-stretching’.

For extremely long DNA molecules, such as larger than 20 kb, in order to sustain electrophoretic migration, DNA molecules must adopt extended conformations preferentially aligned in the electric field direction. Unfortunately, this mode of migration is accompanied by a drastic reduction in the size dependence of electrophoretic mobility, making separation of long DNA fragments under continuous electric fields extremely challenging if not impossible.

Early attempts to overcome these limitations explored reducing the extent of molecular alignment either by lowering the electric field strength or by employing sieving gels with very large pores. Neither of these methods is ideal in practice, however, because lowering the electric field results in prohibitively long separation times while large-pore gels are mechanically fragile and difficult to synthesize. It was subsequently discovered that an additional dynamic process of reorientation could be introduced by periodically changing the direction and magnitude of the applied electric field. This process contributes an additional size dependent component to the electrophoretic mobility, with smaller sized fragments able to reorient more quickly than larger molecules and thereby migrating faster. These pulsed field gel electrophoresis (PFGE) techniques, first described by Schwartz and Cantor in 1984 [15], are now widely used and have greatly extended the range of DNA fragment sizes that can be separated, even up to tens of megabases [15, 16, 17].

2.3 Pulsed field gel electrophoresis

Pulsed field gel electrophoresis is a powerful tool that could separate DNA fragments from tens of kilo bases to few mega bases. The separation depends on periodically switching the electric field direction. Generally, longer DNA fragments respond to the field changes more slowly than the shorter ones, so that their movement is delayed. By studying the relationship between molecular size and velocity, it was found that DNA molecules demonstrate both size-dependent and size-independent velocity when

subjected to field orientation changes. Once a new field appears, DNA molecules align from random conformation to the field direction in a size dependent way. When the steady state is reached, size-dependent velocity is no longer valid, and is replaced by the size-independent velocity. Thus, for a given pulse frequency, longer fragments can not reach the steady state before pulse switching, while the shorter ones could migrate with steady state velocity, resulting in the larger ones lagging behind of the smaller ones.

In terms of instrumentation, a variety of designs has been developed to perform PFGE (as demonstrated in Figure I.3) and can be broadly classified according to how the electric field is modulated. In one case, field inversion gel electrophoresis (FIGE), the electric field direction is periodically alternated by 180° with different combinations of magnitude and pulse time applied in each direction in order to maintain a net forward migration. FIGE was first introduced in 1986, and proven to be useful for large DNA fragments separation [18]. FIGE methods are attractive because the electric field remains uniform throughout the gel minimizing distortion of the shape and spacing of the separated bands. These methods are also relatively straightforward to adapt for use in capillary-based formats [19, 20, 21, 22]. Furthermore, the set up of the FIGE system requires minimum instrumentation and FIGE system can be easily combined with other techniques, such as direct blotting electrophoresis [18]. A caveat, however, is that electrophoretic mobility may exhibit a non-monotonic dependence on fragment length depending on details associated with the pulsed field profile and experiment conditions employed [23, 24, 25, 26]. A second category of instrumentation includes designs where

the electric field is alternated over angles less than 180°. One popular example is the contour-clamped homogeneous electric field (CHEF) configuration where a hexagonal electrode arrangement is employed to alternate the electric field over an angle of 120° [27]. Use of an angle less than 180° makes it easier to maintain net forward migration, and a more well-defined relationship between mobility and fragment size is often observed. Spatial variations in the electric field may be produced, however, that can distort the band shapes and migration paths. Other configurations have been developed with the aim of minimizing these effects and allow more complex field profiles and pulsing patterns to be generated, including designs where either the gel or electrodes are mechanically rotated (rotating gel electrophoresis (RGE) and rotating field electrophoresis (RFE), respectively) and arrangements where the electric field is applied across the thickness of the gel (transverse alternating field electrophoresis (TAFE)) [17]. All these designs are have their own advantages and are widely used to separate large DNA fragments.

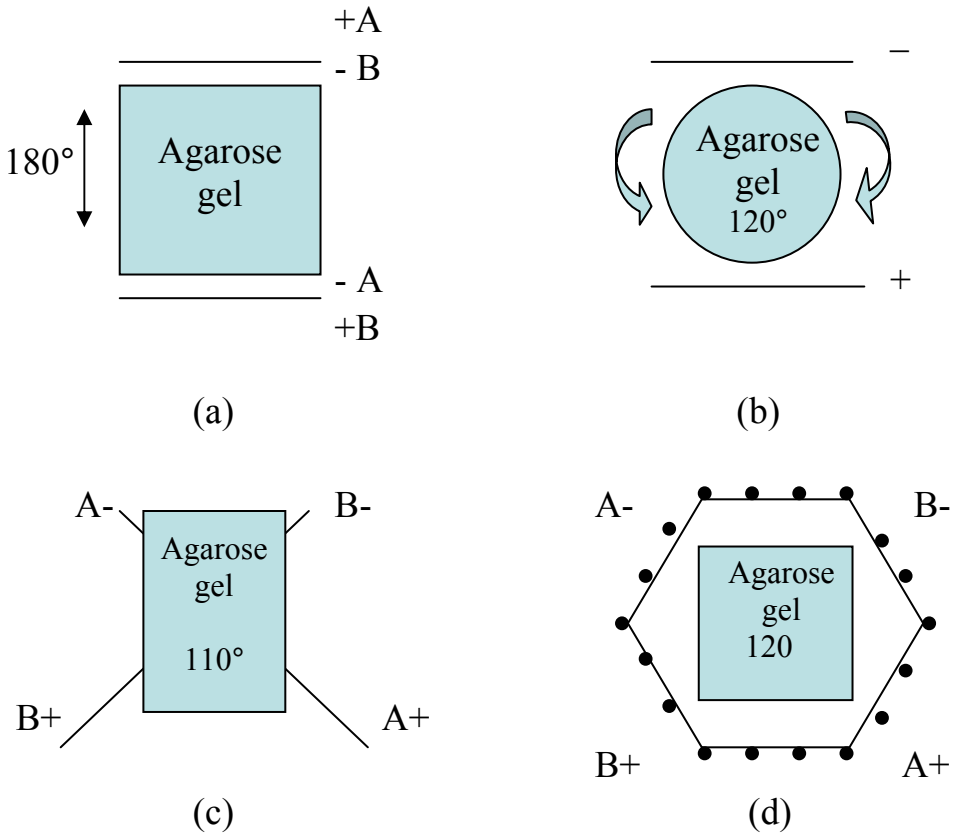

Figure I.3. Pulsed field gel electrophoresis configurations. (a) Field inversion gel electrophoresis (FIGE). Electric field orientation is alternated between A and B. DNA moves upward when A electrodes are active, and moves downward while B electrodes are active. (b) Rotating gel electrophoresis (RGE). Constant electric field is applied with rotating gel platform. (c) Transverse alternating field electrophoresis (TAFE). Gel is orientated vertically. Two pairs of electrodes are active alternatively, forcing DNA sample to zigzag through the gel. However, the final path of DNA is straight for the uniform electric field across the gel. (d) Contour-Clamped homogenous electric fields (CHEF). It has twenty-four point electrodes, which equally distribute around the hexagonal contour to give uniform electric fields. Sample runs straight lanes in the gel.

PFGE methods are important in a variety of applications including analysis of microbial genomes, large-scale restriction mapping and analysis of chromosomes, detection of chromosome breaks, and purification of genomic DNA. PFGE has also been widely used in clinical research to provide information of microbial genomes. For example, in 1990's, *Salmonella agona* infections increased abruptly in England and Wales. In order to identify and subdivide of isolates, the Laboratory of Enteric Pathogens used PFGE for the molecular fingerprinting of *S. typhi*, and for subdivision within epidemic phage types of *S. enteritidis*. Similarly, Ribot et al. from Centers for Disease Control and Prevention used PFGE for subtyping *Campylobacter* isolates [28]. Examples of applications in long-range physical mapping of chromosomes include Dally and coworkers, who used PFGE to construct physical and genetic maps of the Spiroplasma kunkelii CR2-3x chromosome [29]. Large DNA molecules can also be purified using PFGE by extracting the resolved bands after electrophoresis. PFGE is also employed in the process of large-fragment cloning, as for example, in the work of Lai et al. where size ladders for supercoiled and open circular DNA were constructed using bacterial artificial chromosome (BAC) clones. The size of the BAC inserts could then be estimated simply by running a PFGE in parallel with the intact undigested DNA [30]. PFGE is playing a major role in physical mapping of a human chromosome in Human Genome Project, the goal of which is to obtain the entire sequence of human DNA [31].

Furthermore, PFGE can be used to identity different DNA topological forms. For example, Chu et al. investigated separating mixtures of linear (1 – 12kb marker) and

supercoiled (5 kb plasmid) DNA and noticed that the different forms followed different migration paths in the gel. Linear molecules migrated in a gentle arc, supercoiled plasmid DNA migrated in a second dimension beyond the path of the arc, and nicked plasmid fragments migrated very slowly relative to the supercoiled form [32]. Hightower and Garvey made investigations comparing the behavior in PFGE of supercoiled and linear DNA, and observed that migration of supercoiled fragments was insensitive to pulse time, unlike the case in linear DNA [33, 34, 35]. This information is useful to classify different DNA forms using PFGE. In addition, PFGE can be used to detect chromosome breakage. Terajima et al. demonstrated the effectiveness of PFGE for the early detection of diffuse outbreaks due to Shiga Toxin–producing *Escherichia coli* in Japan [36]. Similar techniques have been used to study genotoxic effects caused DNA breakage in fish blood samples. In addition to bacteria, chromosomes of fungi, yeast, protozoa, plants and mammalian genes have been separated using PFGE [30].

Despite the incredible success of PFGE techniques in broadening the range of DNA fragment sizes that can be effectively separated, some important drawbacks remain. First, PFGE can be extremely time consuming, with run times generally ranging from hours to tens of hours. For example, it takes about 18 hours to resolve DNA fragments less than 1600 kbp using TAFE, but 30 to 40 hours using other systems.[31]. This is partially because the extent to which the electric field can be increased to address this issue is limited by the onset of Joule heating effects. Some progress toward performing high-field separations has been made in capillary systems [37, 38], although high voltage

power supplies are typically required. A second drawback is that most PFGE instruments employ slab gel-based designs that necessarily rely on post-stain detection to visualize the separated bands. This not only adds to the total experiment time, but also means that the separation process cannot be observed while the run is in progress. Consequently, the extent to which the details of DNA migration can be quantitatively studied in order to rationally optimize separation performance is limited. Finally, many commercial PFGE instruments are relatively expensive, a factor that can limit their accessibility both for routine analytical use and for performing fundamental studies. Thus, a need exists for an inexpensive platform to enable rapid PFGE separations to be performed while at the same time incorporating the ability to continuously observe the migrating DNA fragment zones during the course of the run.

3. Single molecule visualization

Gel electrophoresis is a simple and commonly used technology for size fractionation of biopolymers. It is of most importance to molecular biology as an analytical tool. Without gel electrophoresis, molecular biology would never have developed to the extent it has reached today [39]. However, there are still many aspects of the underlying physics of DNA migration when subjected to an applied electric field that are not yet fully understood[39, 40]. This level of fundamental understanding is important in order to enable further improvements separation performance high resolution, high-throughput to be achieved. This has motivated studies aimed at directly observing the behavior of

individual molecules during electrophoresis. Fluorescence microscopy has become a powerful tool that provides great opportunity for researchers to observe DNA molecules migrating through the gel matrix under electric fields, in order to extend the knowledge of dynamics of gel electrophoresis at molecular level.

The first observation of individual DNA molecule undergoing agarose gel electrophoresis was reported by Steven B. Smith's group [41](as shown in Figure I.4). DNA conformations were studied in both steady and pulsed field. According to their report, DNA macromolecules were migrating through the gel with alternation contraction and lengthening movements [41]. U-shapes were observed when the DNA became hooked around [41] by the gel fiber. DNA molecules demonstrated elastic property when stretching both ends at the same time. Moreover, the leading end turned into condensed, leading the rest of the chain move along the path.

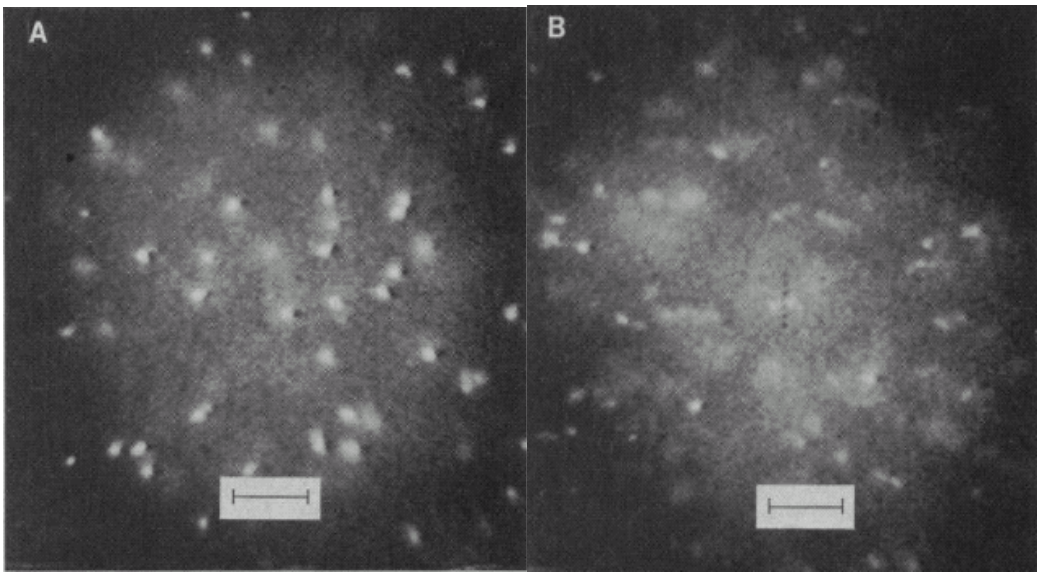

Figure I.4. Images of λ-phage DNA in agarose with (A) no electric field and (B) with 6 V/cm. A 1.5% agarosc (SeaKem ME) suspension in 0.5x tris-boric acids-EDTA buffer (TBE) with 0.5 μg of ethidium bromide per milliliter was melted and brought to 60°C. Then 0.1 μg of λ-phage DNA (BRL) was added to 1 ml of agarose and 15 μ1 of the mixture was placed on a microscope slide preheated at 60°C. A 22-mm #1 cover glass was placed over the sample. After 5 min of cooling, it was coated on two opposite edges with fingernail polish. The microscope consisted of a Nikon MicroPhot FX with an epifluorcscence attachment, a PlanApo 60x NA (numerical operative) 1.4 oil immersion objective, and a 2x magnifier. The depth of focus was 2 μm. The sample was excited in green light and viewed in red. A Varo Noctron 4 image intensifier, an Ikegami 310 vidicon television camera, and a Mitsubishi 359U VCR recorded the image. Infrared light from the excitation source was blocked by using a 3-mm Schott BG38 glass filter. The recorded video images were processed in a Quanta QX-7 image processing system coupled to an IBM PCIAT and photographed from the monitor screen. Each photograph is the average of four frames of NTSC video. Scale bar is 10 μm [41].

Schwartz and Koval reported a similar observation, describing DNA movements under both steady and pulsed field as cycles of elongation and contraction [42]. Detailed study about the effect of pulsed-oriented electrophoresis on DNA conformations were discuessed and it was found that although DNA molecules followed similar cycles in pulsed field as in steady field, the field angle exerted an obvious effect on DNA coil dynamics [42]. In addition, they showed that rapid collapse of the structure can be prevented by switching the field along perpendicular angles.

Following these pioneer studies, considerable efforts were applied to which explaining the motion of indivisual DNA molecule during gel electrophoresis by taking advantage of fluorescence microscopy. Nicholas J. Rampino reported that the migrating rate of DNA can be slow down and ultimately arrested when passing through the gel [43]. The interaction between DNA molecules and gel fiber consisted of unraveling the globular molecules into V-shape, of forming symmetric V-shape occasionally, and of slipping around the gel fiber [43]. Based on the experimental findings, a hypothesis was proposed that the prime mechanism of size separation of DNA in gel electrophoresis may be that the duration of this DNA-gel interaction was proportional to the length of DNA [43].

Pulsed field gel electrophoresis (PFGE) is a technology that overcomes the size limitation of conventional gel electrophoresis and expands the separation range up to few mega basepairs. In another paper of Nicholas J. Rampino, the authors first employed microscopic observation of DNA behavior to explain macro field inversion gel electrophoresis (FIGE) mobility phenomena. According to their report, the degree of retardation appeared proportional to the number of trapped conformations, when trapped conformation per DNA molecules is few [44]. Later, Sergio Gurrieri et al. published the first clear observation of individual DNA molecule passing through the gel during both 90º and 120 º pulsed field gel electrophoresis (PFGE). The differences in movements of single DNA molecules undergoing 90º and 120 º PFGE were demonstrated [45]. In 90º PFGE, the ‘head’ remained the leading end no matter the new field appeared or not, which is not much different from steady field electrophoresis (Figure I.5); while in 120 º PFGE, the previous ‘head’ became ‘tail’ when the field switched [45](Figure I.6).

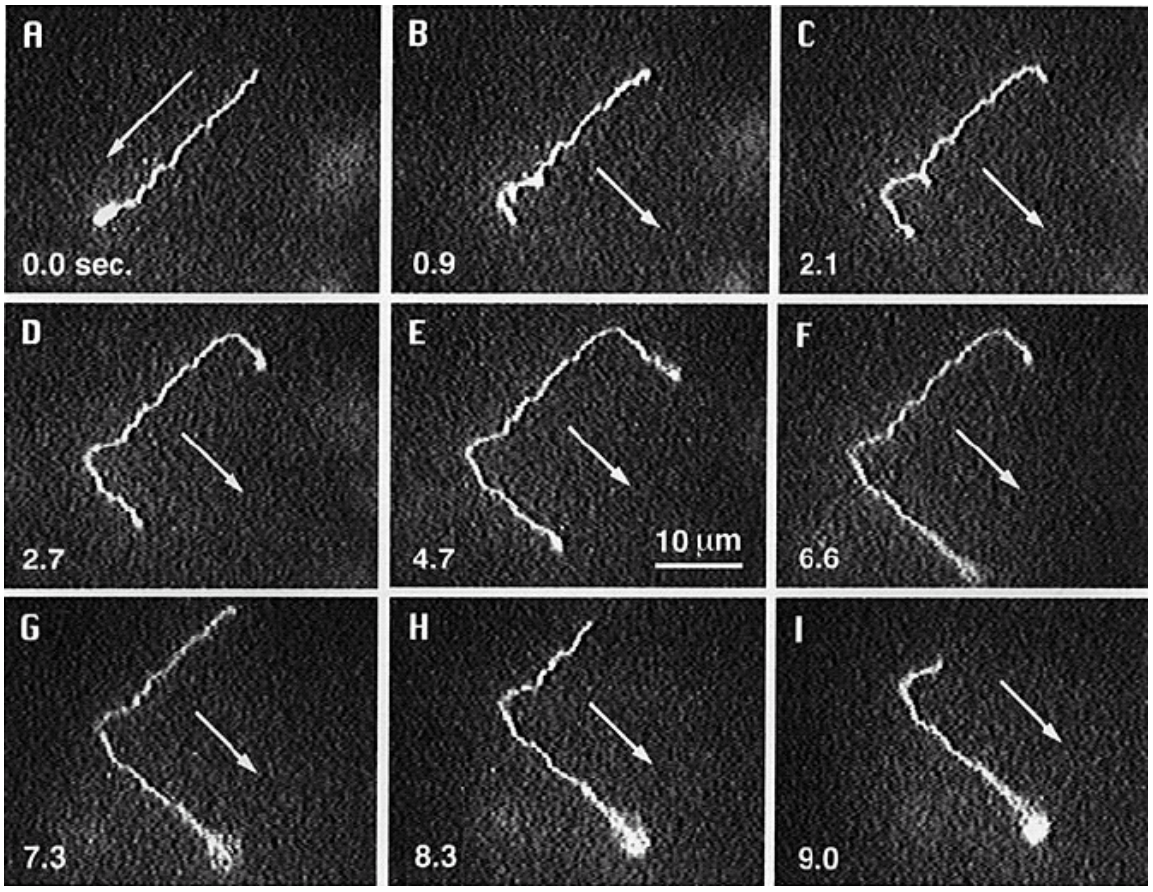

Figure I.5. Example of a T2 DNA molecule during 90° PFGE. The molecule is first moving to the lower left (A) in the direction of the arrow. Then the field is switched to the lower right (B). DNA stained with YOYO-1. Electric field, 10 V/cm [45].

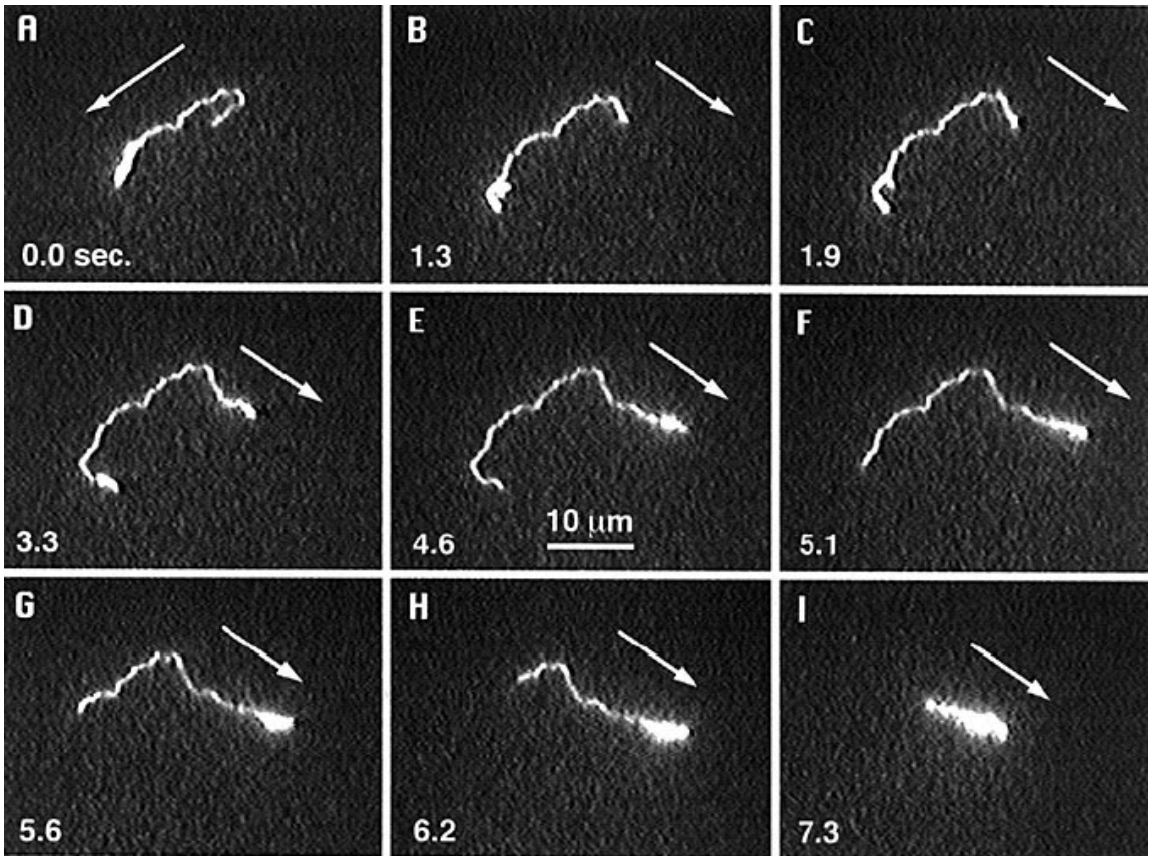

Figure I.6. Example of a T2 DNA molecule during 120° PFGE. The molecule is first moving to the lower left (A). Then the field is switched to the lower right (B). Notice that the 'tail' end of the molecule drives the chain during the reorientation process. DNA labeled with YOYO-1. Electric field, 8 V/cm [45].

Other than usual conformations of DNA molecules observed during both steady and pulsed field gel electrophoresis, there are some other interesting conformations of DNA undergoing gel electrophoresis. In 1990, Sergio Gurrieri et al. observed the kinked configurations of DNA molecules undergoing orthogonal field alternating gel electrophoresis (as shown in Figure I.7) [46], which was the first experimental confirmation of some of the predictions of J. M. Deutsh in 1987 [47]. Also, there was an agreement with other authors (Smith et al., 1989; Schwartz & Koval, 1989) that DNA molecules seldom stretched to the complete elongation under normal electrophoretic field strengths [46].

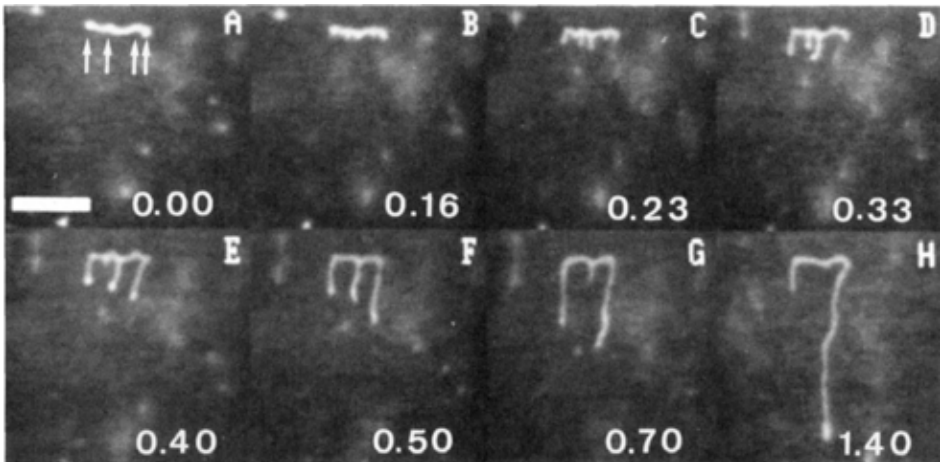

Figure I.7. The demonstration of kinks formation [46].

A ‘W’ conformation was detected by Konstantin Starchev et al. (as shown in Figure I.8) [48] using birefringence under sine wave electric fields, which was not found in steady field. The reason for the formation of ‘W’ conformation was explained, that is mostly because the sine wave could slow down the inversion of the field which favored the specific conformation [48].

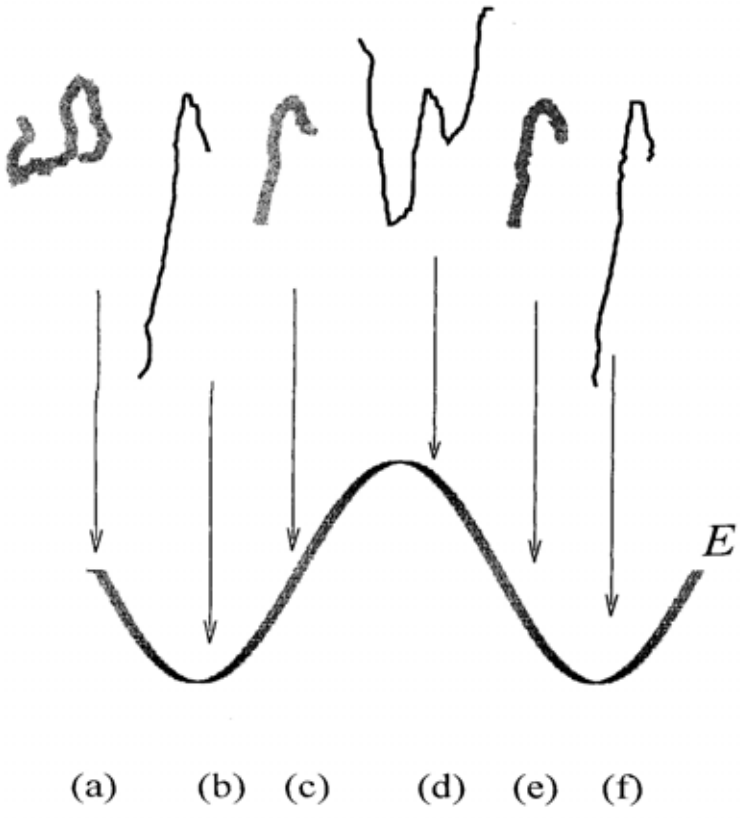

Figure I.8. The demonstration of ‘W’ conformation formation [48]

The possibility of manipulating and observing single DNA molecules has also helped to advance our understanding of polymer physics. This was demonstrated in a series of studies by Chu et al. where DNA molecules (4~43 μm in length) were covalently attached to polystyrene beads so that the behavior of the tethered DNA could be observed as the fragments become stretched and ultimately fully extended by an external flow shown in Figure I.9 [51]. Relaxation time and extension length were studied [40] [50, 51, 52], with results in qualitative agreement with a theoretical scaling prediction.

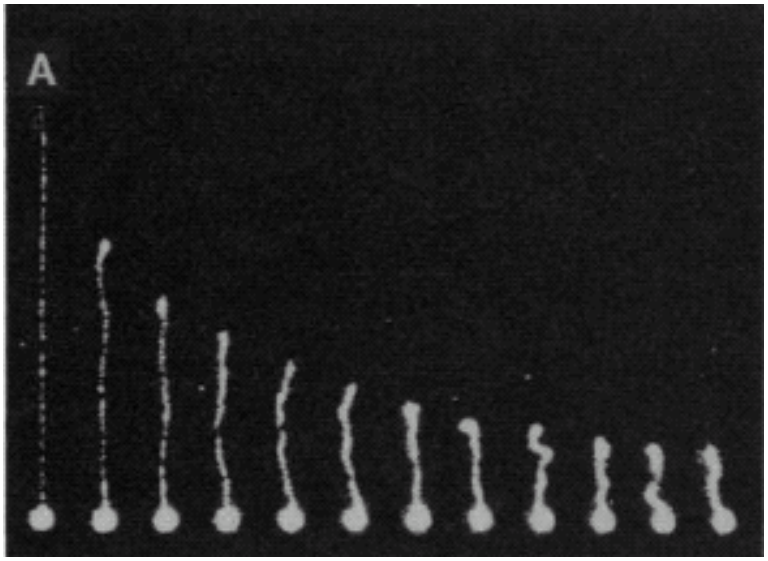

Figure 1.9. Relaxation of single molecule of DNA. DNA is stretched to its full length about 39 μm. Frames are spaced at 4.5 s intervals [51].

Later, the same group used elongational flow to stretch λ DNA and determined the probability distribution of extension states. The distribution of molecular configurations occurring at the highest strain rates was determined, and indicated that a simple model consisting of two beads connected by a spring did not provide an adequate description. These experiments were also notable for providing experimental validation of reptation models by allowing direct observation of tube-like motion of λ DNA manipulated with optical tweezers [50]. In tube-like motion study, fluorescent labeled DNA molecules was manipulated and observed in the entangled solution of none fluorescent labeled DNA. DNA molecules were tethered with beads at one end of each chain, and stretched to various conformations, such as kinks and loops. Relaxation was studied, and the result was DNA molecules were found approximately followed the same tube path defined by their initial contour [50]. Figure I.10 demonstrates the tube-like motion of a relaxation DNA molecule [50].

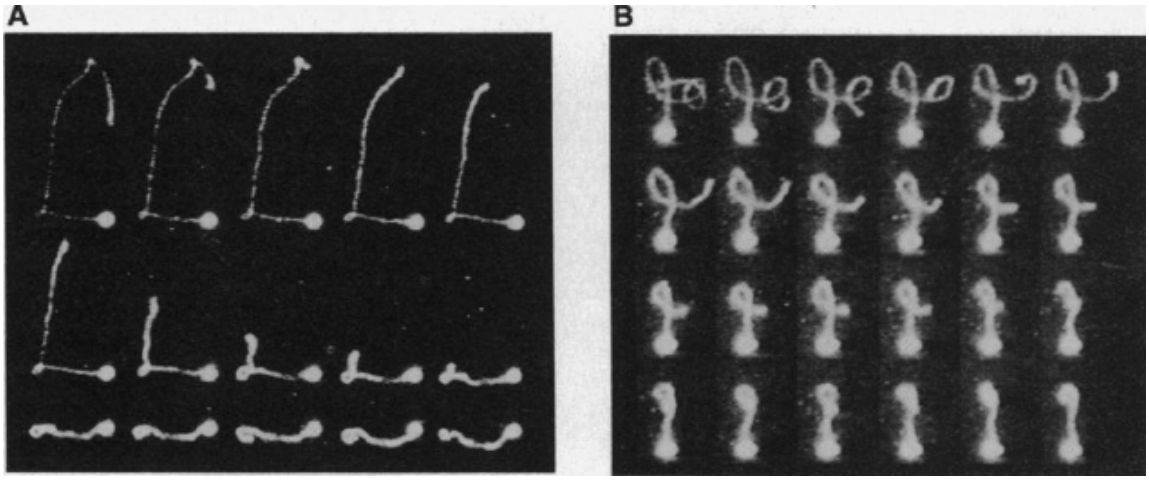

Figure I.10. Example of relaxation motion of DNA. (A) A demonstration of the tube-like motion of a relaxing DNA molecule in a concentrated polymer solution. (B) A demonstration of DNA relaxation along a contorted path drawn with the optical tweezers by manipulation of the bead [50].

Doyle et al. have fabricated microfluidic devices incorporating micron-scale insulating obstacles that allow collisions experienced between electrophoretically migrating λ-DNA and the obstacle to be observed. Rates of stretching and lengths of the fully extended molecules were measured, and it was found out that the hooking probability depends on the Deborah number between the range of 0.5>De>30[53]. Reccius et al. investigated extended λ-DNA confined in nano channels where a free extension process occurred when the electric field was switched off. The extension length and decompression time were measured, and could be explained by scaling arguments. Recently, novel techniques for stretching DNA were reported, such as entropic stretching [49], which is simply based on physical confinement. Generally, manipulating DNA molecules provides us additional information about the physical properties of DNA, also extends our ability for better controlling DNA during electrophoresis, which may later be applied for developing a novel electrophoresis technology in the future.

Single molecule visualization technology provides us great opportunity to directly observe the factors affecting DNA movement, and reveal the interaction between DNA molecules and gel fibers during electrophoresis. This information is the basics to develop new technology for better DNA separation in the future.

4. Quantum dot nanoparticles

Quantum dot nanoparticles are nano scale atom clusters, which consist of a core, shell and coating. The core is made from a nanometer-scale crystal of a semiconductor material (CdSe), containing a few hundreds to a few thousands of atoms. The semiconductor shell (ZnS) surrounds and stabilizes the core, and improves the optical and physical properties of the material. The core-shell material is further coated with a polymer shell that allows the materials to be conjugated to biological molecules and to retain their optical properties. For example, streptavidin can be covalently attached on the surface of quantum dot nanoparticles through ester coupling reaction, which provides quantum dots streptavidin conjugates high specific biological activity. The size of the conjugate is the as the same scale as a macromolecule or protein (about 15 to 20 nm). Figure I.11 demonstrate the structure of straptavidin functionalized quantum dots conjugate.

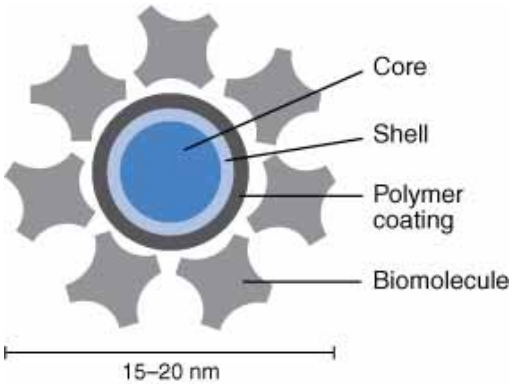

(a)

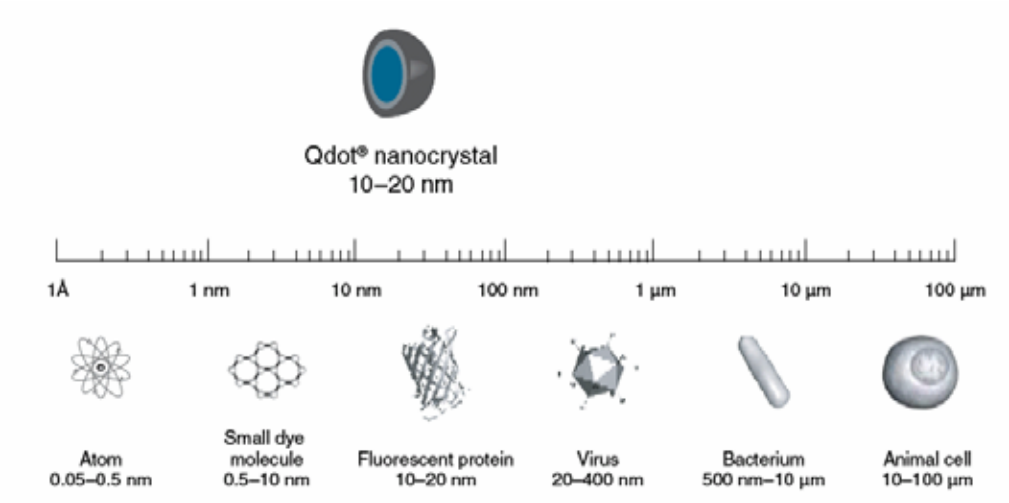

(b)

Figure I.11. The structure of quantum dot. (a) Schematic of the overall structure of a Qdot streptavidin conjugate, from Invitrogen, Inc. (b) Demonstration of relative size of Qdot streptavidin conjugates, from Invitrogen, Inc [54].

Quantum dots are flurophores, which are substances that absorb photons of light and re-emit photons at a different wavelength. Quantum dots are a kind of material that extremely efficient to generate fluorescence. They have brighter fluorescence and greater photo-stability than traditionally used organic fluorophores. Fluoresce of quantum dots are generated through the formation of excitons, or coulomb-correlated electron-hole pairs, which provides longer lifetime than organic fluorophores.

Quantum dots have a broad range of spectrum, and each individual has a narrow, symmetric emission spectrum with the emission maximum near 525 nm, 565 nm, 585nm, 605 nm, 625 nm, 655nm, 705nm, or 800 nm. Commercialized quantum dots have direct relationship between the physical size and emission wavelength. Therefore different sized quantum dots demonstrate different color of fluorescence. Figure I.12 shows the absorption and emission profiles of commercial quantum dots from Invitrogen.

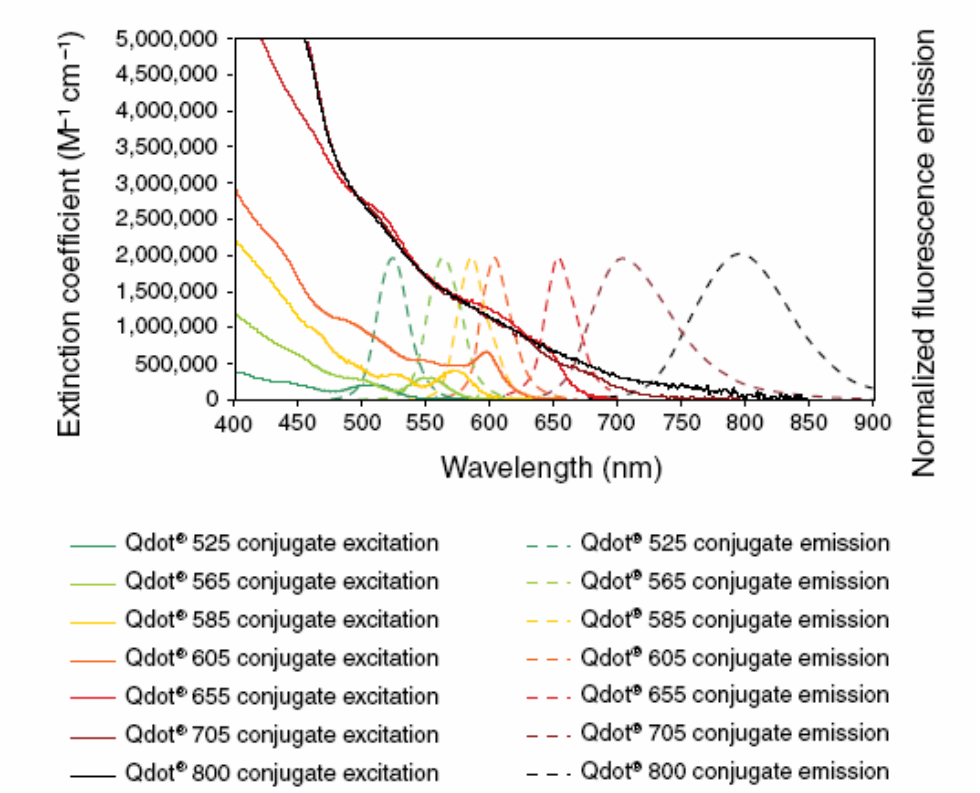

Figure I.12. Absorption and emission profiles of quantum dot nanoparticles from Invitrogen, Inc [54].

As a semiconductor material, Quantum dot nanoparticles have attracted extensive interest in biology and medicine for their unique optical and electronic properties. It is used for in vitro imaging of fixed cells and tissues, intracellular organelles and molecules, and membrane surface. Furthermore; it is efficient for in vivo targeting of cells, tissues, organs and tumors. It can detect low-abundance antigens, and becomes a great alternative method for western blotting that provides exceptional sensitivity and

broad linear range of detection, which has significant advantage over traditionally use colorimetric and chemiluminescence methods. Recently, quantum dots have been reported as an efficient method for nucleic acid detection [55]. For example, Zhang's group constructed a two-color quantum dots for nucleic acids detection which provided rapid and sensitive detection results [55]. Quantum dot technology provides great oppoturnity helping scientists to discover more information about the molecular events in tumor cells and early diagnosis.

5. Objectives

Pulsed field gel electrophoresis (PFGE) has become a well-established technique for fractionation of DNA fragments ranging from kilobases to megabases in length. PFGE methods are important in a variety of applications including analysis of microbial genomes, large scale restriction mapping and analysis of chromosomes, detection of chromosome breakage, and purification of genomic DNA. But despite this widespread importance, PFGE separations usually suffer from an undesirable combination of long experiment times (often approaching tens of hours), the need to apply high voltages (often approaching tens of kV, requiring expensive switching power supplies), and difficulties in observing separation progress during the course of the run.

We have recently made two key innovations that, when combined, could potentially overcome many of these limitations. First, we have developed methods to construct

DNA–quantum dot conjugates in order to determine their influence on separation performance. Conjugates are constructed by complexation between streptavidin functionalized quantum dots and end-biotinylated lambda DNA. The attached quantum dots can then be further modified through binding interactions with biotinylated single-stranded DNA primers. By using different combinations of quantum dots of various size and primers of various lengths, both the size and charge density of the quantum dot complex at the ends of each lambda DNA molecule can be precisely manipulated. We have explored these effects using real-time single molecule imaging to directly observe the conformations adopted by individual DNA molecules and their interactions with the gel matrix during electrophoresis. These experiments have helped us to identify physical mechanisms through which the quantum dot and primer conjugates alter electrophoretic migration under various electric field conditions. Second, we have developed a miniaturized PFGE apparatus capable of separating DNA fragments tens of kilobases in length within 3 hours using a modest applied potential of 20 V. The device is small enough to be imaged under a fluorescence microscope, permitting the migrating DNA fragments to be observed during the course of the separation run. We have validated the operation of this device by using it to investigate how separation resolution in field inversion gel electrophoresis (FIGE) is affected by parameters including the ratio of forward and backward voltage, pulse time, agarose gel concentration, and temperature. These data allow us to quantify the dependence of DNA mobility on fragment size.

The goal of this research is to combine these innovations to develop new methods that may help us understand and manipulate the nanoscale interactions between DNA molecules and hydrogel sieving matrices during gel electrophoresis in order to improve separation speed and resolution over a broad range of DNA fragment sizes.

Objective 1: Single Molecule Visualization of DNA-Quantum Dot Conjugates. We investigate the migration of single DNA molecules incorporating quantum dot complexes attached at one or both ends. This architecture will allow us to adjust both the size and charge of the quantum dot complex. Single molecule motion is observed under application of electric fields with different orientations and pulsing parameters. Image analysis is then performed on an ensemble of DNA fragments to identify different interaction modes and their relative frequencies, as well as to quantify the extension length, entanglement probability and the reorientation time associated with each mode.

Objective 2: Bulk Pulsed Field Gel Electrophoresis Studies. The insights gained from the single molecule studies are combined with pulsed field gel electrophoresis experiments using the miniaturized instrumentation we have developed. We construct quantum dot conjugated DNA size ladders for use in these experiments that will allow us to observe how separation performance is influenced. These experiments will also show us the extent to which observations made in single molecule studies of long DNA fragments can be extrapolated over a wider size range, and may also help to identify which modes

of interaction between the migrating DNA and the gel contribute most favorably to separation performance.

CHAPTER II

A SIMPLE AND INEXPENSIVE MICRO-SLAB GEL DNA ELECTROPHORESIS SYSTEM WITH REAL TIME FLUORESCENCE DETECTION*

In this Chapter, we demonstrate an example of the miniaturization of gel electrophoresis device. We describe the construction of a simple yet powerful gel electrophoresis apparatus that can be used to perform size selective separations of DNA fragments in virtually any laboratory. This system employs a micro-slab gel format with a novel gel casting technique that eliminates the need for delicate combs to define sample loading wells. The compact size of the micro-slab gel format allows rapid separations to be performed at low voltages using sub-microliter sample volumes. Real time fluorescence detection of the migrating DNA fragments is accomplished using an inexpensive digital microscope that directly connects to any personal computer with a USB interface. The microscope is readily adaptable for this application by replacing its white light source with a blue LED and adding an appropriate emission filter. Both polyacrylamide and agarose gels can be used as separation matrices. Separation performance was characterized using standard double-stranded DNA ladders, and correct sizing of a 191

---

* The material reported in this chapter is reprinted with permission from: An inexpensive microslab gel DNA electrophoresis system with real-time fluorencence detection by Chen, X.; Ugaz, V. M., *Electrophoresis* 2006, *27*, 387-393.

base pair PCR was achieved in 10-20 minutes. The low cost and simplicity of this system makes it ideally suited for use in a variety of laboratory and educational settings.

1. Materials and methods

1.1 Assembly of micro-slab gel system

Micro-slab gels were cast between a bottom plate of 30 x 24 mm microscope cover glass (Golden Seal, Fisher Scientific, Pittsburgh, PA) and a sheet of overhead transparency film (3M, Minneapolis, MN) cut to the same size (Figure II.1). First, the cover glass was affixed to a larger glass plate using two strips of aluminum tape. The glass plate served as an electrically insulating support surface for the gel assembly, while its optical transparency permitted the fluorescently labeled DNA to be illuminated from below. The electrically conductive aluminum tape also served as the electrodes used to apply a potential across the gel. For these experiments, adhesive aluminum film used to seal conventional multi-well PCR plates (Fisher Scientific) was cut into strips approximately 2 mm wide. We also investigated the use of adhesive copper film, but found that upon application of a voltage, electrochemical interactions with the ionic buffer environment produced an undesirable blue coloring in the gel that obscured fluorescence from the migrating DNA bands. Next, two plastic spacer strips were positioned at the edges of the cover glass and oriented perpendicular to the aluminum electrodes in order to define

the gel thickness. Spacer thicknesses of 0.4 and 0.6 mm were cut directly from plastic shim stock (McMaster-Carr, Chicago, IL).

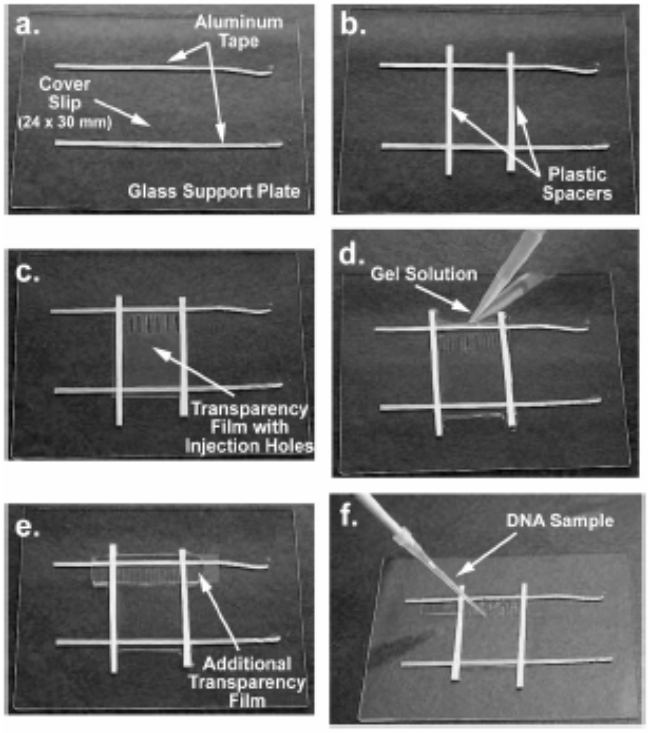

Figure II.1. Assembly, casting and loading of microslab gels. (a) Mounting of bottom cover slip on glass support plate with electrically conductive aluminum tape. (b) Positioning of plastic spacers to define gel thickness. (c) Overlay of transparency film coated with BindSilane incorporating holes to define location and shape of sample loading wells. (d) Pipetting the gel solution into the gap between the bottom cover slip and the upper transparency film. (e) Placement of second transparency film strip to further define sample loading well size and shape. Polyacrylamide gel will not polymerize in the exposed area. (f) Loading of DNA samples into the individual wells area. (f) Loading of DNA samples into the individual wells after gel polymerization [56].

The use of transparency film as the top plate is advantageous not only because it is readily available, inexpensive, and durable, but because it also permits a variety of different injection well shapes and sizes to be easily constructed. We investigated the use of rectangular, circular, and triangular injection well structures. Triangular injection wells were produced by manually cutting triangles directly in the film; while circular and rectangular injection wells were produced using ordinary hole punches (McGill, Marengo, IL). An issue with transparency film is that the polyacrylamide gels adhere poorly to the surface leaving a gap through which DNA preferentially migrates rather than traveling through the gel matrix. This problem was alleviated by wiping the inner surface of the transparency film with PlusOne BindSilane (Amersham Biosciences Corp., Piscataway, NJ) to promote surface adhesion. The BindSilane solution was applied to the surface using a Kimwipe towelette and allowed to air dry.

The transparency film was gently held in place by hand while polyacrylamide gel solution was pipetted into the gap between the top and bottom plates, after which surface tension forces were sufficiently strong to hold the top plate in place. The size of the injection wells could be further manipulated by partially covering the holes in the top plate using a second strip of transparency film. Since the polymerization reaction is inhibited by the presence of oxygen, the gel did not form in the exposed portion of the hole. Using this technique it is possible to precisely adjust the size of the injection hole to match the desired volume of sample to be loaded into the gel. Once polymerization was completed, the strip partially covering the holes was gently removed and the

remaining unpolymerized solution was wicked out of the injection wells using a Kimwipe towelette.

Gels were also cast between two glass plates using the same procedure described above, except that injection holes were drilled in top cover glass using an electrochemical discharge process. Then, after pipetting a gel solution between the plates, pins were inserted through the holes in order to define the loading wells. Although use of a glass top plate avoids gel adhesion issues encountered with the transparency film, difficulties associated with drilling the holes and the lack of flexibility in producing holes of different shapes and sizes makes this a less attractive option.

1.2 Gel preparation

Micro-slab gels were cast using both crosslinked polyacrylamide and agarose. Polyacrylamide gels were prepared by diluting as-supplied 50 %T LongRanger gel solution (Cambrex Bio Science, Walkersville, MD) in appropriate amounts of deionized water and 10x Tris-Borate-EDTA (TBE) buffer (Bio-Rad Laboratories, Hercules, CA) to obtain final gel concentrations of 4.75 and 5.25 %T in 1.5x TBE. Prior to casting, 7µl of a 10 % w/v aqueous ammonium persulfate solution and 3 µl of N,N,N',N'-Tetramethylethylenediamine (both from Bio-Rad Laboratories, Hercules, CA) were added to a 1 ml aliquot of the desired concentration of gel solution and gently mixed by stirring with the pipette tip. A 200-300 µl volume of this mixture was then dispensed

into the gap between the top and bottom gel plates using a 1,000 µl pipettor, after which it was allowed to polymerize for at least 25 minutes. Agarose gels were prepared by dissolving agarose powder (Bio-Rad Laboratories, Hercules, CA) in a 1x TBE buffer solution. The gel casting process was identical to that used for polyacrylamide, except that the molten agarose solution was loaded rapidly enough to fill the entire volume between the gel plates before it began to harden. The gel was then allowed to cool for at least 15 minutes, after which injection wells were fashioned by cutting away the agarose inside the top plate holes with a pin.

1.3 DNA sample preparation

Separations were performed using a 100 base pair double stranded DNA ladder (Bio-Rad Laboratories, Hercules, CA) and a PCR product. The PCR product consisted of a 191 base target associated with membrane channel proteins M1 and M2 of the influenza-A virus. Optimized buffer/dNTP mix and primers were obtained in a kit from Maxim Biosciences (forward and reserves primer sequences were: 5'-GCAGCGTAGACG-CTTTGTCCAAAAT-3' and 5'-CAGCCCCCATCTGTTGTATATGAG-3'). Standard reactions contained 15 µl optimized buffer/dNTP mix, 5 µl primer mix, 4.25 µl ddH_2O, and 0.5 µl template DNA (3.9 kb, 5 x 10^5 copies), all included in the PCR kit, and 0.05 U/µl of AmpliTaq Polymerase (Applied Biosystems, Foster City, CA). Thermocycling

was performed using a 3-temperature cycling protocol (anneal: 61 °C, extend: 72 °C, denature: 95 °C, 35 cycles). DNA samples were pre-stained by adding 3 µl of a 100x SYBR-Green I (Molecular Probes, Eugene, OR) solution to 7 µl of DNA.

1.4 Electrophoresis conditions

After casting, the micro-slab gel assembly was mounted on the microscope stage, and the aluminum electrodes were connected to a DC power supply (Model E3612A, Agilent Technologies, Palo Alto, CA). Approximately 0.5-0.8 µl of fluorescently labeled DNA was then pipetted into each injection well, and electrophoresis was performed by applying 40-50 V across the electrodes for 10-20 minutes. Although some bubbling occurred at the electrode surfaces, the separation was not affected as long as the electrodes were not positioned near the injection wells. All runs were performed at room temperature.

1.5 Computer microscope refit

An inexpensive computer microscope (QX3 Plus, Digital Blue, Marietta, GA) was used for visualization of the migrating DNA (Figure II.2 a, b). This microscope connects directly to the USB port of a personal computer, and offers three levels of magnification (10x, 60x, and 200x). The 10x magnification setting was mainly used in order to provide the widest field of view of the migrating bands. Software to control the microscope and perform image and video capture is available for both Microsoft Windows and Apple Macintosh platforms (Macintosh support is achieved using the free miXscope application available from EdH Software (www.edhsw.com)). The QX3 microscope's CMOS sensor captures images at a resolution of 320x240 pixels, subsequently interpolated to 512x384 pixels for display by the microscope software [57]. An updated version of the microscope has since become available (Model QX5) which claims to provide higher resolution.

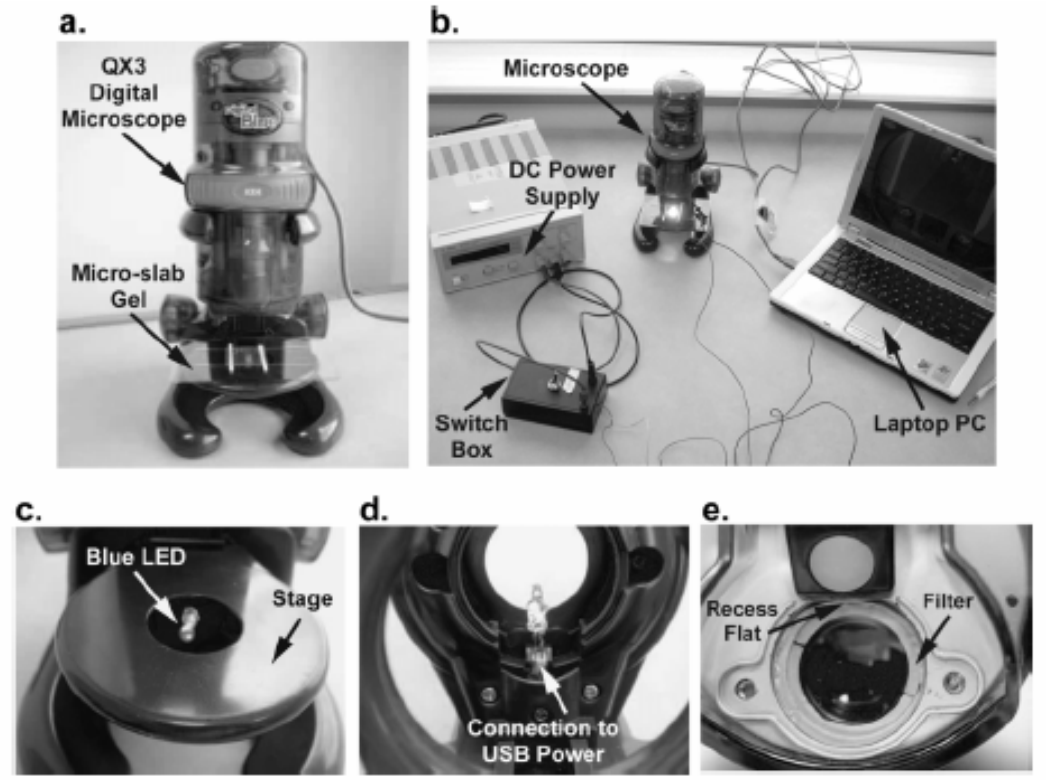

Figure II.2. Illustration of QX3 Plus microscope based detection system. (a) Mounting of micro-slab gel on microscope stage. (b) Overview of complete electrophoresis setup. Connections to the DC power supply were made using test clips and a homebuilt switch box. (c) Top view of modified stage showing positioning of blue LED illumination source. (d) Bottom view of stage in (c) depicting connection of blue LED to lamp socket for USB power. (e) Positioning of emission filter underneath objective cover in microscope housing [56].

Visualization of the fluorescently labeled DNA samples with the QX3 Plus microscope required two simple modifications: The white light source supplied with the microscope was replaced with a blue light source and an appropriate emission filter was added. An inexpensive blue light source was constructed by replacing the light bulb inside the microscope stage with blue LEDs (many combinations are possible, however we obtained good results using Part # 67-1747-ND, Digi-Key Corporation, Thief River Falls, NJ). The LEDs we selected provide a peak output wavelength of 470 nm, with an intensity of 1000 mcd and a 30° viewing angle. Wider viewing angles are available to provide more diffuse illumination, but generally at the expense of overall intensity. Most importantly, these LEDs were selected such that their power requirements (3.5 V, 30 mA) allow them to be directly connected to the lamp socket in the microscope stage in order to draw power entirely from the USB connection, thereby eliminating the need for an additional power source (Figure II.2 c, d) (According to the manufacturer, the tungsten bulbs supplied with the QX3 Plus operate at 3.5 V and 300 mA). The circular white plastic diffuser located in the center of the stage platform was also removed to permit maximum illumination intensity from the LED array. Next, the clear plastic protective cover over the objective lens was removed, and a 530 nm long pass filter (Part # NT46-059, Edmund Optics, Inc., Barrington, NJ) was inserted to reject the blue light so that only the fluorescent DNA was visible (Figure II.2e). The clear plastic cover was then replaced and held the filter securely in place. Positioning the scope on a dark surface (such as a black lab bench top) reduced background illumination and enhanced overall contrast. Additional filters and optics can be installed to more precisely define

excitation and emission spectral characteristics, or to allow a variety of other microscopy techniques to be employed (an excellent resource for scientific applications of the QX3 is provided on the Molecular Expressions website hosted at Florida State University).

2. Results and discussion

A series of electrophoresis experiments were performed using 4.75 and 5.25 %T polyacrylamide gels (Figure II.3 a, b). The 10x objective provided sufficient magnification to image all bands in the ladder at both gel concentrations. Proper adjustment of the LED lamp is necessary in order to both align the illuminated area with the objective and to provide uniform light intensity over the entire field of view. With proper positioning, it is possible to observe DNA migration in several lanes simultaneously, and the QX3 Plus microscope allows both still images and video clips of the separation to be recorded. If a wider field of view is desired than is possible with the 10x objective, the gel assembly can be photographed using a conventional UV trans-illuminator setup used with ordinary benchtop electrophoresis gels (Figure II.3 c).

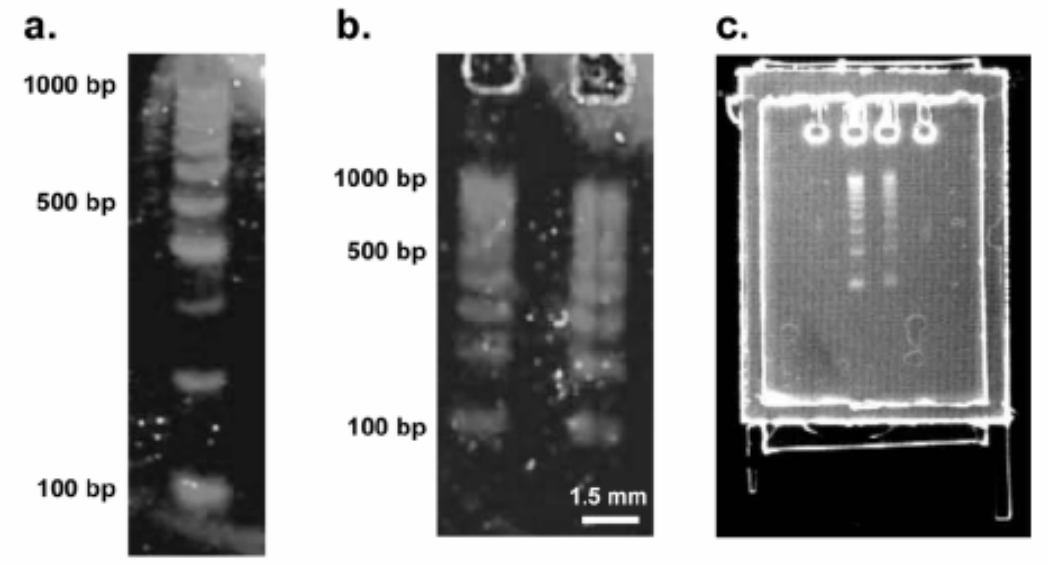

Figure II.3. Separation results using micro-slab gel electrophoresis system. (a) Separation of 100 base pair DNA ladder in a 4.75 %T crosslinked polyacrylamide gel (E = 20 V/cm, run time = 10 min). (b) Separation of 100 base pair DNA ladder in a 5.25 %T crosslinked polyacrylamide gel (E = 20 V/cm, run time = 10 min). (c) Photograph of gel in (b) taken under a conventional UV trans-illuminator showing the entire micro-slab gel assembly [56].

All separation runs were performed in 10-20 minutes electric fields of approximately 20 V/cm (electric current remained relatively constant during the course of the run). The ability to resolve the migrating fragments under these conditions is attributable to several benefits of the micro-slab gel format. First, the compact size of the gel cassettes allows electrophoresis to be performed in a high surface area to volume environment that greatly enhances dissipation of Joule heating. Consequently, runs can be performed at higher electric fields without significantly increasing the temperature or inducing thermal gradients within the gel, both of which contribute to broadening of the separated zones [58]. Secondly, and perhaps most importantly, the ability to construct small and precisely defined loading well structures within the gel allows the width of the injected sample zone to be greatly reduced. By loading only the amount of sample necessary to fill the well, stacking at the gel interface occurs almost immediately upon application of the electric field due to the large mobility difference between the DNA sample in free solution and in the gel. Consequently, the sample already confined within the small sample well volume becomes even more highly focused at the gel interface. It is likely that with proper design even higher electric fields could be applied in order to achieve more rapid separations, although we did not explore this possibility.

As an example of a typical analytical application, we used the micro-slab gel apparatus to perform a multilane separation of a 191 base pair product of a PCR reaction and a 100 base pair ladder (Figure II.4a). Correct sizing of the PCR product was achieved in 15 minutes using sample volumes less than one microliter. In addition to polyacrylamide,

agarose gels can also be employed in the micro-slab gel format as illustrated by separation of a 100 base pair ladder in a 2% agarose gel (Figure II.4 b). Device operation is virtually identical to polyacrylamide gels, with the exception of the process used to create the sample loading wells. Nevertheless, the ability to employ agarose gels greatly expands the size range of DNA fragments that can be separated using this apparatus.

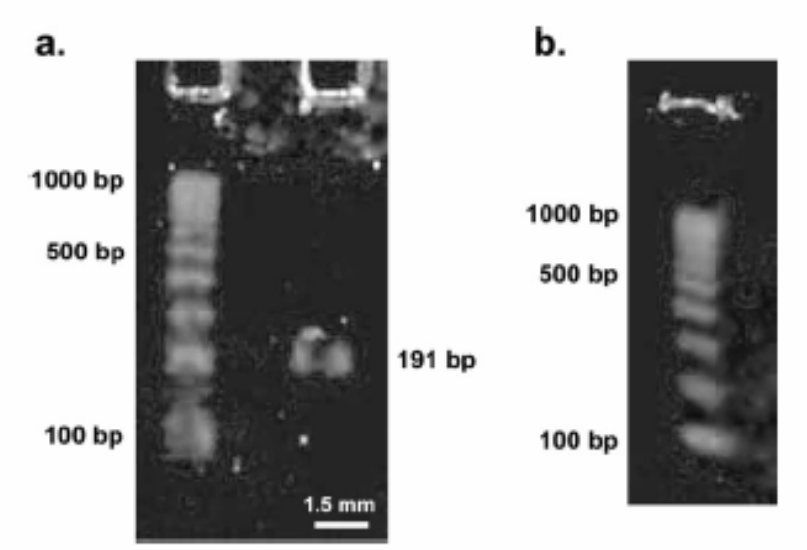

Figure II.4. Separation examples. (a) Sizing of a PCR product using micro-slab gel system (5.25 %T crosslinked polyacrylamide gel, E = 20 V/cm, run time = 15 min). (b) Separation of 100 base pair DNA ladder in a 2% agarose gel (E = 20 V/cm, run time = 20 min) [56].

Despite its simplicity, this micro-slab gel apparatus offers performance comparable to or even exceeding that of similar systems (Table III.1). In terms of sample quantity, the sub microliter volumes required are at least an order of magnitude less than conventional benchtop systems. However, delicate combs are not required during gel casting and sample loading can be performed using standard pipettors. In addition, the ability to employ a wide range of gel formulations identical to those used at the macroscale makes this apparatus readily adaptable to existing laboratory protocols and workflow. The ability to perform separations in 10-20 minutes, depending on the application and required level of resolution, offers the capability of providing results much more rapidly than with conventional benchtop systems. Finally, and perhaps most importantly, detection and imaging of the migrating bands can be achieved using a digital microscope that easily interfaces with most personal computers. Not only is this system orders of magnitude less expensive than conventional laboratory gel documentation systems, it is also portable and allows the separation process to be monitored in real time.

Table II.1 Comparison of conventional and micro-slab gel electrophoresis systems [56].

Feature	Portable	Maurer and Dati[4]	Guttamn's [5]	Convensional
separation platform	25 ×30×0.6 mm	75×25×1 mm	180×75×0.19 mm	250×100 mm
gel volume	0.5 ml		2 ml	20ml
special buffer system	no		yes	yes
buffer	TBE/polyacrylamide or agarose		TBE/agarose or agarose and LPA mixture	TAE/agarose
gel pouring method	pipette	continuous gradient gel system	syringe	directly pouring
comb requried	no	yes	no	yes
cooling system	no	no	yes	no
sample	DNA, PCR product	protein	DNA, PCR product, Protein	DNA, PCR product, Protein
sample amount	0.5~0.8 µl	1~5 µl	0.25 µl	10 µl
sample injection	pipette	capillary	membrane mediated loading	pipette
gel preparation and loading time	5mins		10mins	35mins
separation time	25mins	100 mins	25mins	60mins
gel storage	yes	no	no	no
detection system	blue LEDs and filter bult in a toy computer microscope	post-stain	scanning laser-induced fluorescence/avalanche photodiode detection	post-stain
detection time	immediate		immediate	10 mins~few hours
detection system cost	~100 USD			

3. Conclusion

The micro-slab gel system presented here offers an inexpensive and greatly simplified instrument for performing routine gel electrophoresis experiments. This system combines the benefits of the microslab format (enhanced heat transfer that allows operation at higher electric fields, reduced sample volumes), a novel gel casting technique that eliminates the need for delicate combs to define sample loading wells, and a simple modification to an inexpensive digital microscope to provide the ability to achieve rapid separations with sufficient resolution for use in a variety of analytical applications. The attractive combination of cost and simplicity make this system particularly attractive for use in educational settings as a platform to allow gel electrophoresis techniques to be introduced in a broader range of courses at virtually any level. Currently, the QX3 Plus microscope is available for approximately $60 US, making it possible to assemble a complete system including DC power supply for well under $200 US if an existing PC is used. Because it is even feasible for students to build and operate their own DNA electrophoresis apparatus, a unique opportunity exists to greatly enhance the science and engineering curriculum by stimulating and developing interdisciplinary skills, particularly in areas at the interface between the chemical and life sciences. In addition to electrophoresis, the ability to easily image fluorescently labeled species using various combinations of dyes, excitation wavelengths, and emission filters has wide applicability to expand the observation and study of particle and molecular behavior spanning a wide range of length scales.

CHAPTER III

DNA MIGRATION STUDIES USING A HIGH-SPEED MINIATURIZED FIELD INVERSION GEL ELECTROPHORESIS SYSTEM

In Chapter II, we introduced an inexpensive micro-slab gel electrophoresis device. However, the device can not resolve the DNA fragments size above 10kb. In this chapter, we describe the design and operation of a miniaturized FIGE apparatus which is capable of separation large DNA fragments. A thin 2 x 2.6 cm agarose gel is cast in the device, loaded with a fluorescently labeled dsDNA sample, and subjected to a specified alternating forward and reverse voltage pulse sequence. Since the device is small enough to be placed under a fluorescence microscope, the separation process can be monitored in real time during the course of the run. We investigate separation performance using a 2.5 kb dsDNA sizing ladder incorporating fragment lengths ranging from 2.5 to 35 kb, and demonstrate that separations of this sample can be achieved within 3 hours using very low voltages. The importance of reorientation processes in PFGE suggests that the pulse time and electric field magnitude in each direction are parameters that can be adjusted to optimize separation performance. We investigate this further by using our device to quantitatively study the influence of forward and backward electric field strength, pulse time, agarose gel concentration, and temperature on separation resolution and DNA fragment mobility. Good agreement is observed with comparable studies in literature. We hope that this device design will offer a simple and convenient platform

that may enable future studies of DNA migration in PFGE to be performed quickly and inexpensively.

1. Materials and methods

1.1 Device construction

A miniaturized PFGE device was constructed as shown in Figure III.1. First, an outer buffer reservoir was created by affixing four 8 mm-tall Plexiglas strips in a rectangular arrangement on top of a glass base plate using epoxy. Next, a set of four holes were drilled through each of two smaller 5 mm-tall strips in order to allow two 28 gauge platinum wires to be inserted into each strip and extended along its length (i.e., parallel to the bottom glass surface, approximately 2 cm long). These plastic strips were then mounted to the glass plate using epoxy and separated by a distance of 2.6 cm yielding two independently addressable pairs of horizontal electrodes oriented at 180° with respect to each other. Finally, two additional 5 mm tall strips were placed outside the electrode strips in order to create sidewalls that enclose an area for casting the agarose gel. These sidewalls were not permanently affixed to the lower glass plate so that the gel to could be removed for further analysis if necessary.

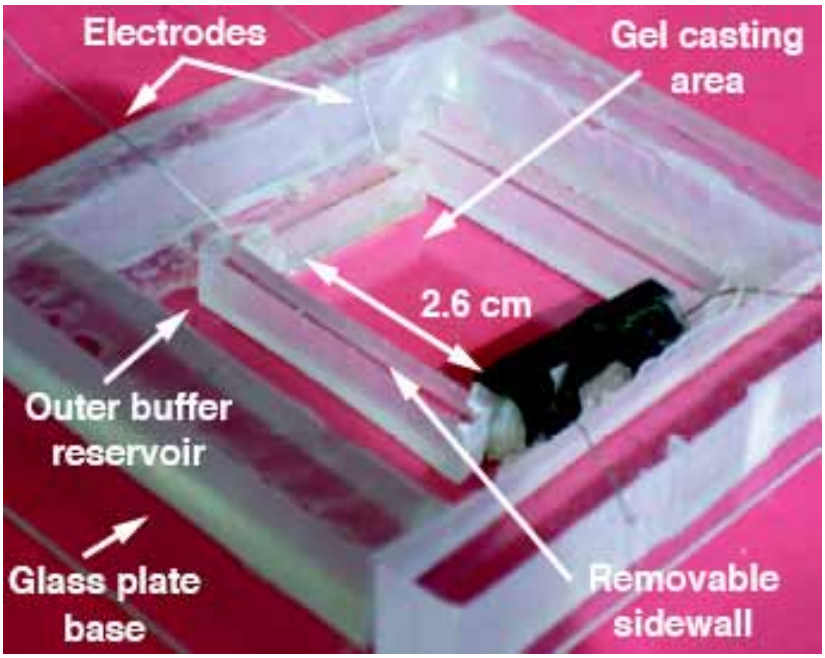

Figure III.1. Photograph of the miniaturized FIGE apparatus. After casting the gel and loading a DNA sample, the entire device is placed on a temperature controlled stage and observed under a fluorescence microscope.

1.2 DNA sample and gel preparation

All separations were performed using a 2.5 kb dsDNA ladder containing fragment sizes ranging from 2.5 to 35 kb (2.5 kb Molecular Ruler; Bio-Rad Laboratories, Inc., Hercules CA). Samples were prepared by mixing 7 μL of the DNA ladder with 3 μL of 100x SYBR-Green fluorescent dye (Invitrogen/Molecular Probes, Carlsbad CA) and 1 μL of 6x Orange Loading Dye solution (Fermentas Inc., Hanover MD). Electrophoresis gels were prepared by dissolving an appropriate amount of agarose powder (Certified Megabase Agarose; Bio-Rad Laboratories, Inc., Hercules CA) in 1x Tris/Boric Acid /EDTA (TBE) buffer solution (Extended Range TBE; Bio-Rad Laboratories, Inc., Hercules CA). Gels were then cast by pipetting a sufficient amount of molten agarose to cover the electrodes mounted on the plastic strips in the casting area (~ 2.5 mL). A homemade plastic comb with 1.6 x 0.5 mm teeth was then inserted to define several loading wells, and the gel was left to cure at room temperature for at least 15 minutes. After curing, a razor blade was used to cut a thin gap between the gel and the electrode wires at each end of the casting area. This step helped to prevent accumulation of bubbles generated at the surface of the platinum wires so that they could not distort the electric field and interfere with the separation. The comb was then gently removed, an 0.8 μL aliquot of the DNA sample mixture was pipetted into each injection well, and 0.5x TBE running buffer solution was added to cover the gel.

1.3 Electrophoresis procedure

Once the gel was cast and loaded, the entire device was placed on a thermally controlled stage whose temperature was regulated using a thermoelectric element. Most runs were performed at 15 °C, unless otherwise indicated. The two sets of electrodes were connected to an Agilent E3646A dual output DC power supply (Agilent Technologies, Inc., Santa Clara CA) and controlled using a custom program written in LabVIEW (National Instruments, Austin TX) that allowed the field direction to be periodically alternated. For the purposes of this study, pulse sequences were chosen such that the electric field in the forward direction was fixed at 7.7 V/cm (20 V applied potential), and both the forward and backward pulse times were set to be equal. Using this setup, a square wave pulsed field profile was achieved by switching between the two outputs of the power supply with a 250 ms zero-field delay between each forward and reverse pulse. Detection was performed by observing the gel using an Olympus SZX-12 fluorescence stereoscope (Olympus America Inc., Center Valley PA) and a CCD-300 cooled CCD camera (Dage-MTI, Michigan City IN).

1.4 Data analysis

Electrophoretic migration was characterized by analyzing digitized images recorded at regular time intervals during the course of the run in order to determine the incremental distance traveled by each migrating band. Displacements were measured in units of pixels, converted to units of distance using a calibration standard, and then used to calculate mobility $\mu = v / E_{avg}$, where v is the migration velocity (i.e., displacement ÷ time) and E_{avg} is the average electric field strength during the pulse sequence. Mobilities computed over several time intervals were then averaged to obtain a final value. Image analysis and calculations were performed using in-house code written in MATLAB (The Mathworks, Inc., Novi MI). Measurements were taken after 3 h of run time unless otherwise noted, and in most cases data from at least three separation runs were averaged.

The digitized images were also used to characterize the ability to distinguish adjacent migrating bands in terms of a separation resolution parameter R defined as the distance between two peaks relative to the sum of their half widths

$$R = (x_2 - x_1)/(w_1 + w_2) \quad \text{(III-1)}$$

where x_i is the position of band i and w_i is the half width of band i. Resolution calculations were performed using an in-house MATLAB code. Briefly, a spatially averaged intensity profile is plotted across a user-defined region spanning multiple bands and the location of the maximum intensity value of each peak is manually selected along

with the minima on either side. The selected peaks are then fitted to a Gaussian distribution function using an optimization procedure, after which the standard deviation σ is calculated. The total width of each peak is defined as 2 σ, yielding an expression for separation resolution of the form

$$R = (x_2 - x_1) / (\sigma_1 + \sigma_2) \quad \text{(III-2)}$$

When plotting data, the calculated resolution between two peaks is assigned to an intermediate average fragment length (e.g., the resolution value between the 10 and 12.5 kb bands is plotted as corresponding to an intermediate fragment size of 11.25 kb at the midpoint between the two bands). We note that this peak analysis is performed on a snapshot of all bands in the gel at a single point in time, as opposed to finish-line detection where data is acquired at a fixed downstream location.

2. Results and discussion

2.1 General observation

We performed an initial series of experiments to test the effectiveness of the FIGE device in separating the DNA fragment sizes present in the 2.5 kb molecular ruler. These studies also provided an opportunity to assess the extent to which separation resolution is enhanced relative to running in a continuous field mode. Fluorescence images representative of typical separation conditions are shown in Figure 2 for runs performed

in under both continuous field and FIGE modes in 45 min and 3 h respectively. In the continuous field separation, bands corresponding to fragments longer than about 12.5 kb experience compression and are difficult to resolve. In contrast, the same bands are clearly distinguishable when the separation is performed under FIGE conditions. It can also be seen that in both cases bands corresponding to the shortest fragment sizes (2.5 and 5 kb) appear much fainter than the others as a consequence of their increased rate of diffusional broadening. Since this rapid decrease in fluorescence intensity makes it difficult to accurately locate and fit the peak shapes with acceptable reproducibility, we do not include separation resolution data for the 2.5 and 5 kb bands. Performing the separation at a higher gel concentration would reduce the rate of broadening and allow fragments in this size range to be better resolved. Finally, we note that the images in Figure III.2 do not show evidence of band inversion effects over this fragment size range for the separation conditions employed in these experiments.

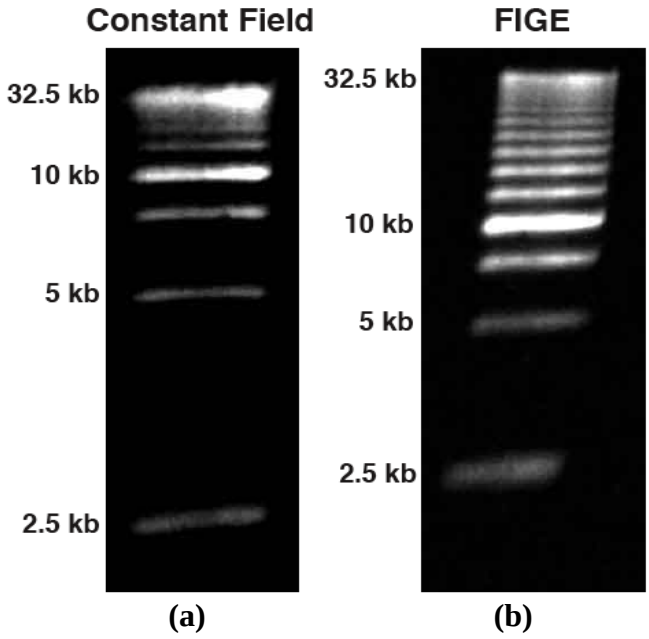

Figure III.2. Comparison of separation results for gel electrophoresis performed in continuous field and field inversion modes (2.5 kb molecular ruler dsDNA sample, 1% agarose gel, T = 15ºC). (a) Continuous field mode, E = 5 V/cm, 45 min run time. Bands corresponding to fragment sizes larger than 12.5 kb experience compression and are difficult to resolve. (b) Field inversion mode with E_{fwd} = 7.7 V/cm, E_{rev} = 2.2 V/cm (α = 3.5), $t_{fwd} = t_{rev}$ = 800 ms, and a 3 h run time. Nearly all bands are resolvable.

2.2 Influence of electric field

Since the magnitude, direction, and timescale of the applied voltage are periodically changed during the course of a separation run, it is useful to define an average electric field in terms of the difference between the forward and reverse components weighted by the time period over which each field component is applied. [16]:

$$E_{avg} = E_{fwd}\left(\frac{t_{fwd}}{t_{total}}\right) - E_{fwd}\left(\frac{t_{rev}}{t_{total}}\right) = \frac{E_{fwd}t_{fwd} - E_{rev}t_{rev}}{t_{fwd} + t_{rev} + t_0} \qquad \text{(III-3)}$$

Here, E_{fwd} and E_{rev} are the electric field magnitudes in the forward and reverse directions; t_{fwd} and t_{rev} represent the pulse time (i.e., the time during which the electric field is applied) in the forward and reverse direction; and t_0 expresses the time interval associated with switching the electric fields between the forward and reverse directions (the electric field strength is zero during this time). We used a value of t_0 = 500 ms to account for the 250 ms zero-field delay between each forward and reverse pulse in our setup. Thus, a positive value of E_{avg} indicates net migration in the forward direction.

First, we investigated the effect of changing the relative magnitudes of applied potential in the forward and reverse directions. These effects were isolated by holding the pulse time in both the forward and reverse directions constant at 800 ms, while the forward potential was maintained at 20 V (E_{fwd} = 7.7 V/cm). The relative magnitudes of forward and reverse potential are expressed in terms of a voltage ratio $\alpha = E_{fwd} / E_{rev}$. It is evident from the data in Figure III.3 that after 3 h of run time, the separation resolution remains

relatively unchanged over the range of α investigated, with the possible exception of the lowest and highest values (1.5 and 6.0 respectively) where resolution is noticeably lower for fragments shorter than 20 kb.

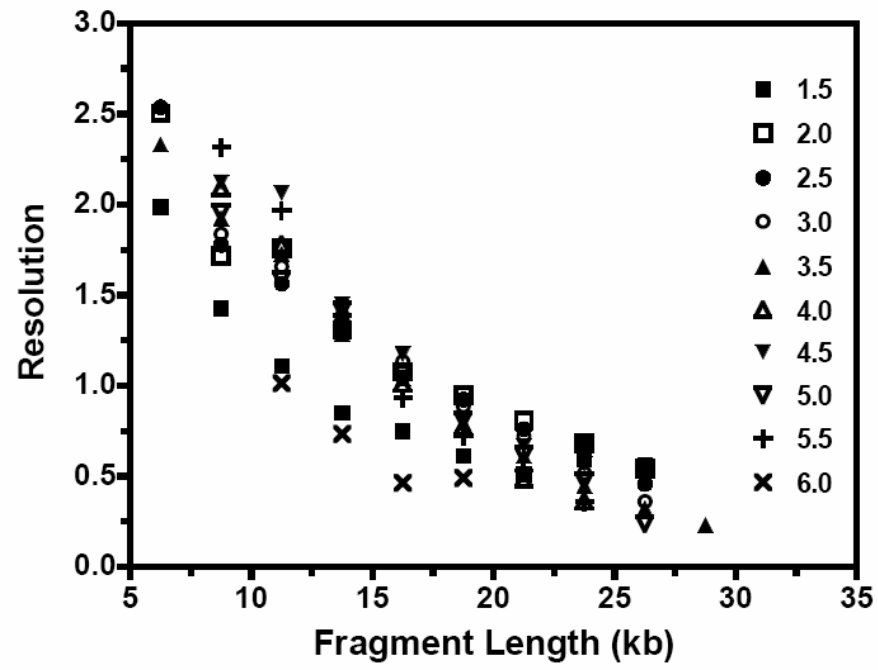

Figure III.3. Effect of changing the ratio of forward and reverse electric field strength ($\alpha = E_{fwd} / E_{rev}$) on separation resolution. The value of E_{fwd} was held constant at 7.7 V/cm with $t_{fwd} = t_{rev}$ = 800 ms. Experiments were performed in a 0.8% agarose gel, at T = 15 ºC for a run time of 3 h.

A second parameter related to the electric field is the pulse time, or the time over which the potential is held constant in each direction. Again, it can be seen that resolution follows the same general trend of decreasing with increasing fragment size as the pulse time is varied over a range of 100 to 1500 ms. (Figure III.4a). When the data are plotted as a function of pulse time, however, the presence of a local maximum (or a mild transition) is evident in the vicinity of 800 ms (Figure III.4b). Although we are not able to offer an explanation for this, we note that in general the pulse duration must be long enough to permit sufficient relaxation and reorientation of the migrating fragments to take place in order to exert an appreciable impact on the size dependence of electrophoretic mobility. In the FIGE mode, these parameters must be chosen so that a net average electric field in the forward direction is maintained. Different electrophoretic mobility and separation resolution behavior are achievable by employing various combinations of these parameters since they each exert an influence over the DNA migration process.

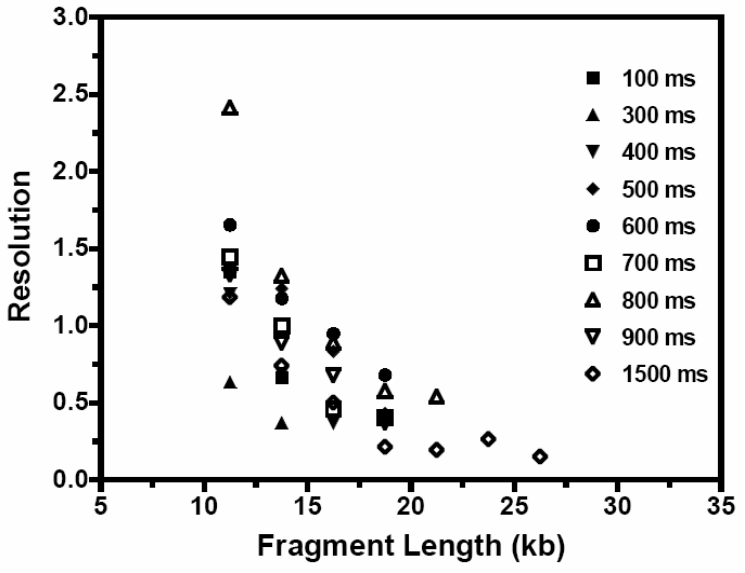

(a)

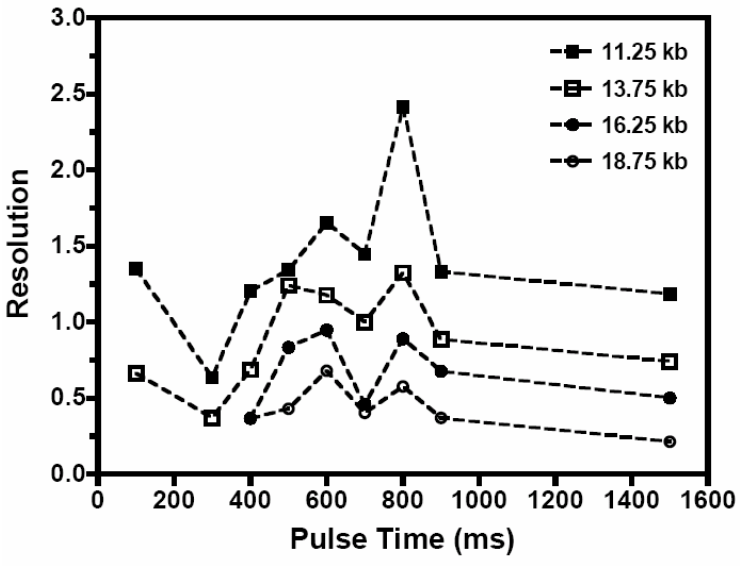

(b)

Figure III.4. Effect of changing the pulse time ($t_{fwd} = t_{rev}$) on separation resolution. (a) Resolution as a function of fragment length, and (b) resolution as a function of pulse time. Experiments were performed in a 0.8% agarose gel, at 15 ºC for 3 hours with E_{fwd} = 7.7 V/cm, E_{rev} = 2.2 V/cm (α = 3.5).

2.3 Influence of temperature

The data in Figure III.5 suggest that separation resolution does not change appreciably as the run temperature is increased from 15 to 20 °C, however a decrease in resolution occurs as the temperature is increased further to 35 °C. In most pulsed field methods, separations are performed at temperatures in the vicinity of 15 °C in order to minimize the effects of diffusional band broadening during the relatively long run times required. In the case of our miniaturized system, these results suggest the possibility of running at higher electric fields to achieve even faster separations because the miniaturized slab gel format promotes more efficient heat transfer to more effectively dissipate the effects of Joule heating. Additionally, the temperature distribution within the thin gel slab is uniformly distributed, allowing direct lane-to-lane comparisons to be made in a straightforward manner.

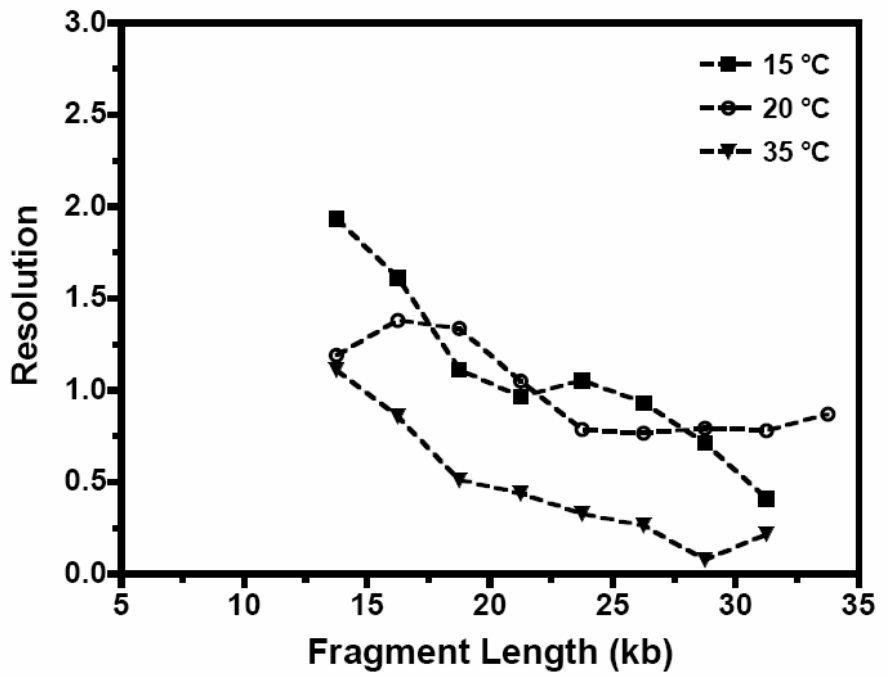

Figure III.5. Effect of temperature on separation resolution. Experiments were performed in a 0.8% agarose gel, at 15 ºC for 3 hours with E_{fwd} = 7.7 V/cm, E_{rev} = 2.2 V/cm (α = 3.5), and $t_{fwd} = t_{rev}$ = 800 ms.

2.4 Influence of gel concentration

Increasing the agarose concentration from 0.6 to 1% is largely accompanied by an increase in separation resolution over the entire range of fragment sizes studied. Increasing the concentration further from 1 to 1.3%, however, results in a slight decrease in resolution, as shown in Figure III.6. This decrease is likely an indication that 3 h of

run time is no longer sufficient to adequately resolve all the bands at this high gel concentration. Thus, a gel concentration in the range of 0.8 to 1% appears to provide optimum resolution under the separation conditions investigated here while maintaining a good balance between performance and run time.

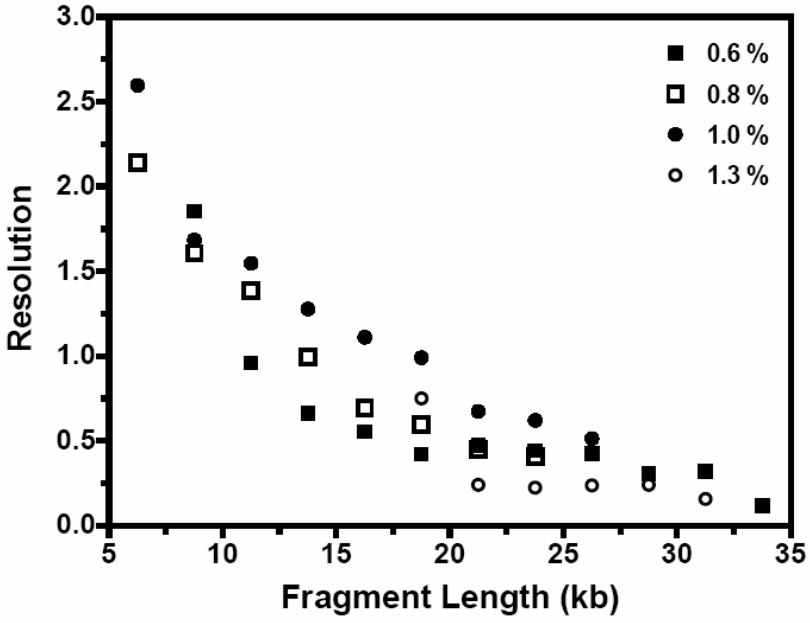

Figure III.6. Effect of gel concentration on separation resolution. Experiments were performed at 15 ºC for 3 hours with E_{fwd} = 7.7 V/cm, E_{rev} = 2.2 V/cm (α = 3.5), and t_{fwd} = t_{rev} = 800 ms.

2.5 Size dependence of electrophoretic mobility

In continuous field electrophoresis, DNA migration is typically expressed in terms of a mobility $\mu = v$ / E, where v is the migration velocity of a given fragment. Since the direction and magnitude of the electric field are periodically changing in a FIGE experiment, we use the average electric field defined in equation (3) to calculate mobility. Figure III.7 shows the size dependence of mobility for DNA fragments in the 2.5 kb molecular ruler, where it is evident that the mobility at a given fragment size does not appear to change significantly over the range of agarose gel concentrations studied.

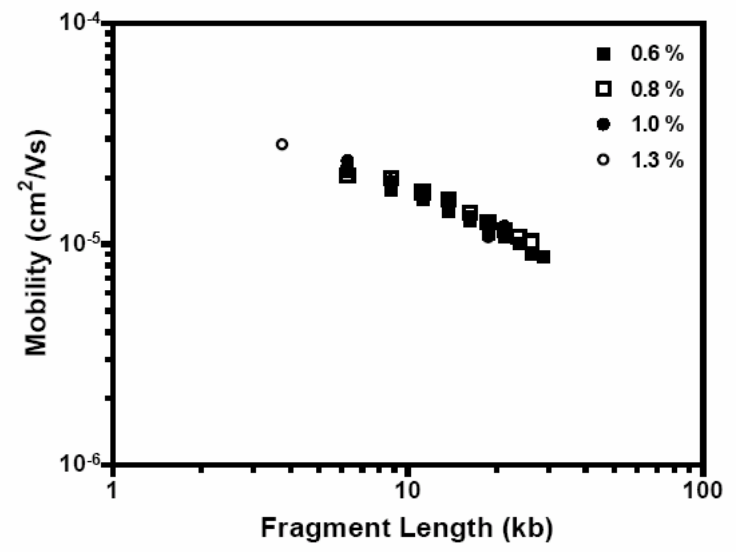

Figure III.7. Double logarithmic plot of mobility versus DNA fragment size at different agarose gel concentrations. Experiments were performed at 15 ºC for 3 hours with E_{fwd} = 7.7 V/cm, E_{rev} = 2.2 V/cm (α = 3.5), and $t_{fwd} = t_{rev}$ = 800 ms.

Furthermore, we observe a mobility scaling close to $\mu \propto N^{-0.5}$ (Table III.1), as opposed to the N^{-1} usually observed in continuous field gel electrophoresis (N can be taken as the fragment length in base pairs). A qualitative explanation for this scaling behavior may lie in the mechanism by which DNA migration is influenced by the applied electric field. In FIGE mode, the DNA molecules are subjected to an electrostatic force that repeatedly alternates between the forward and reverse directions. When the field direction is switched, shorter fragments quickly change their migration direction while larger molecules are able to respond less quickly. In the case of very long fragments, the DNA may only experience partial reorientation without a significant change in migration speed or direction during the reverse pulse. The reversal in migration direction experienced by smaller fragments during a portion of each pulse sequence (under a given set of pulse parameters) would thus be accompanied by a decrease in net forward mobility, thereby reducing the size dependence of the mobility scaling. Choosing combinations of field strength and pulse time that impart a net forward migration approaching that in a continuous field would be expected to yield scalings closer to N^{-1}.

Table III.1. Summary of observed size dependence of DNA fragment mobility for FIGE-mode separations performed in this work and comparison with the results of comparable experiments reported in literature. The figure numbers in the original manuscripts from which mobility scalings have been computed are indicated below the citation of each paper in the first column. *The mobility scaling values in the last column indicate the exponent z associated with the mobility size dependence $\mu \propto N^z$.

Reference	This work	Birren et al. [59]			Sobral and Atherly. [60] (figure 3d-f)	Heller et al. [61] (figure 1c)	Kim & Morris [62] (figure 6)
Measurement	Mobility ($\mu=v / E_{avg}$)	Displacement			Mobility ($\mu=v / E_{avg}$)	Velocity	Mobility ($\mu=v / E_{avg}$)
Format	Miniature slab gel	Slab gel			Slab gel	Capillary	Capillary
Gel	0.6% agarose 0.8% agarose 1.0% agarose 1.3% agarose	1.0% agarose			0.8% agarose 1.0% agarose 1.2% agarose	1% HPC	0.0033% HEC
Buffer	0.5x TBE	0.5x TBE			0.5x TBE	1.0x TBE	0.5x TBE
T (°C)	15	13			13	25	Not stated
Run time	3 h	10h			7-10h	1h	4mins
E_{fwd} (V/cm)	7.7	9	9	6	5.7	243	200
α	5.7	1.5	1.5	1.0	1.0	3.0	2.4
t_{fwd} (ms)	800	800	200	500	1200	10	14
t_{rev} (ms)	800	800	200	200	400	10	14
E_{avg} (V/cm)	4.0	7.5	7.5	6.0	5.7	162	142
Mobility scaling*	-0.53 (0.6%gel) -0.47 (0.8%gel) -0.50 (1.0%gel) -0.47 (1.3%gel)	-0.39	-0.61	-0.58	-0.50 (0.8%gel) -0.47 (1.0%gel) -0.52 (1.2%gel)	-0.18	-0.07

Further insights can be gained by comparing these scalings with those reported in previous investigations of FIGE-based DNA migration (only a subset of the larger body of PFGE literature). We noted earlier that operation under pulsed electric field conditions necessitates defining the electric field strength in terms of an averaged quantity (equation (III-3)). Alternatively, the need to specify an electric field can be eliminated altogether by quantifying DNA migration in terms of displacements or velocities of the migrating bands rather than mobilities. Both of these approaches need to be reconciled, however, in order to make comparisons between our data (expressed in terms of mobility) and the results of previous studies (expressed in terms of velocity or displacement). We attempted to do this by converting displacement and/or velocity data reported in previous publications into mobility values using the electric field and pulsing parameters employed in each study. Migration data was extracted directly from digitized images of data plotted in each publication using GraphClick software (Arizona Software). In this way, we were able to compare the scalings of mobility with fragment size that we observed with what has been reported in previous studies. These results are summarized in Table III.1, where we have considered only a subset of PFGE literature involving FIGE-based separations of double-stranded DNA fragments in a size range comparable to that used in our experiments.

Birren et al. investigated electrophoresis of linear dsDNA fragments in terms of relative migration distance using three different sets of pulsing parameters with values of E_{avg} in the vicinity of 6 – 8 V/cm [59]. Under conditions where E_{fwd} was greater than E_{rev} (α =

1.5) and $t_{fwd} = t_{rev}$, a stronger size dependence of electrophoretic mobility was observed at longer pulse times. When E_{fwd} was set equal to E_{rev} ($\alpha = 1$) with $t_{fwd} > t_{rev}$, a scaling of $\mu \propto N^{-0.58}$ was observed, roughly in between the other two values. Sobral and Atherly investigated FIGE migration of both linear and supercoiled DNA ladders at agarose concentrations of 0.8, 1.0 and 1.2% with pulse times varying over a wide range from 0.12 to 120 s [60]. Considering the case of linear dsDNA with fragment sizes in the range of 2 – 12 kb and run conditions closest to those employed in our experiments (i.e., $E_{fwd} = E_{rev} = 5.7$ V/cm, $t_{fwd} = 1.2$ s, $t_{rev} = 0.4$ s) yields mobility scalings very close to $\mu \propto N^{-0.5}$ at all three agarose concentrations, consistent with our observations.

FIGE-mode mobility studies have also been performed in capillary electrophoresis systems. These systems are of interest due to their considerably shorter run times (generally less than one hour) resulting from the ability to apply higher electric fields than are possible in slab gels instruments. Different techniques are also used to detect the migrating bands, with slab gel instruments employing post-stain detection with intercalating dyes while capillary methods operate in a finish-line detection mode whereby dye is present in the running buffer and binds to the DNA fragments during the course of the separation. Heller et al. investigated migration of linear dsDNA fragments in the 100 – 10000 bp size range in a 1% HPC sieving matrix using pulse conditions corresponding to $E_{fwd} = 243$ V/cm and $E_{rev} = 81$ V/cm ($\alpha = 3$) and $t_{fwd} = t_{rev}$, and observed a scaling of $\mu \propto N^{-0.18}$ [61]. Kim and Morris also investigated FIGE-based separations of linear dsDNA fragments in the 8.3 – 48.5 kb size range using a capillary

system containing ultradilute HEC and PEO sieving gels [62]. Remarkably, a level of resolution sufficient to distinguish all fragments in the DNA sample could be achieved in run times of less than 4 min, although mobilities were found to be weakly size dependent under these conditions with $\mu \propto N^{-0.07}$. A strong dependence on pulse time was also observed whereby mobilities exhibited a weak but uniform size dependence under some pulsing conditions, but developed a much stronger size dependence for fragment sizes between about 20 – 30 kb at other pulse times.

Two important observations can be made from the comparison between our data and the results of previous studies. First, the scalings of mobility with fragment size that we observe (e.g., $\mu \propto N^{-0.5}$) appear to be generally consistent with those previously observed in FIGE-based separations performed in slab gel instruments under similar conditions. Interestingly, the experiments of Bierren et al. with $t_{fwd} = t_{rev}$ incorporate pulse parameters most closely matching ours (in a 1% agarose gel) but yield a mobility scaling of $\mu \propto N^{-0.39}$ which deviates somewhat from our observations, possibly attributable to the different values of α employed or the switching delay t_0 included in our pulse sequence. Secondly, there is a significant difference in mobility scaling between experiments performed in capillary instruments as compared with slab gels, with the capillary data exhibiting a much weaker size dependence. This may be a consequence of the higher electric fields employed in the capillary experiments (about 100 times those used in slab gels) that would promote a more fully extended DNA conformation during a greater fraction of the total pulse time. These high fields,

however, are also accompanied by considerably faster pulse times that may counteract these effects somewhat. It is likely; however, that separation performance could be improved by further optimization of pulsing parameters.

3. Summary and conclusion

We have described the design, construction, and operation of a miniaturized PFGE device and have demonstrated its effectiveness for performing rapid FIGE-mode separations of dsDNA fragments in the 2 – 35 kb size range. In addition to faster run times, the compact design offers advantages of reduced reagent consumption and improved heat transfer, potentially making it possible to run at higher electric fields. We then used this device to investigate the relationship between electrophoretic mobility and DNA fragment size, and found results in general agreement with previous studies in slab gel systems. These comparisons also highlight a lack of systematic experimental data spanning a broad range of operating conditions. These data are of critical importance in order to fully characterize and understand the complexities of DNA migration in pulsed field systems, and ultimately to enable rational selection of optimal separation parameters (e.g., combinations of field strength and pulse time). This deficiency has been due in large part to the lack of a convenient and accessible experimental platform that would allow careful study of these phenomena. We hope that instrumentation like the miniature apparatus we introduce here will help address this need and stimulate future studies in this area.

CHAPTER IV

SINGLE MOLECULE OBSERVATION ON DNA-QUANTUM DOT CONJUGATES DURING GEL ELECTROPHORESIS

Quantum dot nanoparticles have emerged as a powerful tool for fluorescent labeling of biomolecules. In this chapter, we investigate gel electrophoresis of DNA–quantum dot conjugates at single molecule level in order to determine their influence on separation performance. Conjugates were constructed by complexation between streptavidin functionalized quantum dots and end-biotinylated lambda DNA. The attached quantum dots could then be further modified through binding interactions with biotinylated single-stranded DNA primers. By using primers of various lengths, this construction allowed both the size and charge density of the quantum dot complex at the ends of each lambda DNA molecule to be precisely manipulated. A miniaturized agarose gel electrophoresis system was also constructed in order to enable visualization of the migrating fragments using a fluorescence microscope.

1. Materials and methods

1.1 Device construction

In order to allow the gel electrophoresis process of DNA quantum dots conjugates be directly imaged within the working distance of the microscope's 100x oil immersion objective, agarose gel had to be cast in a thin layer. Briefly, the gel was cast between the glass plate and a coverslip. Two parallel strips of aluminum tape were affixed approximately 30 mm apart on the surface of to a glass plate to serve as the electrodes. Next, a 10 μL aliquot of molten agarose containing the DNA sample to be imaged was pipetted in between the aluminum strips, and a coverslip was carefully pressed down on top to allow the agarose to flow and fill the entire gap between electrodes. The outside perimeter of the coverslip between electrodes was then sealed with clear acrylic nail polish to reduce evaporation, but the aluminum strips were left exposed so that bubbles could escape and fresh electrophoresis buffer could be periodically applied. Figure IV.1 is the simple schematic of gel casting process.

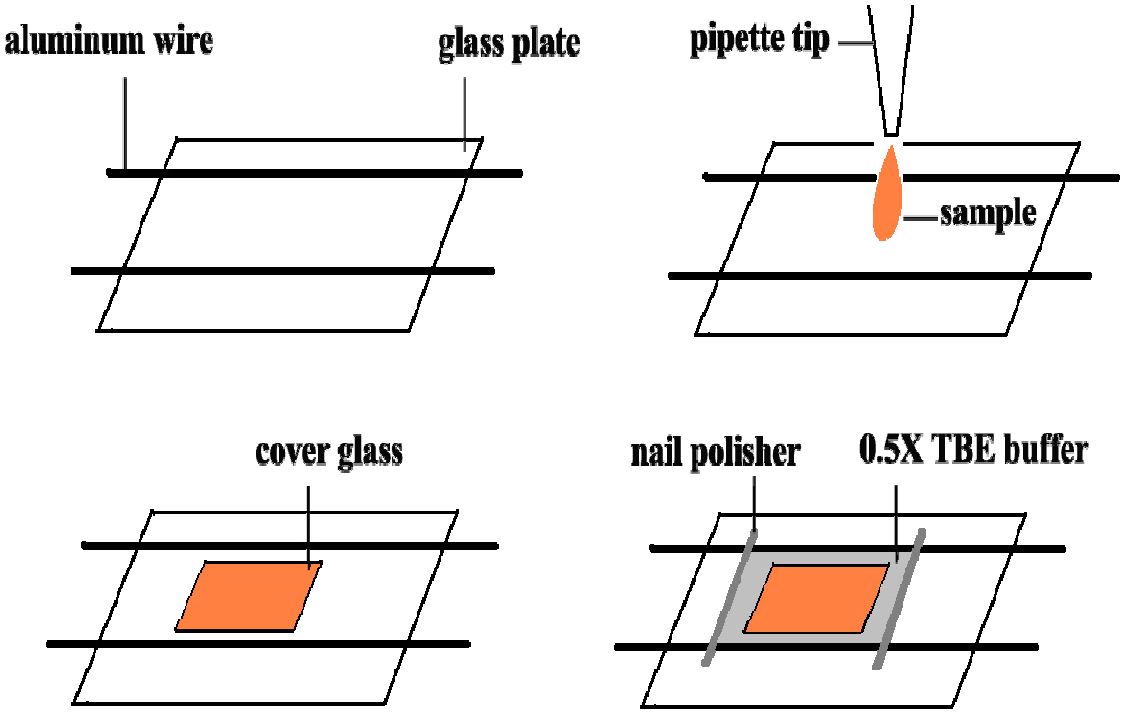

Figure IV.1. Schematic of gel casting process for single molecule studies of DNA migration in agarose gels.

1.2 Sample preparation

Construction of DNA quantum dots conjugate relies on the streptavidin-biotin interaction [63], the strongest known non-covalent biological interaction (Ka = 10^{15} M^{-1}) between protein and ligand. There are two steps to prepare DNA quantum dots conjugates. First, the 12 base overhang at each end of λ DNA molecule was biotinylated, after which, striptavidin functionalized quantum dots were attached to form the conjugates.

To biotinylate the DNA, biotinylated dCTP was added to fill in the overhang of λ DNA. A 50 µl reaction was prepared, by adding 5 µl of 10X polymerase buffer (New England BioLabs), 25 µl of sterile water (New England BioLabs) and 20 µl λ DNA (New England BioLabs). In order to break up the sticky ends of λ DNA the mixture was heated to 65° C for seven minutes in the thermal cycler. Then 100X molar excess of dATP, dGTP, dTTP and biotinylated dCTP (Invitrogen, Inc.) was added to the mixture. Along with 0.5 µl of Klenow DNA polymerase was added in to start the reaction to fill the 5' overhang. The reaction was carried on at room temperature for 30 minuets. Finally, excess EDTA (ethylenediaminetetraacetic acid) was added in to stop the reaction. The reaction products were purified using drop dialysis (0.025 µm pore size, Millipore, Inc.) and the concentration was measured by absorbance at 260 nm using a NanoDrop ND-1000 spectrophotometer.

Next, the purified biotinylated λ DNA and streptavidin functionalized quantum dots (Qdot 605 from Invitrogen; emission wavelength is 605 nm) were diluted to a proper concentration respectively, making the concentration of quantum dots 100X excess than that of λ DNA. This is to ensure each DNA molecule binds (one at each end). The λ DNA and quantum dots were mixed well and incubate for 5 mins at room temperature to allow enough time for the conjugates to form. To label the DNA molecules, 3% YOYO dye was added to the mixture, which gave optimized fluorescence images with minimum background. 0.1mg/ml glucose oxidase, 0.018 mg/ml catalase and BME (β-

mercaptoethanol) were also added, in order to minimize photo bleaching of the fluorescent dye.

The conjugates could be further modified with biotinylated single-stranded DNA primers. We used primers with lengths of 10, 20, 30, and 40 bases (Integrated DNA Technologies) as a means to discretely alter the amount of negative charge concentrated at the quantum dots on the ends of the larger DNA molecule. Primers were first heated up to 65 ºC for 10 minutes to denature. Then 100X excess biotinylated primers was added to the conjugates mixtures and incubate for 5 minutes on bench before adding the fluorescence dye. Because each quantum dot has multiple bonding sites, the excess primers ensure every quantum dot can be fully covered by primers.

Upon completion of all modifications, we verified the formation of monodisperse populations of DNA, quantum dot, and primer conjugates by gel electrophoresis. A distinct band associated with the conjugate served as an indication that the binding process yielded a homogeneous product (e.g., no significant fractions of quantum dots bound to multiple λ DNA fragments, etc.).

1.3 Gel casting and electrophoresis

Fluorescently labeled DNA conjugates were mixed with an aliquot of 0.8% agarose gel. Agarose gel was stored in a 55°C incubator, in order to keep its liquid state. Before mixing with DNA conjugates, the agarose gel was taken out and put on the bench for a while in order to avoid degrading the constructed conjugates by increasing the temperature too much. Gel casting should be done in a short time, so that the gel won't harden inside the pipette tip.

The loaded and assembled electrophoresis device was placed on the stage of a Zeiss Axioskp 2 microscope and the DNA molecules were imaged using a 100x oil immersion objective under mercury arc illumination with a GFP filter set. Images were acquired using a Hamamatsu C-2400 SIT camera and digitized for analysis. An electric field of 14 V/cm was applied for continuous field electrophoresis study. DNA migration behavior under pulsed field conditions was studied as well. A power amplifier (TREK, model 603) and a function generator (WAVETEK, 5MHz sweep generator) were used to generate pulsed pattern; so that field inversion and 120 degree pulsed field electrophoresis can be achieved.

1.4 Data analysis

In order to quantitatively characterize the difference in motion between bare λ DNA and λ DNA nanoparticle conjugates during gel electrophoresis, three electric field conditions were applied: continuous field, 120 degree pulsed field and field inversion, the extension length and the entanglements probability were measured. For extension length, an in-house MATLAB code was created that generates a circle enclosing the area occupied by each DNA molecule. The maximum diameter of the circle represents the maximum extension length of DNA molecules, which is demonstrated in Figure IV.2 Using this method, we tracked an ensemble of individual λ DNA–quantum dot conjugate molecules over time the maximum extension lengths they experienced during migration. The resulting data can be plotted as a histogram of maximum extension lengths. For the measurement of entanglements, the number of hooked situation was counted over more than 600 total movements. The ratio of the entangled and total movements represents the level of entanglements.

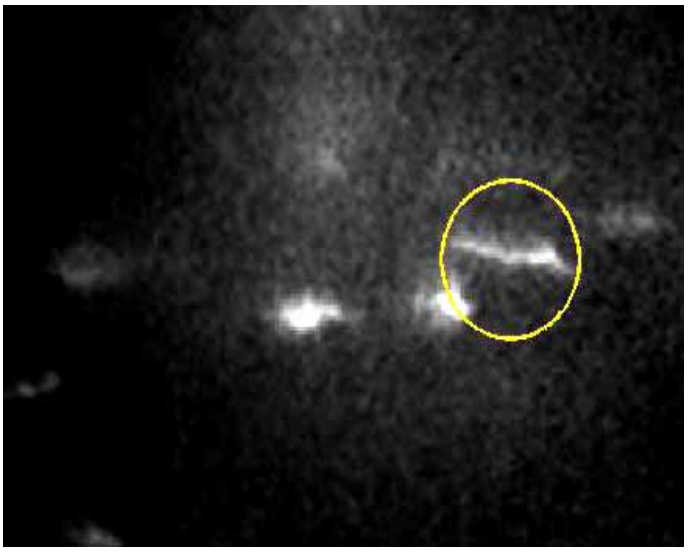

Figure IV.2. Example of in-house Matlab program. The circle generated by in-house Matlab program is used to evaluate the length of single DNA molecule during electrophoresis.

A calibration target was imaged under the same conditions to allow length scales in units of pixels to be converted to distance units. An ensemble of 25–50 molecules and around 600 movements was selected for quantitative analysis. The manual nature of the analysis process made it very time consuming to study larger sample sizes.

2. Results and discussion

2.1 Qualitative observations

The tables in the Appendix summarize the range of DNA conformations we observed during electrophoresis. These results suggest that the DNA molecules adopt different conformations under gel electrophoresis when their charge to size is changed by modifying the ends with both electrically neutral quantum dots and charged quantum dots (complexed with primers). Once neutral quantum dots are attached at both ends of the DNA molecule, electrostatic forces may become focused in the middle of the chain instead of at the ends, possibly causing the middle of chain to move ahead, as an alternative to the head first motion observed in un-modified λ DNA molecules. When the quantum dots were bonded with the 20bp-Cy5 primer, both charge and size are increased at the two ends of the chain, resulting in easy hooking and slow releasing. Since the center of the chain moving ahead was also observed in this case, it could be an evidence that the increasing size is dominant than the increasing charge.

Initial visualization experiments were performed using both bare λ DNA and DNA-quantum dots conjugates under continuous field gel electrophoresis. These results show that the DNA molecules adopt very different conformations under gel electrophoresis when their charge and/or size characteristics are altered by modifying the ends with both weakly charged quantum dots and negatively charged quantum dot-primer complexes.

Middle-move-ahead conformation was captured, as shown in Figure IV.3. The dynamics was altered as single-stranded primers were attached to the quantum dots, which increased the net negative charge at both ends of the migrating DNA molecule. It took them longer time to get released once they got trapped by gel fibers (Figure IV.4).

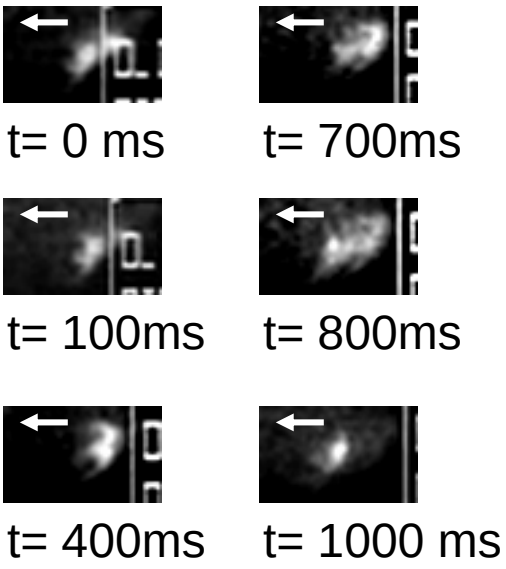

Figure IV.3. The demonstration of middle-move-ahead movement of a λ DNA-quantum dot conjugate in continuous field gel electrophoresis. Electrophoresis was performed in 0.8% agarose gel under E=14 V/cm.

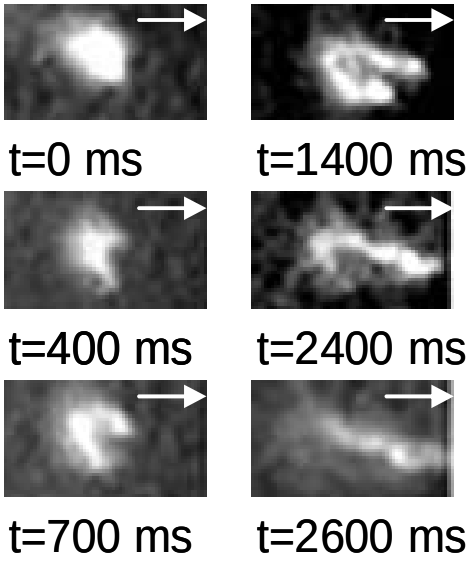

Figure IV.4. Slow releasing of the primer decorated λ DNA-quantum dot conjugate in continuous field gel electrophoresis. When DNA molecule was hooked by gel fibers, a "U" shape was formed. And both arms of the "U" were extending forward at approximately the same speed, which causes the long "U" shape period. Electrophoresis was performed in 0.8% agarose gel under E=14 V/cm.

The visualization of single molecule electrophoresis was also preformed under 120 degree pulse field and field inversion gel electrophoresis. Images were consistent with what we observed under continuous field conditions. Middle-moving-ahead movement occurred more often for λ DNA-quantum dots conjugate particularly during 120 degree pulse field gel electrophoresis. Figure IV.5 is a series of images showed how the middle-moving-ahead movements of λ DNA-quantum dots conjugates undergo in continuous field, field inversion and 120 degree pulsed field gel electrophoresis.

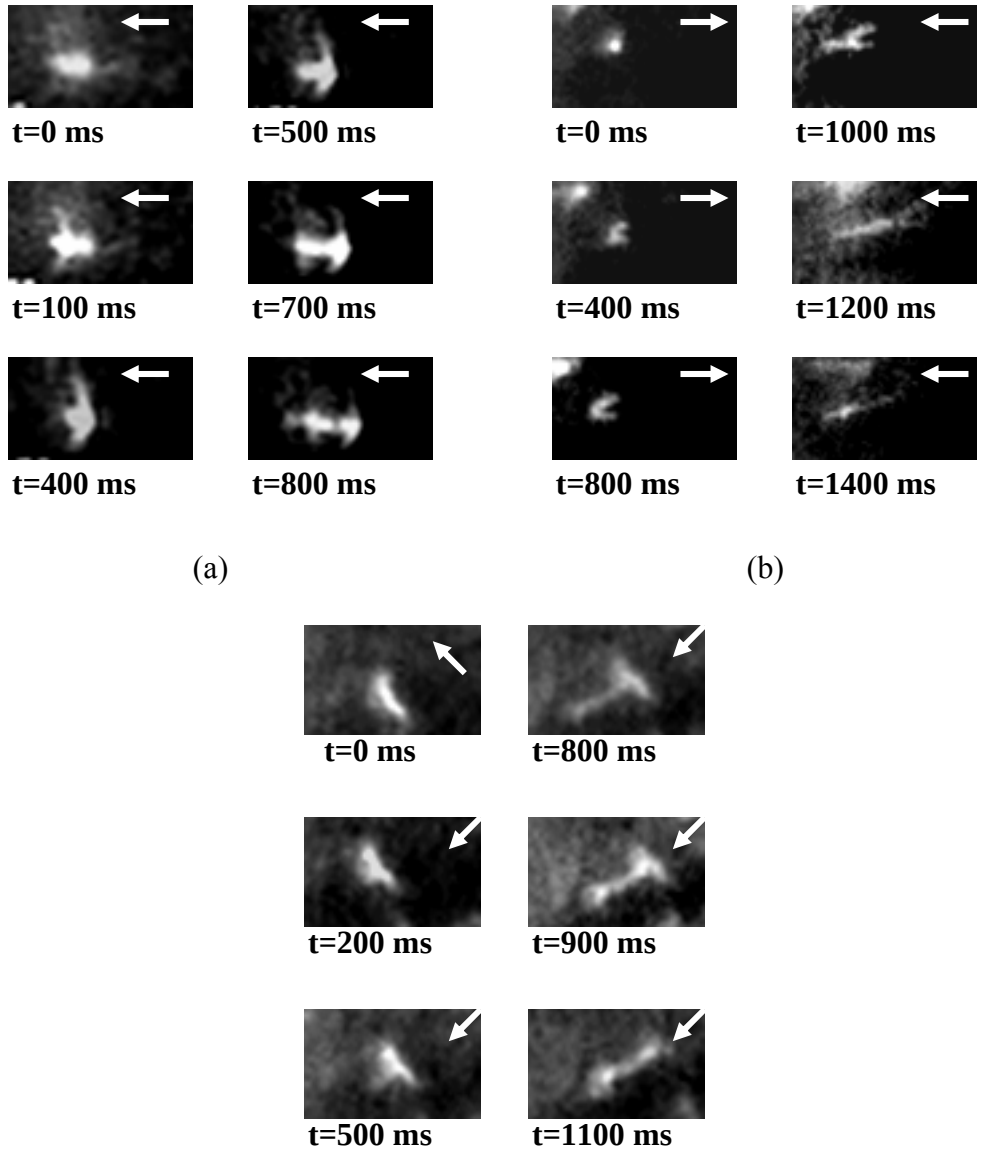

Figure IV.5. Example of middle-move-ahead conformation. Middle-move-ahead conformation of λ DNA quantum dots conjugate in (a) steady field gel electrophoresis, E=20 V/cm (b) FIGE. Qdots were modified by attaching 20 bp primers, E_{fwd}=25 V/cm, E_{rev}=8 V/cm, t_{fwd}=t_{rev}=2s (c) 120 PFGE, E=30 V/cm, t=5s. 0.8% agarose was used in all there fields.

2.2 Quantitative measurement

2.2.1 Extension length

We compared the histograms of extension length of bare λ DNA, λ DNA-quantum dot conjugates and λ DNA with primers attached to the quantum dot complex under continuous field, 120 degree pulse field and field inversion (Figure IV.6). For the pulsed field experiments, we chose pulse times long enough for DNA molecules to re-orientate to the new field direction, and the measurements were taken when electric field was switched. The comparison shows that λ DNA-quantum dot conjugates display the longest extension length in both continuous field and 120 degree pulsed field, yet, shortest length in field inversion. This could be because weakly charged quantum dots may become more easily to be hooked on gel fibers. The reduced random reorientation at the hooked end caused by the weak charge, may then make it more difficult to be released while the other end continues to move forward, resulting in longer extension in continuous field. Figure IV.7 shows the snapshots of the extension behavior of weakly charged quantum dots-λ DNA conjugates.

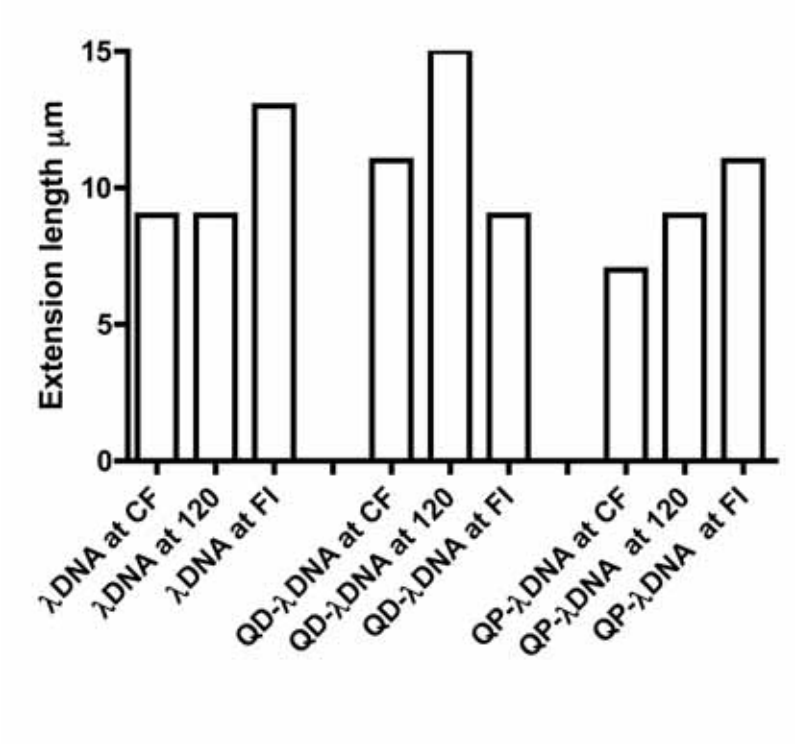

Figure IV.6. The comparison of histograms of the extension length. The extension length of bare λ DNA, λ DNA-quantum dots conjugates, and the primer decorated λ DNA-quantum dots conjugates were measured in continuous field, field inversion and 120 degree pulsed field gel electrophoresis. The electric fields were for steady field E=13V/cm; for 120 degree pulsed field E=15V/cm in both direction; and for field inversion pulsed field E_{fwd}=28V/cm, E_{rev}=8.5V/cm. In the plot, lambda, lambdaQ, lambdaQP represent bare λ DNA, λ DNA quantum dots conjugates, and 20bp(Cy5) primer decorated λ DNA-quantum dots conjugates respectively. And CF, FI, 120 correspondingly represents continuous field, field inversion and 120 degree pulsed field gel electrophoresis.

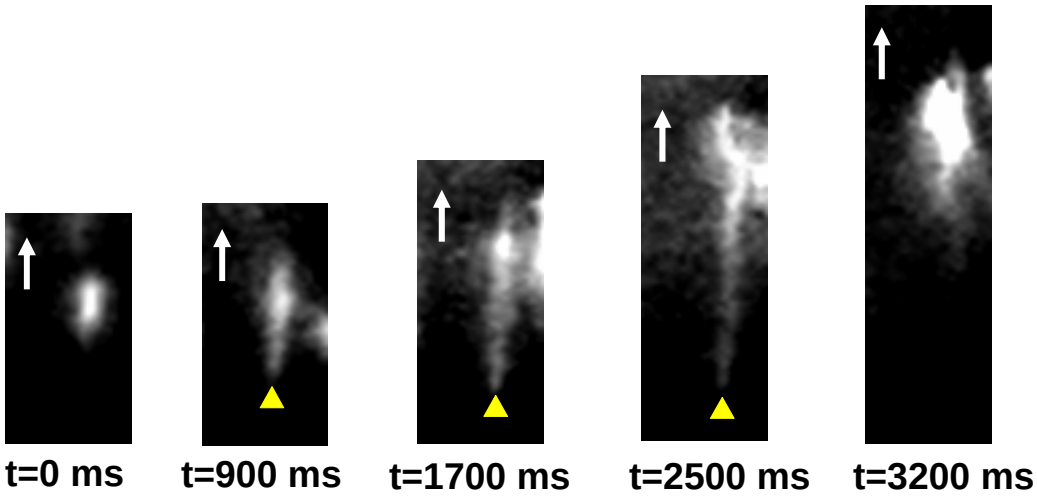

Figure IV.7. Example of extension. In steady field gel electrophoresis, λ DNA-QD conjugate was stretched to about 22 μm under *E*=13 V/cm. One end of DNA chain was fixed while the other end was moving forward.

In 120 degree pulsed field, the electric field angle forces QD-DNA to adopt longer contour in order to align to the electric field. But in field inversion field, DNA molecules are aligning parallel to the electric field responding to two horizontal electric forces. The electric force acting on the primer-decorated QD is stronger than it on the weakly charged QD at the end of the DNA due to the extra net charge from the primers, resulting in the longer extension length of primer-decorated QD-DNA conjugates. Both QD and primer-decorated QD-DNA conjugates may have longer reorientation time than bare λ DNA, but the frequently switched the electric fields may also not allow the conjugates to extend fully. Therefore the extension length of bare λ DNA in field inversion pulsed field is statistically the longest.

2.2.2 Entanglement

We also calculated the entanglement probability of bare λ DNA, λ DNA-quantum dot conjugate and primer decorated λ DNA-quantum dot complex under continuous field, 120 degree pulsed field and field inversion pulsed field gel electrophoresis(Figure IV.8).

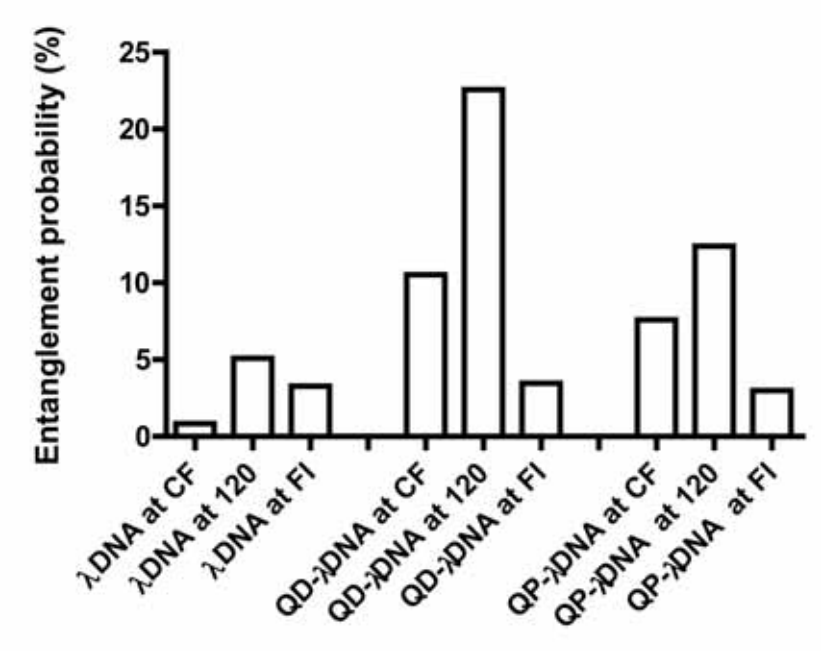

Figure IV.8. The comparison of histograms of the entanglement probability. The entanglement possibility of bare λ DNA, λ DNA-quantum dots conjugates, and the primer decorated λ DNA-quantum dots conjugates were measured in continuous field, field inversion and 120 degree pulsed field gel electrophoresis. Electric fields were for steady field E=13V/cm; for 120 degree pulsed field, E=15V/cm in both direction; and for field inversion pulsed field, E_{fwd}=28V/cm, E_{rev}=8.5V/cm. In the plot, lambda, lambdaQ, lambdaQP represent bare λ-DNA, λ-DNA quantum dots conjugates, and 20bp(Cy5) primer decorated λ-DNA quantum dots conjugates respectively. And CF, FI, 120 correspondingly represents continuous field, field inversion and 120 degree pulsed field gel electrophoresis.

The results show that bare λ DNA has the fewest entanglements in continuous field gel electrophoresis. However, the entanglement probability of λ DNA in pulsed field, including 120 degree pulsed field and field inversion, increases, and especially in the 120 degree pulsed field. This support the idea that increased gel fiber-DNA interaction helps to separate large DNA fragments (> 20kb). This is why the separation of large DNA can be achieved in pulsed field gel electrophoresis, but not in continuous field gel electrophoresis. QD-λ DNA conjugates may have the highest entanglement possibility, particularly in 120 degree pulsed field, because the end attached quantum dots are more easily hooked on gel fibers and their neutral charge make them even difficult to release. A series of interesting images of QD-λ DNA conjugates were also captured, in which "M" conformations were observed shown in Figure IV.9. This special conformation is the example of the strong entanglement of QD-λ DNA conjugates in gel electrophoresis.

When additional negative charge is added at each end of the DNA molecule, the ends can more easily move to find ways of escaping from hooking. Thus, λ DNA with primers attached to the quantum dot complex shows less probability of entanglements than λ DNA-quantum dot conjugate.

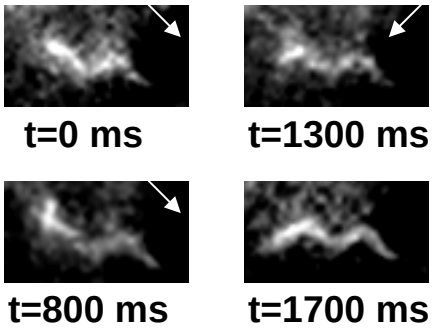

Figure IV.9. Example of 'M' conformation. In 120 PFGE, λ DNA-QD conjugate showed an 'M' conformation. The right end of the chain was hooked by gel fibers, and the left end moved up and down with the electric field. However, the whole chain can never escape the hooking situation no matter how the left end moved. Experiment conditions are E=30 V/cm, t=1s, 0.8% agarose.

It is interesting to notice that in continuous field, both λ DNA-quantum dot conjugate and the primer decorated λ DNA-quantum dot complex released slowly from hooking. However, the mechanisms of these two slow release modes appear to have different physical origins. For λ DNA with quantum dots, once a molecule becomes hooked by a gel fiber, its two arms continue to move in the field direction trying to escape the entanglement. However the weakly charged quantum dots restrict motion of the chain ends that would otherwise promote release. On the other hand, the free end continues to move forward, often resulting in nearly full extension of molecule. For primer decorated λ DNA-quantum dot conjugates, the charge density is greater at the ends. Thus, once it becomes hooked by a gel fiber both ends continue to move forward causing it to remain in a hooked conformation for a longer time.

2.2.3 Reorientation time

Based on the experiments, we found that the characteristics of bare λ DNA and its conjugates demonstrated dramatic differences in 120 degree pulsed field. Therefore, a further investigation on the reorientation time of bare λ DNA and its conjugates were preformed under 120 degree pulsed field gel electrophoresis. A histogram in Figure IV.10 was plotted according to which bare λ DNA took the shortest time to re-align to the new coming field, while λ DNA-quantum dot conjugates need the longest time to re-orientate. This may be due to the extra resistance produced by attaching QD and primer-

decorated QD to the ends of DNA. This result is consistent with the extension length measurements.

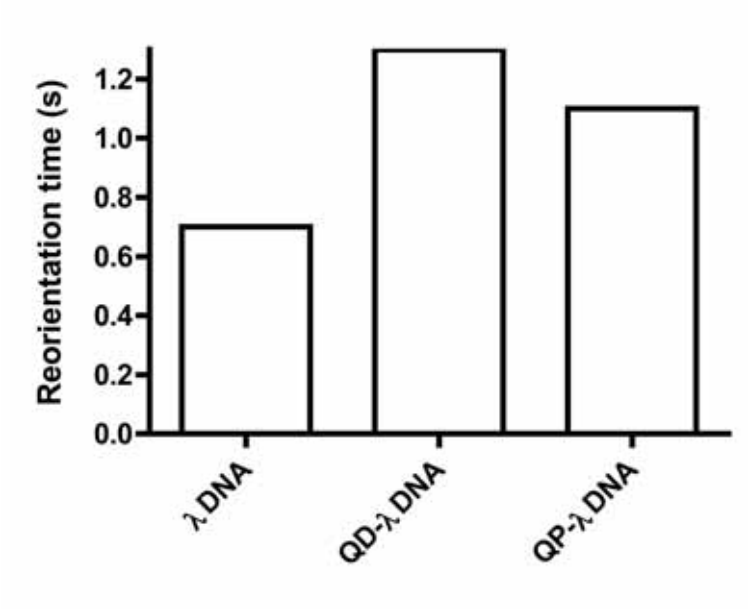

Figure IV.10. The comparison of the histograms of the reorientation time. The comparison of the histogram of reorientation time of bare λ DNA, λ DNA-quantum dot conjugate and primer decorated λ DNA quantum dot complex under 120 degree pulsed field (E=15V/cm in both direction, frequency=0.2 hz). In the plot, lambda, lambdaQ, lambdaQP represent bare λ DNA, λ DNA-quantum dots conjugates, and 20bp(Cy5) primer decorated λ DNA-quantum dots conjugates respectively.

2.2.4 The extension length between different primer-decorated QD-DNA

Finally, the extension length between different sized primer-decorated QD-λ DNA was studied using an in-house Matlab program and a histogram was generated as shown in Figure IV.11. According to the data, 30bp-primer-decorated QD-λ DNA and 40bp-primer-decorated QD-λ DNA have slightly longer extension length, comparing with 20bp-primer-decorated QD-λ DNA and 20Cy5-primer-decorated QD-λ DNA. The increased primer length brings more charges to the ends, where the electric force may be stronger. When Cy5 molecules are attached to the 20 bp primer, the size increased with a decrease in charge, so the extension length of 20Cy5-primer-decorated QD-λ DNA was lower than 20bp-primer-decorated QD-λ DNA. 40bp-primer-decorated QD-λ DNA dose not show obviously higher extension lengths than 30bp-primer-decorated QD-λ DNA, possibly because the increased charge is compatible with the increased size by adding 40 bp primers. Also, it may be that when primer size reaches certain point, the binding sites on the QD may become blocked by the size and the random movements of the primer.

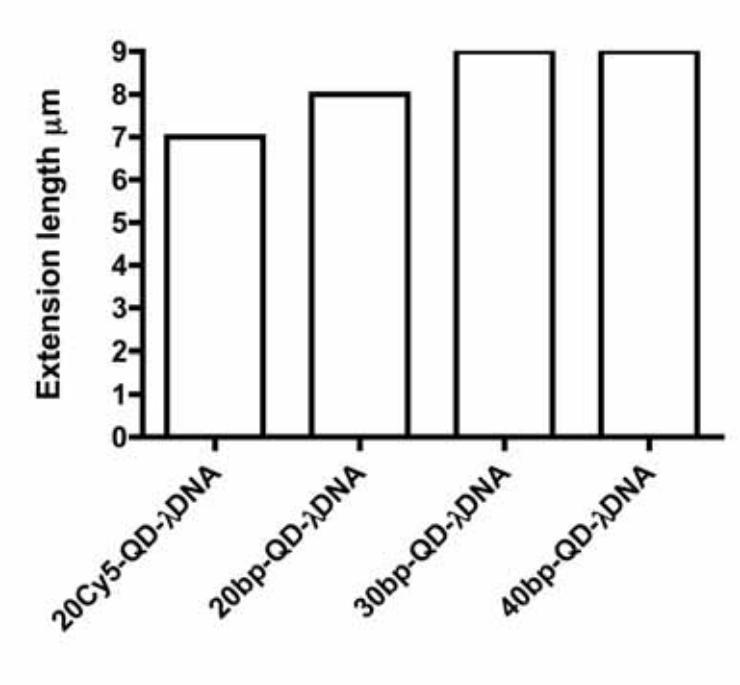

Figure IV.11. The comparison of the histograms of the extension length. Λ DNA-quantum dots conjugates were attached with different sized primers (20 bp primers, Cy5 molecule attached 20bp primers, 30bp primers and 40bp primers) under steady field gel electrophoresis (*E*=13V/cm). Here, lambdaQ-20bp-Cy5, lambdaQ-20bp, lambdaQ-30bp and lambdaQ-40bp represent 20 bp (Cy5) primer decorated λ DNA-quantum dots conjugates, 20 bp primer decorated λ DNA-quantum dots conjugates, 30 bp primer decorated λ DNA-quantum dots conjugates, and 40 bp primer decorated λ DNA-quantum dots conjugates respectively.

3. Conclusion

These preliminary studies show that adding primer decorated quantum dot complexes to λ-DNA can change its electrophoretic mobility. Observations of single molecules reveal that the DNA molecules exhibit different conformations and migration dynamics that depend on the relative size and charge density of the complexes. This suggests that DNA-quantum dot complexes provide a mechanism to manipulate the nanoscale interactions between the DNA and the sieving gel that in turn define overall separation performance.

CHAPTER V

SEPARATION OF DNA-QUANTUM DOT CONJUGATES IN HIGH-SPEED MINIATURIZED FIELD INVERSION GEL ELECTROPHORESIS SYSTEM

In chapter IV, we have demonstrated the electrophoretic behavior of quantum dot-DNA conjugates at the single-molecule level. When end-labeled with quantum dots and different sized primer decorated quantum dots, the extension length, entanglement probability, and reorientation time of λ DNA showed different behavior under continuous field, field inversion, 120 degree pulsed field conditions. In this chapter, we describe construction of a DNA ladder whose fragments are end-labeled with quantum dots and primer-decorated quantum dots. Electrophoresis of the quantum dot-DNA conjugate ladder was performed in the high-speed miniaturized field inversion gel electrophoresis system discussed in chapter III, and differences in mobility between conjugates were investigated. Correlating the macro-scale electrophoretic migration behavior to the observations at single molecule level, can help us understand how to manipulate DNA in order to achieve improved separation.

1. Materials and methods

1.1 Sample preparation

In order to create different sized DNA fragments, a restriction digest reaction was performed. λ DNA was used as the template for KpnI enzyme (New England Biolabs) that cuts in two locations yielding three bands of length: 29942 bp, 17057 bp and 1503 bp respectively. All of the fragments contain 4 base pair overhang of the sequence GTAC-3'at each end. In each reaction, 1 μg of the template DNA was added in to total 50 μl reaction volume, and 20 reactions were carried out at the same time to produce sufficient product. After the reactions were completed, all products were collected and concentrated to about 250 μl in volume. 50 μl of the concentrated product was then pipetted on to a paper filter (0.025 μm pore size, Millerpore, Inc.) for the first drop dialysis process to remove excessive enzyme and salt from the restriction digest reaction. After one to two hours of purification, the sample was recollected and the concentration was measured using the NanoDrop spectrometer.

The measured concentration values were converted to a molar basis and the same process of biotinylation described in chapter III was performed. 45 μl of purified restriction digest product (about 70~80 ng/μl) was mixed with 5 μl of 10X reaction buffer. The mixture was incubated in the thermalcycler at 65 ° C for 10 minutes to break up the sticky ends. dATP, dGTP, dTTP and biotin-dCTP were diluted to a appropriate

concentrations and added to the mixture to make 100x molar excess of the DNA sample. 0.5 μl of Klenow enzyme (Progema, Inc.) was then added to the mixture for biotinylation. The reaction was carried on at room temperature for 30 minutes and stopped by adding 2 μl 0.5M EDTA (Invitrogen, Inc.). After the reaction was completed, the products underwent a second drop dialysis purification overnight in order to remove the enzyme, dNTPs and salt. The concentration of the biotinylated product after the second dialysis was measured by NanoDrop and ranged from 70~80 ng/μl.

Quantum dots (1 μM, Invitrogen), 10base-biotin primer (100 μM, Intergrated DNA Technology), 20base-biotin primer (100 μM, Intergrated DNA Technology), 20bp-Cy5-biotin primer (100 μM, Intergrated DNA Technology), 30base-biotin primer (100 μM, Intergrated DNA Technology), and 40base-biotin primer (100 μM, Intergrated DNA Technology was diluted by 100 folds. Instead of adding quantum dots to the entire purified biotinylated product, only 2 μl of diluted quantum dots were added to 2 μl of biotinylated product to make at least 1000x molar excess of the DNA sample. The mixture was incubated at 37 °C for 20 minutes, allowing the quantum dots to adequately attach to the DNA molecules. Next, to construct primer-decorated quantum dot DNA conjugates, 2 μl of diluted primer was added to the quantum dot-DNA conjugate mixture and incubated for another 10 minutes at 37 °C, making the concentration of primer 100x excess of the quantum dots.

For quantum dot-DNA conjugates and primer-decorated quantum dot-DNA conjugates, no fluorescent dye was added to the sample mixture, while for regular restriction digest products, 2 µl 100 X SYBR Green (Invitrogen, Inc.) was added to 8µl of total volume.

1.2 Gel electrophoresis

0.6%, 0.8% and 1% agarose gels were used for electrophoresis. The gels were cast into the miniaturized field inversion gel electrophoresis device; and allowed to harden for 20 minutes. A razor was used to slice along the electrodes to avoid direct contact of gel and the electrodes, as the heat generated during electrophoresis may cause air bubbles to break the gel. A comb was inserted about one fourth the length of the gel downstream from the anode. 3 µl of each sample was injected into each well to ensure the bands could be visualized due to the low concentration of the DNA. 0.5 X TBE was used as the running buffer. A function generator (WAVETEK, 5MHz sweep generator) and a power amplifier (TREK, model 603) were used to generate the pulsed field. A square pulse pattern was adopted with 10 V/cm forward and 3.5 V/cm reverse, at 1.136 Hz frequency.

2. Results and discussion

2.1 Qualitative observations

After end-labeling the restriction digest products with quantum dots, the bands appear sharper and clearer than the original restriction digest product (Figure V.1). This is probably because the excessive fluorescent dye molecules added to the original RD product may interact with the DNA in a complex way, while only the two quantum dots attached to each conjugate provide enough fluorescence to be detected.

Also, for fluorescence dye labeled DNA, longer fragments appear brighter than shorter ones (Figure V.1). When sample contained a broad range of DNA sizes, either the longer fragments sometimes were over exposed in order to see the shorter ones; or the shorter ones were sacrificed to see the longer fragments clearly. However, the DNA fragments end labeled with quantum dots provide uniform fluorescence intensity if equal molar concentrations are presented. Therefore, a broad range of DNA sample can be visualized clearly at the same time.

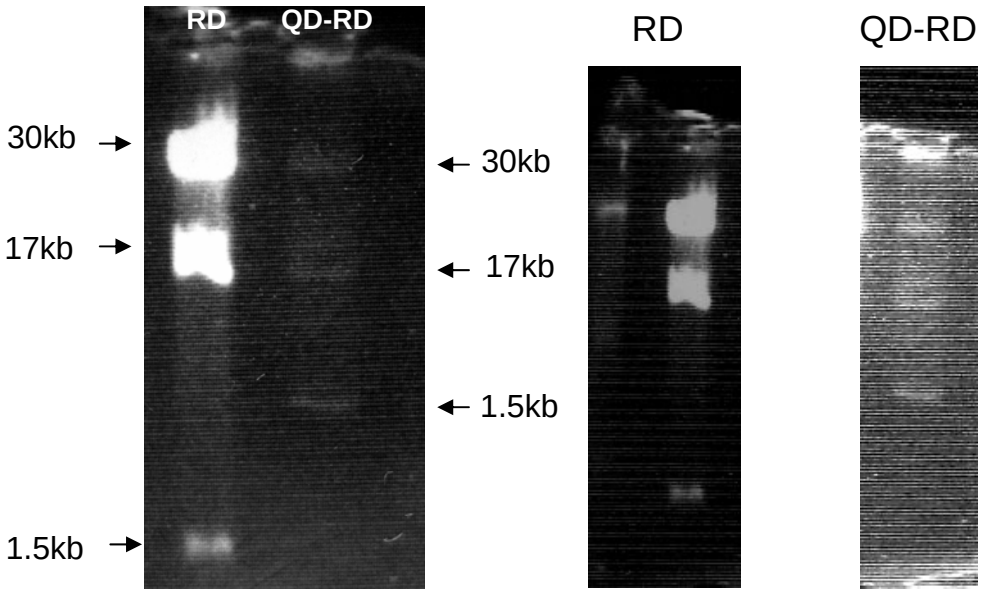

(a) (b)

Figure V.1. The gel image of non-modified restriction digest products and quantum dot end labeled restriction digest products. (a) Left lane is the non-modified restriction digest products, and the right lane is quantum dots end labeled restriction digest products. Samples were run in 1% agarose gel by FIGE. E_{fwd}= 11 V/cm and E_{Rev}=5.5 V/cm, t_{fwd}= t_{Rev} =440ms. 0.5X TBE was used as running buffer. (b) The brightness and contrast were adjusted to show detail more clearly.

In conventional PFGE, DNA samples of broad size range can hardly be resolved in a single gel because it is difficult to reduce readable distance between small and large DNA bands. For example, in order to see the top bands clearly, longer experiment times are desired that may cause small bands to move out of the gel. However, when DNA samples are end labeled with quantum dots, the bands are not only sharper, but the smaller DNA fragments migrate closer to the larger ones. Accordingly, the separation distance for broad-size-ranged DNA is shorted, which allows the slab gel electrophoresis device to be further miniaturized.

2.2 Quantitative observation

Electrophoresis was performed in 0.6%, 0.8% and 1.0% agarose gels respectively. The samples are labeled as follows: RD(restriction digest product), RD-QD conjugates (restriction digest product-quantum dot 605 conjugates), RD-QD-10bp (restriction digest product-10 bp primers covered with quantum dot 605 conjugates), RD-QD-20bp (restriction digest product-20 bp primers covered with quantum dot 605 conjugates), RD-QD-20bpCy5 (restriction digest product-20 bp-Cy5 primers covered with quantum dot 605 conjugates), RD-QD-30bp (restriction digest product-30 bp primers covered with quantum dot 605 conjugates), RD-QD-40bp (restriction digest product-40 bp primers covered with quantum dot 605 conjugates).

In order to evaluate the difference in migration of the conjugates, electrophoretic mobility was measured shown in Figure V.2. The Average electric field (equation (III-3) in Chapter III) was employed to calculate mobility for FIGE experiments.

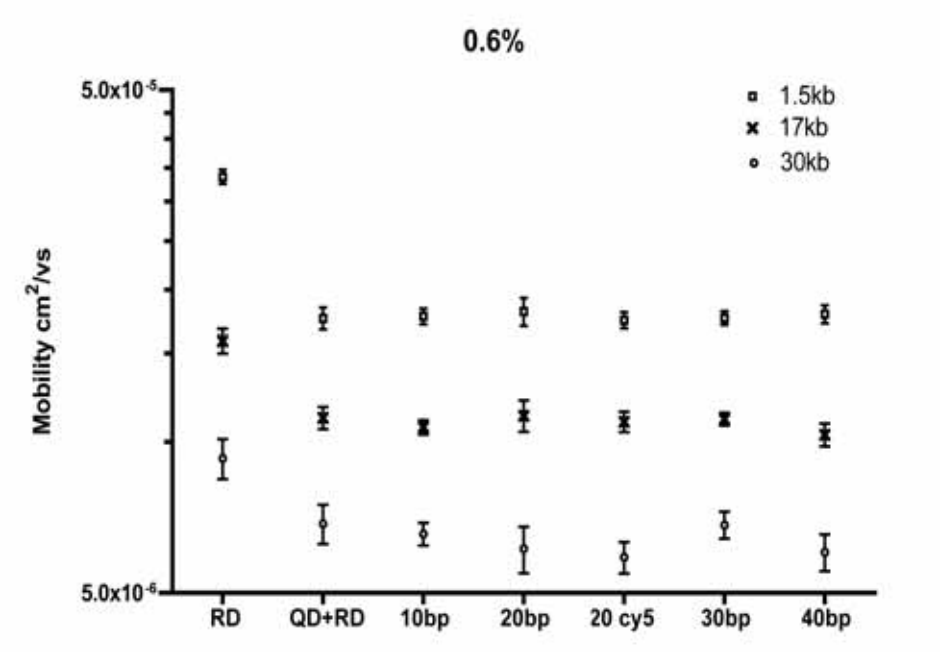

(a)

Figure V.2. Semi-log plot of the mobility of RD and the conjugates. (a) Electrophoresis was running in 0.6% gel. (b) Electrophoresis was running in 0.8% gel. (c) Electrophoresis was running in 1.0 % gel. In the plot, 10bp, 20 bp, 20Cy5, 30bp, 40bp correspond to restriction digest product-10 bp, 20bp, 20bp-Cy5, 30bp, 40bp primers covered quantum dots 605 conjugates respectively. A squared pulse pattern was adopted to generate field inversion field, and E_{fwd}= 10V/cm and E_{Rev}=3.5 V/cm, t_{fwd}=t_{Rev} =440ms. 0.5X TBE was used as running buffer.

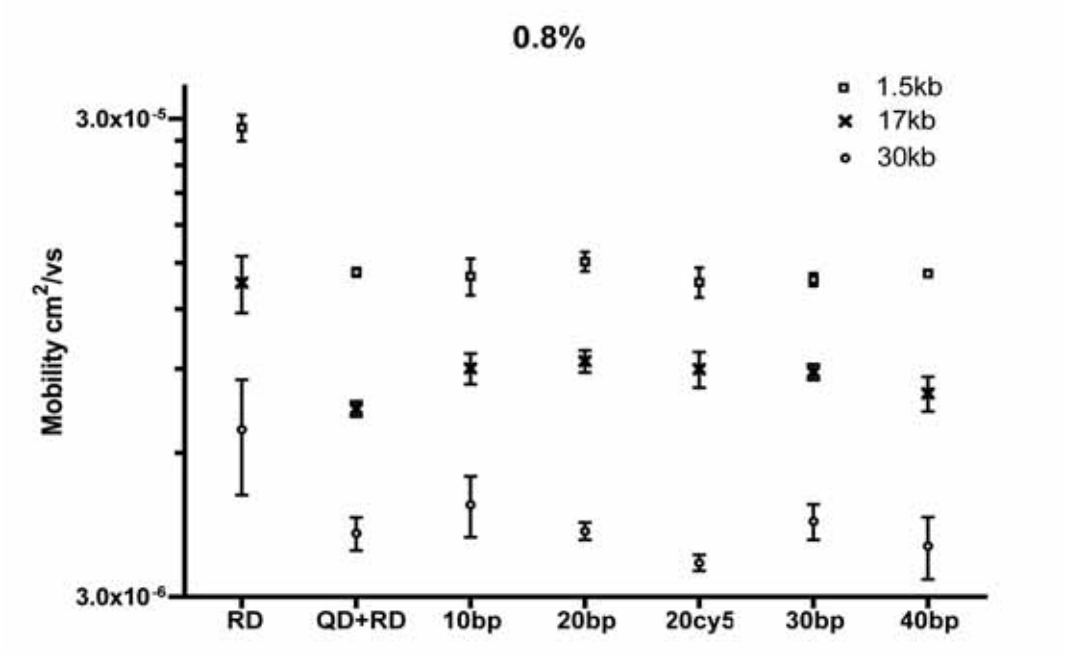

(b)

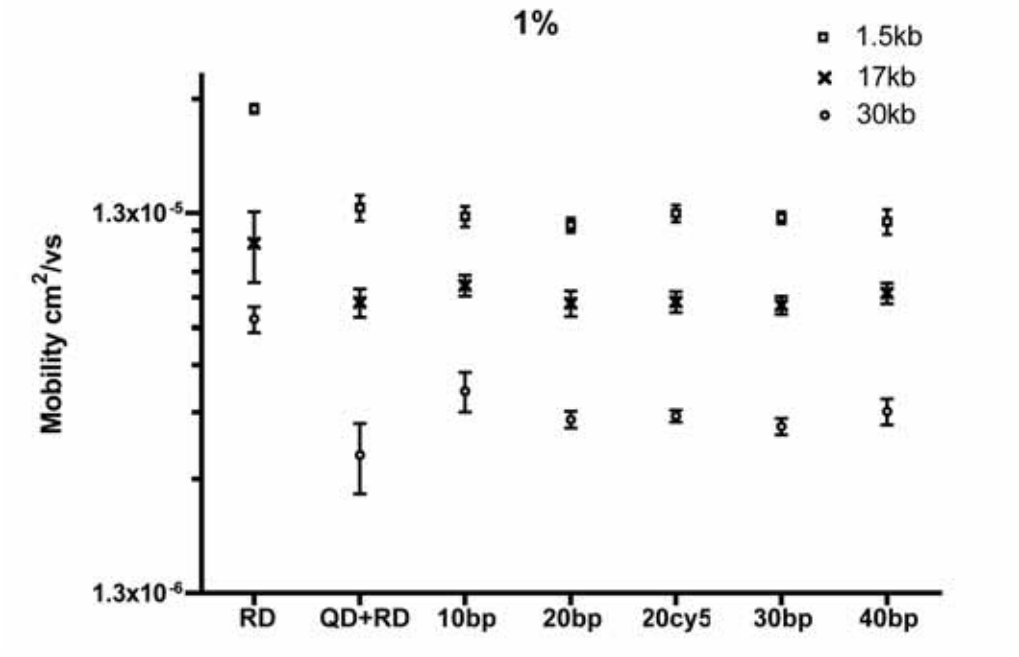

(c)

Figure V.2. Continued.

Generally, the mobilities of RD are higher than the conjugates in all three gel concentrations. The mobilities are only slightly different in the 1.5kb fragments among all DNA conjugates. With the increase of DNA size, the variance of mobility becomes obvious. When gel concentration increases, variance of mobility is also noticeable.

In order to investigate the influence of quantum dots end label on the mobility of the conjugates, experiments with only primer-decorated quantum dots were performed. The mobilities of the primer-decorated quantum dots were measured and shown in Figure V.3. From Figure V.3, the mobility of primer-decorated quantum dots is at least twice as fast as the original RD. Once they form conjugates, however mobility are reduced and become slower than original RD (shown in Figure V.2). This may due to the enhanced interaction with the gel fiber when conjugates form. If the fiber-DNA interaction dominants over the changing charge and size, it could explain why all conjugates appear to slow down. Notice that when the gel concentration decreases, fewer fiber-DNA interactions occur, thereby promotes the conjugates to move with slightly higher mobility (as shown in Figure V.2 (a)).

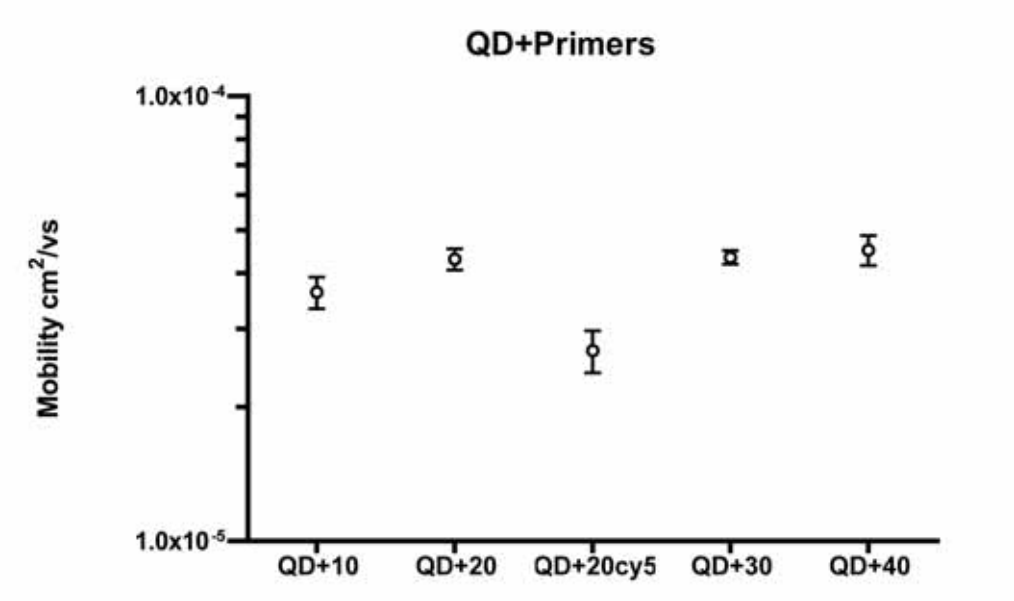

Figure V.3. The semi-log scale of mobility of primer-decorated quantum dots. Experiments were run in continuous field with 1% agarose gel under E=10.8 V/cm. For all the samples in this figure, no fluorescent dye was added.

The conjugates can be classified into two groups according to the charge of the end label: weakly charged QD conjugates (RD-QD) and the negatively charged QD conjugates by binding primers to the QD. From Figure V.2, we found that with the increase in gel concentration and DNA fragment size, weakly charged QD conjugates showed slower mobility than the primer-decorated conjugates. In Chapter IV, a series of visualization experiments on the bare lambda DNA and the lambda DNA-QD/primer-decorated conjugates were performed during electrophoresis. Recalling the results from

Chapter IV, quantum dots labeled DNA conjugates exhibited higher entanglement probability, owing to quantum dots-fiber interactions. Once quantum dots conjugates become hooked, they take longer to release because the weakly charged QDs suppress the random re-orientation of the ends. On the contrary, when primers are bonded to the QDs, the charge is increased at the ends, which helps the DNA to escape from the gel fiber due to the enhanced the random reorientation of the ends. This may explain the slower mobility of weakly charged QD conjugates relative to negatively charged QD conjugates observed here.

When the fiber-DNA interactions are less intense, the influence from the mobility of primer decorated QDs can be seen in the mobility of the small size conjugates. For example, in 0.6% agarose gel, the mobility of 1.5kb conjugates follows a similar trend as the primers decorated QDs. RD-QD-20bpCy5 is the slowest in migration and RD-QD-40bp is the fastest one, RD-QD-20bp and RD-QD-30bp are comparable. But this trend becomes less obvious due to the fiber-DNA interaction when the gel concentration increases.

A semi-log plot of mobility vs. gel concentration also known as a Ferguson plot, can be used to determine particle size and free solution mobility which is related to the net surface charge [64]. Figure V.4 shows the Ferguson plots of RD and the conjugates at different DNA fragment sizes.

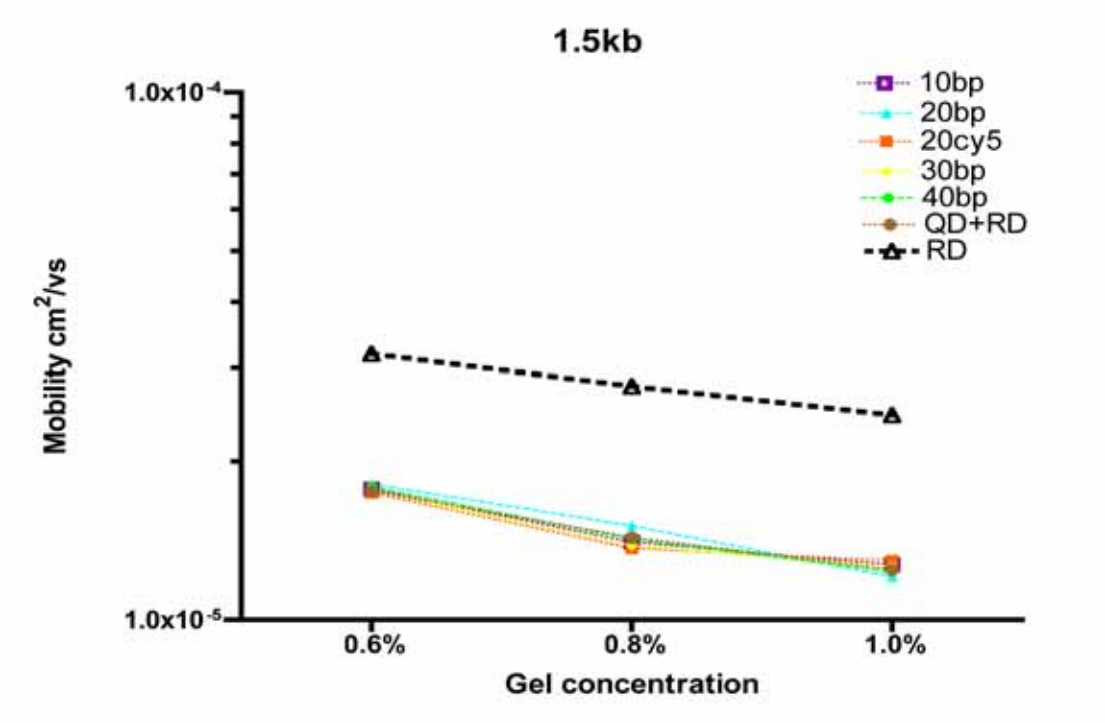

(a)

Figure V.4. Ferguson plot of RD and RD-QD/primer-decorated QD conjugates. (a) log mobility vs. gel concentration at 1.5kb. (b) log mobility vs. gel concentration at 17kb. (c) log mobility vs. gel concentration at 30kb. All experiments were performed in FIGE, E_{fwd}= 10V/cm and E_{Rev}=3.5 V/cm, t_{fwd}= t_{Rev} =440ms. 0.5X TBE was used as running buffer.

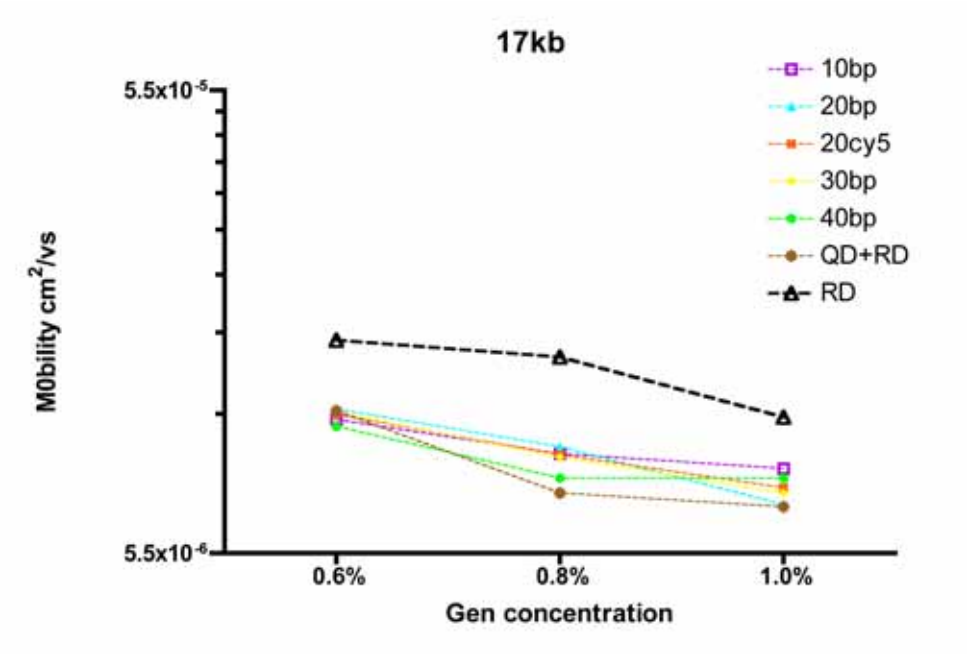

(b)

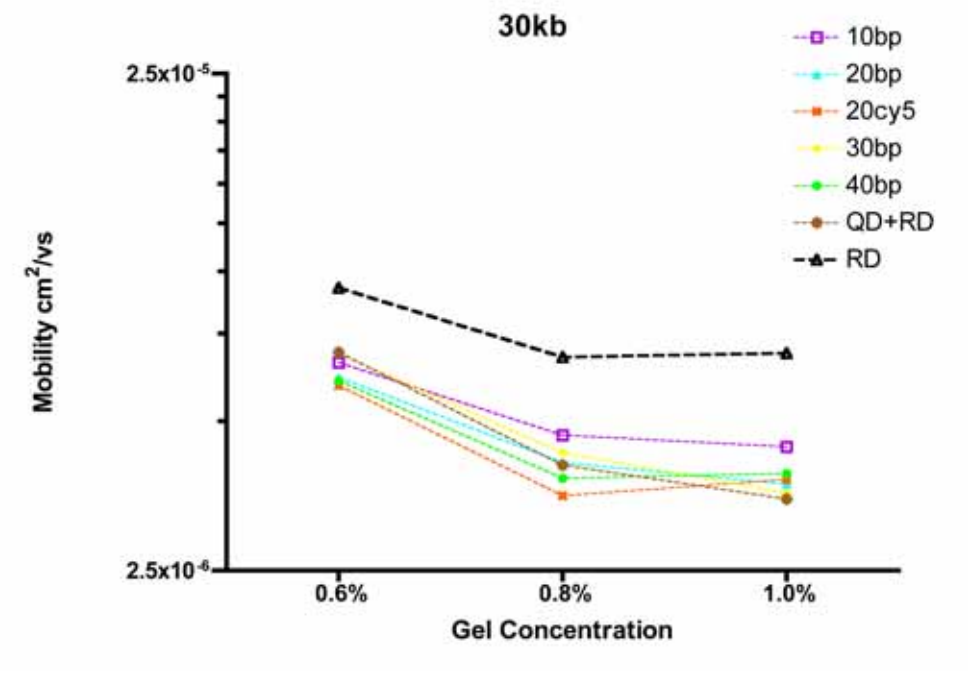

(c)

Figure V.4. Continued

The linearity of the RD at 1.5kb (Figure V.4 (a)) suggests that the conformation of 1.5 kb RD fragment during electrophoresis can be modeled as a sphere. RD-QD/primer-decorated QD conjugates demonstrate approximately linear relationship between log mobility and gel concentration, so that they can be also assumed to migrate with sphere-like conformations in all three gel concentrations. The trend lines of the conjugates are also close together, from which the conjugates can be described as sharing the same molecular weight and charge at 1.5kb. This may help explain the similar mobility of the conjugates at 1.5kb (Figure V.2). In addition, the slope of the conjugates is greater than the slope of RD, suggesting that the molecular weight of the conjugates is higher than the RD due to the additional size of the QD. This provides an explanation to the higher mobility of RD than conjugates in Figure V.2. Generally in this region, both the RD and the conjugates are migrating through the gel as spheres, so that less fiber-DNA interactions arise, and the molecule size and net charge dominate the migration behavior.

However, the relationship between the log mobility and the gel concentration of both RD and the conjugates become nonlinear at 17kb and 30kb. Under these conditions, the DNA molecules are too large to migrate through the gel as spheres, so that an extended conformation must be adopted in order to move through the gel by reptation. Accordingly, more fiber-DNA interactions occur, which becomes a major factor affecting DNA migration mobility. When gel concentration is low (0.6%), the conjugates are move at close mobility (Figure V.4. (b), (c)), and with the increase of gel concentration, difference in the mobility of the conjugates becomes more obvious.

3. Conclusion

Pulsed field gel electrophoresis (PFGE) of QD end-labeled DNA provides improved detection by producing sharp and clear band images, overcoming the drawback of using fluorescence dye and allowing a broad size range of DNA fragments to be visualized clearly at the same time. Moreover, it shortens the distance of the DNA sample which has broad size range, so that small and large DNA fragments can be separated in one gel. This also provides opportunity to separate DNA ladders in miniaturized electrophoresis device.

Electrophoretic migration behavior is also investigated by measuring the mobility of DNA sample. Generally, QD/primer-decorated QD-DNA conjugates have similar mobilities that are slower than the non-modified DNA sample. When the gel concentration is low, the fiber-DNA interactions are minimized so that the mobility of DNA conjugates becomes influenced by the additional size and charge from QD and the primer-decorated QD end label. With increase in gel concentration and fragment size, fiber-DNA interactions become predominant, so that mobility differences between the conjugates become apparent.

CHAPTER VI

CONCLUSIONS

1. Summary

Electrophoresis is an important analytical method employed in molecular biology and medicine. However the procedure can be laborious and time consuming. Therefore, development of high-throughput, sensitive, time and labor saving electrophoresis technology is of great demand.

With the development of miniaturization technology, capillary and microchip electrophoresis devices have attracted great interest and have already demonstrated their advantages for fast separations. However, practically speaking, slab gel electrophoresis is still the preferred technology in many molecular biology labs because it is simple to operate and, provides capability for lane-to-lane comparison so that the controls, standards and samples can be run at the same time in one single gel to allow differences in samples to be detected. Hence, the miniaturization of slab gel electrophoresis is appealing for practical needs. In addition, miniaturization of pulsed field gel electrophoresis devices for analysis of large DNA fragments is attractive, as the separation time in pulsed field gel electrophoresis is at least ten times longer than the ordinary slab gel electrophoresis. Also, large DNA can only be separated in pulsed field

gel electrophoresis, because the mobilities are only weakly size dependent, which causes all sized fragments to migrate through the gel at the same speed.

Currently, there are several technical concerns for pulsed field gel electrophoresis: 1. Shortening separation time without reducing the separation resolution using high voltage. 2. Miniaturizing the device size. When a DNA sample containing multiple bands ranging from small DNA fragments to large ones, there is a certain limit below which incomplete separation occurs, i.e. when top bands resolves, the bands at the bottom may have be moving out of the gel.

In this dissertation, we first constructed a miniaturized field inversion gel electrophoresis device with the dimension 2 x 2.6 cm. A dual output power supply controlled by LabView program was used to generate a square wave pulse sequence. Separation performance was evaluated by measuring the resolution and mobility of a standard DNA ladder ranging from 2.5kb to 35kb. It was shown that the separation time of the DNA ladder was reduced to less than 3 hours, in contrast to the standard running time 15 hours separated by the manufacture of the DNA ladder. Yet, good resolution was achieved as well. Because of the small size of the device, the band migration could be visualized under a fluorescence microscopy during the separation process, so that the factors that affect the resolution such as the ratio of forward and reverse electric field, pulse time, gel concentration and temperature can be studied. This could not be achieved in conventional FIGE because of detection difficulties caused by the device's size. DNA

migration in FIGE was investigated by studying the relationship between mobility and gel concentration as well as mobility and DNA fragments size. The mobility at a given fragment size does not change significantly over the range of gel concentrations studied. In addition, a mobility scaling close to $\mu \propto N^{-0.5}$ is observed, as opposed to N^{-1} usually observed in continuous field. This scaling behavior may lie in the mechanism by which DNA migration is influenced by the applied electric field. Thus, understanding the mechanism of DNA migrating in pulsed field gel electrophoresis is a key to improve the separation performance.

The miniaturized FIGE device proved to be efficient in separating large DNA fragments in a short time, and is reliable to produce experimental data for separation resolution and mobility analysis. The failure in separation of large DNA fragments in continuous field is basically due to the uniformly distributed charge along DNA chain stretching out responding to the applied electric field, so that resistance generated by the gel matrix relatives constant, resulting in the identical migrating speed of all sized DNA. When pulsed fields applied, the interaction between gel fibers and DNA is increased resulting in differences in reorientation time that restore size-dependent mobility.

In our project, we constructed DNA conjugates by binding striptavidin functionalized quantum dots to end biotinylated DNA. By adding QD end labels, the gel-DNA interaction during electrophoresis is altered, which may have influence on the separation performance in pulsed field gel electrophoresis. In order to understand the behavior of

the QD labeled conjugates during gel electrophoresis, single molecule visualization experiments were performed. Interestingly, conformations where the middle of the molecule moves ahead were observed in QD end labeled DNA conjugates, as opposed to the end leading motion observed in non-modified DNA gel electrophoresis. This is possibly caused by focusing of the electric force is in the middle of the chain once neutral quantum dots are attached to both ends of the DNA molecule.

Qualitative measurements were performed, where the extension length, entanglement probability and reorientation time were analyzed. Weakly charged QD-λ DNA conjugates displayed higher extension lengths than the primer-decorated QD-λ DNA conjugates and the bare λ DNA in continuous field and 120 degree pulsed field, in contrast to the lower extension length in field inversion. This is possibly because weakly charged quantum dots may make it easier for the DNA to become hooked on gel fibers, and the reduced random reorientation at the hooked end caused by the neutral charge may make it more difficult to release, resulting in longer extension in continuous field. Similarly in 120 degree pulsed field, the wide angle of the electric field forces the free end to take longer contour to align with the field while another one end is stuck. However, in field inversion, DNA molecules align parallel to the electric field and respond to two horizontal electric forces. The electric force acting on the QD at the end of the DNA is not as strong as the force on primer-decorated QD due to the extra net charge on the primers, which may cause DNA to be less stretched. Frequently switched fields dose not provide the opportunity for QD-DNA conjugates to extend as they do in

continuous field. Therefore the extension length of QD-DNA conjugates in field inversion field is lower than that in continuous field.

A second observation is that the entanglement probability of bare λ DNA is increased in 120 degree and field inversion pulsed field gel electrophoresis compared with in continuous fields. This supports the idea that increased gel-fiber interaction helps resolve large DNA fragments during gel electrophoresis. The primer-decorated QD-λ DNA conjugates generally have lower entanglement probability than weakly charged QD-λ DNA conjugates, because the increased charge on the QD provided by the primers enhances the random motion that helps the hooked end to find a way to escape.

The reorientation time in 120 degree pulsed field gel electrophoresis is investigated, under which QD-λ DNA conjugates, primers-decorated QD-λ DNA conjugates, and bare λ DNA demonstrate significant differences. Here bare λ DNA has the shortest reorientation time, while the QD-λ DNA conjugates take the longest time to re-align to the new coming field. This may caused by the extra drag by adding QD and primer-decorated QD to the ends.

Finally, the extension length between different sized primer-decorated QD- λ DNA was studied. Although the difference is not dramatic, the 30bp-primer-decorated QD- λ DNA has slightly longer extension length. This shows the forces acting on the DNA may vary with different end charge, as well as the fiber-DNA interaction.

The investigation on the behavior of DNA-QD conjugates during both continuous field and pulsed field gel electrophoresis at molecular level provided useful information on the separation mechanism of both bare DNA and the DNA-QD conjugates. It looks promising that by combining the methods of end labeling QD and primer-decorated QD to DNA molecules and performing electrophoresis in miniaturized FIGE, the separation of large DNA fragments can be improved.

We constructed a three band DNA ladder by restriction digest and labeled the products with QD and the primer-decorated QD. Electrophoresis was performed in miniaturized FIGE, and mobility was measured. According to the overview of the separation results, QD end-labeled DNA conjugates provide sharp and clear background images. Furthermore, the distance between bands is condensed without reducing the band sharpness. By taking advantage of these effects, special ladders can be constructed for further miniaturized slab gel electrophoresis devices that can overcome the drawback of the device size limit caused by using conventional DNA ladders.

The electrophoretic mobility of bare restriction digest products (RD) is apparently higher than the mobility of QD and the primer-decorated QD-RD in 0.6%, 0.8% and 1.0% gel concentration. This may because of the increased drag produced by the QD end label. We also notice that at higher gel concentration and larger DNA fragments size, the mobility of QD-RD conjugates appears to be slower than the primer-decorated QD-RD. This may be explained by the fiber-DNA interaction. According to information from the

single molecule visualization, QD-DNA conjugates are easily hooked up by gel fiber, and more difficult to escape than the primer-decorated. With the increase of gel concentration and DNA size, the interaction between gel fiber and DNA is increased, that caused the delay on the migration mobility.

When fiber-DNA interactions are weak (i.e. at low gel concentration and small DNA fragments), the mobility of different primer-decorated QD-RD conjugates are comparable. The linearity in Ferguson plots at 1.5kb show that small DNA fragment (1.5kb) can be regarded as spheres moving through the gel. Therefore, less fiber-DNA interactions occur. Although the mobility of the conjugates are not significantly influenced by binding with different primers, the trend in mobility change among conjugates can still be recognized as following the similar trend of the primer-decorated QD alone. However, when DNA fragment size and gel concentration increase, the Ferguson plots lose their linearity, indicating that the DNA and DNA conjugates can be no longer assumed to be spheres, but are instead stretched out. The fiber-DNA interactions dominate the migration behavior in this region, and the variance in mobility among different primer-decorated QD-RD conjugates appears.

Generally, by combining the technology of miniaturizing of FIGE and constructing QD end-labeled DNA, a novel technology to separate large DNA fragments is proved to be successful. The separation performance of large DNA fragments is improved by shortening the separation time, sharpening the bands, providing uniform fluorescence

with low background, condensing the gap between bands without reducing sharpness, enhancing the gel fiber-DNA interactions, and allowing the sample of broad size range to be separated in a single gel. The QD-DNA conjugate ladder is promising to be constructed especially for miniaturized gel electrophoresis devices.

2. Recommendations and future work

In our experiments, QD605 striptavidin functionized quantum dots (from Invitrogen Inc.) are employed in constructing DNA conjugates. The targeted bands are 1.5kb, 20kb and 32kb. In order to evaluate the charge density change of the DNA molecule after complexing QD and primer-decorated QD, the estimation calculation of DNA conjugate size and charge is performed. Here, the radius of gyration (*Rg*) is used to represent DNA size, which is expressed as [65]:

$$R_g^2 = \left[\frac{pL}{3}\left(1 - \frac{p}{L} + \frac{p}{L}[exp(-L/p)]\right)\right] \quad \text{(VI-1)}$$

where L is the contour length of the fragment, which equals to 0.34x bp, and p is the persistence length, about 50 nm in typical electrophoresis buffers [63]. The total length D=2 x Rg. To calculate charge, each base pair roughly carries 2 unit of charge for double stranded DNA, and 1 unit for single stranded DNA. And each quantum dot has 20 bonding sites, which is satisfied by primers. Based on the calculation, the ratio of charge to length of different conjugates is plotted in Figure VI.1.

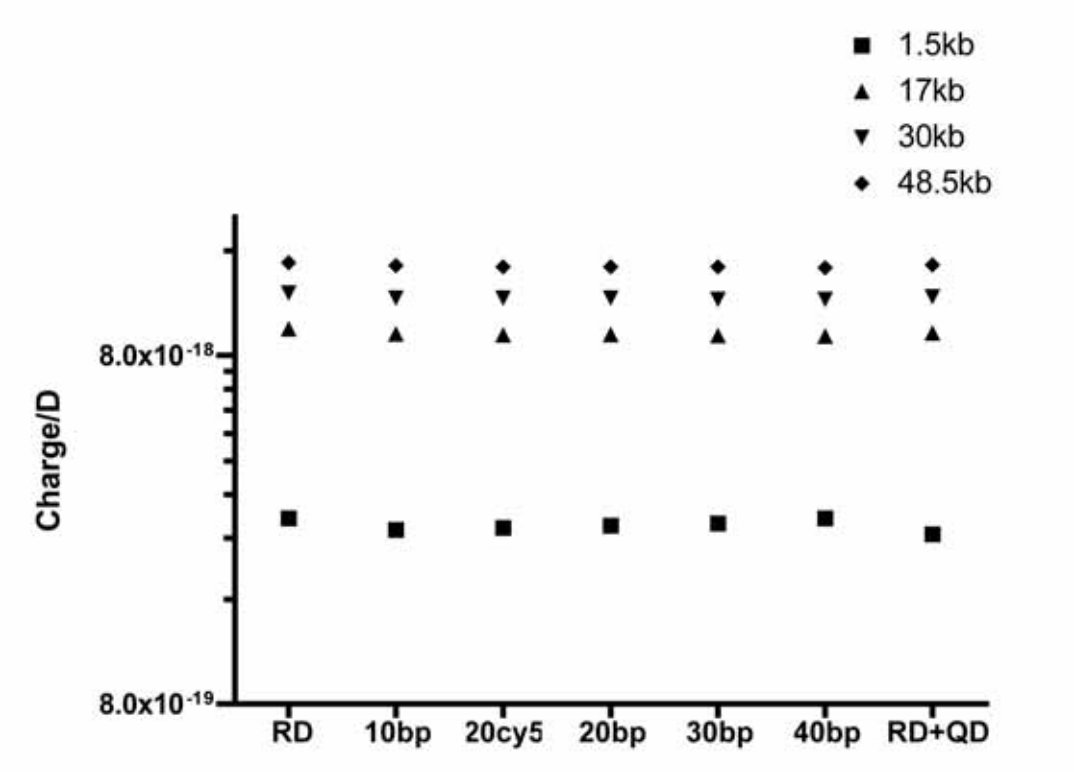

Figure VI.1. The plot of charge to length ratio of DNA and DNA conjugates.

According to Figure VI.1, the charge to size ratio provided by end labeling QD and primer-decorated QD shows more variance at 1.5kb than 17, 30 and 48.5 kb, though the variance is not significant. This demonstrates that the influence from the given size of QD may be more obvious on DNA fragments with size 1.5kb or less. Yet, it appears insignificant when attaching to large DNA fragments above 20kb.

However, the size range of commercial QD is from 15 nm to 20nm, which doses not provide much difference in size. To produce dramatic drag to large DNA fragments above 20kb, QD size is expected to be approximate 30% of the radius of gyration of DNA. One way to obtain the required sized particles is to synthesis them in the lab. By doing it, the size of the particles can be precisely manipulated and the cost will be reduced. Moreover, the biopolymer coating outside the particle can be diverse for different needs.

Applying large particles as the end label, DNA fragments are expected to demonstrate significant slower in mobility comparing with non-modified DNA fragments. Due to the enhanced gel-fiber interaction, separation is less dependent on the pulsed condition and by properly adjusting the QD size and the primers; the separation is expected to be achieved in continuous field gel electrophoresis eventually.

Nevertheless, concerns are raised when DNA fragments are labeled with large particles. First, band inversion phenomena may occur, due to the overwhelmed size increase in

smaller fragments. This can be avoided by choosing the proper sized particle for all sized fragments. Second, synthesis large particle may be difficult. (1) When QD size is above 30nm, it has week optical property. (2) It is critical that other nano particles with large size may not emit certain wavelength once they are excited by light. (3) The nano particles must be monodispersity. Therefore, properly choosing the targeted material is important. Third, can the single stranded primers be replaced by polymer which contains higher charge? This may be the way to manipulate the mobility among different conjugates.

This novel technology has already shown the unique advantage in separation of large DNA fragments. Yet, improvement is still needed. The final success may take a long way to achieve, but good start is half done.

REFERENCES

[1] Troy High School Biology website. http://www.troy.k12.ny.us/.../skinny_genetics.html

[2] Olivera, B. M., Baine, P., Davidson, N., *Biopolymers* 1964, *2*, 245-257.

[3] Szoke, M., Sasvari-Szekely, M., Barta, C., Guttman, A., *Electrophoresis* 1999, *20*, 497-501.

[4] Guttman, A., Ronai, Z., *Electrophoresis* 2000, *21*, 3952-3964.

[5] Maurer, H. R., Dati, F. A., *Analytical Biochemistry* 1972, *46*, 19-32.

[6] Gerstner, A., Csapo, Z., Sasvari-Szekely, M., Guttman, A., *Electrophoresis* 2000, *21*, 834-840.

[7] Guttman, A., Ronai, Z., Khandurina, J., Lengyel, T., Sasvari-Szekely, M., *Chrmatographia* 2004, *60*, S295-S298.

[8] Sasvari-Szekely, M., Gerstner, A., Ronai, Z., Staub, M., Guttman, A., *Electrophoresis* 2000, *21* 816-821.

[9] Lengyel, T., Guttman, A., *Journal of Chromatography A* 1999, *853*, 511-518.

[10] Guttman, A., Barta, C., Szoke, M., Sasvari-Szekely, M., Kalasz, H., *Journal of Chromatography A* 1998, *828*, 481-487.

[11] Shandrick, S., Ronai, Z., Guttman, A., *Electrophoresis* 2002, *23*, 591-595.

[12] Slater, G.W., Noolandi, J., *Biopolymers* 1989, *28*, 1781-1791.

[13] Slater, G.W., Desruisseaux, C., Hubert, S. J., Mercier, J., Labrie, J., Boileau, J., Tessier, F., Pepin, M., *Electrophoresis* 2000, *21*, 3873-3887.

[14] Barron, A. E., Sunada, W. M., Blanch, H. W., *Biotechnology and Bioengineering* 1996, *52*, 259-270.

[15] Schwartz, D.C., Cantor, C.R., *Cell* 1984, *37*, 67-75.

[16] Orbach, M.J., Vollrath, D., Davis, R.W., Yanofsky, C., *Mol. Cell. Biol.* 1988, *8*, 1469-1473.

[17] Burmeister, M., Ulanovsky, L. (Eds.), *Pulsed-Field Gel Electrophoresis,* Humana Press 1991, Totowa, NJ.

[18] Heller, C., Beck, S., *Nucleic Acids Research* 1992, *20*, 2447-2452.

[19] Sobral, B.W.S., Atherly, A.G., *Nucleic Acids Research* 1989, *17*, 7359-7369.

[20] Heller, C., Pohl, F.M., *Nucleic Acids Research* 1989, *17*, 5989-6003.

[21] Lalande,M., Noolandi, J., Turmel, C., Rousseau, J., Slater, G.W., *Proc. Natl. Acad. Sci. USA* 1987, *84*, 8011-8015.

[22] Ito, T., Hohjoh, H., Sakaki, Y., *Electrophoresis* 1993, *14*, 278-282.

[23] Griess, G.A., Rogers, E., Serwer, P., *Electrophoresis* 2000, *21*, 859-864.

[24] Griess, G.A., Serwer, P., *Electrophoresis* 2001, *22*, 4320-4327.

[25] Griess, G.A., Rogers, E., Serwer, P., *Electrophoresis* 2001, *22*, 981-989.

[26] Griess, G.A., Choi, H., Basu, A., Valvano, J.W., Serwer, P., *Electrophoresis* 2002, *23*, 2610-2617.

[27] Chu, G., Vollrath, D., Davis, R.W., *Science* 1986, *234*, 1582-1585.

[28] Ribot, E., Fitzgerald, C., Kubota, K., Swaminathan, B., Barrett, T. J., *Journal of Clinical Microbiology* 2001*, 39*, 1889-1894.

[29] Dally, E. L., Barros, T. S. L., Zhao, Y., Lin, S., Roe, Bruce A., Davis, R. E.,

Canadian Journal of Microbiology 2006*, 52* (9)*:* 857-867.

[30] Min Wang, Eric Lai, *Electrophoresis* 1995*, 16,* 1-7.

[31] Gardiner, K., *Analytical Chemistry* 1991, *63*, 658-665.

[32] Chu, G., Electrophoresis 1989, 10, 290-295.

[33] Hightower. R.C., Metge, D.W., Santi, D.V., *Nucleic Acids Res.* 1987*, 15,* 8387-8398.

[34] Garvey, E.P. and Santi, D.V., *Science* 1986*, 233,* 535-540.

[35] Hightower. R.C. and Santi, D.V., *Electrophoresis* 1989*, 10,* 283-290.

[36] Terajima, J., Izumiya, H., Iyoda, S., Mitobe, J., Miura, M., Watanabe, H., *Foodborne Pathogens and Disease* 2006*, 3,* 68-73.

[37] Heller, C., Pakleza, C., Viovy, J.L., *Electrophoresis* 1995, *16*, 1423-1428.

[38] Y. Kim, M. D. Morris, *Electrophoresis* 1996, *17*, 152-160.

[39] Viovy, J. *Reviews of Modern Physics* 2000, *72,* 813-872.

[40] Ferree, S.; Blanch, H. W. *Biophysical Journal* 2003, *85,* 2539-2546.

[41] Smith, S.; Aldridge, P. K.; Callis, J. B. *Science* 1989, *243,* 203-206.

[42] Schwartz, D. C.; Koval, M. *Nature* 1989, *338,* 520-522.

[43] Rampion, N. J. *Biopolymers* 1991, *31,* 1009-1016.

[44] Rampion, N. J.; Chrambach, A. *Biopolymers* 1991, *31,* 1297-1307.

[45] Gurrieri, S.; Smith, S. B.; Wells, K.S.; Johnson, L.D.; Bustamante, C. *Nucleic Acids Research* 1996, *24,* 4759-4767.

[46] Gurrieri, S.; Rizzarelli, E.; Beach, D.; Bustamante, C. *Biochemistry* 1990, *29,* 3396-3401.

[47] Deutsch, J. M. *Physical Review Letters* 1987, *59,* 1255-1258.

[48] Starchev, K.; Sturm, J.; Weill, G. *Electrophoresis* 1996, *17,* 465-470.

[49] Krishnan, M.; Monch, I.; Schwille, P. *Nano Letters* 2007, *7,* 1270-1275.

[50] Perkins, T. T.; Smith, D. E.; Chu, S. *Science* 1994, *264,* 819-822.

[51] Perkins, T. T.; Quake, S. R.; Smith, D. E.; Chu, S. *Science* 1994, *264,* 822-826.

[52] Ferree, S.; Blanch, H. W. *Biophysical Journal,* 2004, *87,* 468-475.

[53] Randall, G. C., Doyle, P. S., *Physical Review Letters* 2004*, 93,* 058102-1-058102-4.

[54] Invitrogen, Inc. http://probes.invitrogen.com/media/pis/mp19000.pdf.

[55] Zhang, C., Johnson, L.W., *The Analyst* 2006, *131*, 484-488.

[56] Chen, X., Ugaz, M., *Electrophoresis* 2006, *27*, 387-393.

[57] Jelinek, L.; Peters; G., Okuley, J.; McGowan, S. *Intel Technology Journal* 2001, *5*, 1-10.

[58] Barron, A.E.; Blanch, H.W. *Separation and Purification Methods* 1994, *24*, 1-118.

[59] Birren, B.W., Hood, L., Lai, E., *Electrophoresis* 1989, *10*, 1084-1090.

[60] Sobral, B.W.S., Atherly, A.G., *Nucleic Acids Research* 1989, *17*, 7359-7369.

[61] Heller, C., Pakleza, C., Viovy, J.L., *Electrophoresis* 1995, *16*, 1423-1428.

[62] Y. Kim, M. D. Morris, *Electrophoresis* 1996, *17*, 152-160.

[63] Sano, T., Cantor, C.R., *Biological Chemistry* 1990, *265*, 3369-3373.

[64] Tietz, D., Chrambach, A., *Electrophoresis* 1992, *13*, 286-294.

[65] Stellwagen, N. C., *Electrophoresis* 1998, *19*, 1542-1547.

APPENDIX

THE OBSERVATION OF DNA CONJUGATES

DURING GEL ELECTROPHORESIS

A-1. The conformation of λ DNA

NAME	EXAMPLE	COMMENTS
U shape	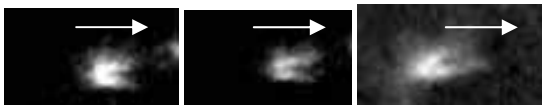	
O shape	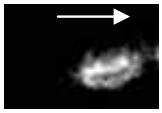	
Half dumbbell	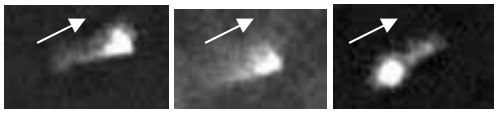	
Triangle	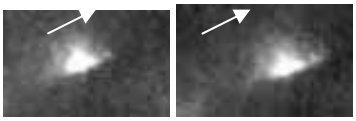	
Mushroom	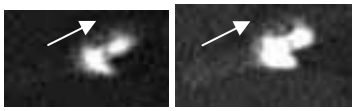	
Line	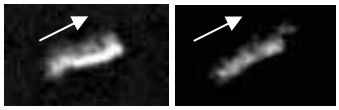	

A-2. The conformation of QD-λ DNA conjugates

NAME	EXAMPLE	COMMENTS
U shape	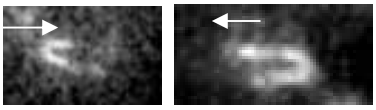	Has a lot of 'U' shape during electrophoresis.
V shape	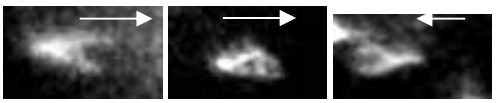	
J shape	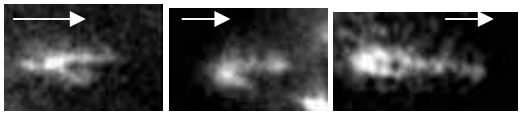	
Half dumbbell	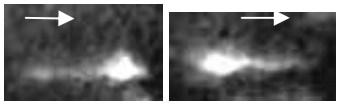	
λ shape	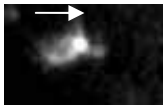	
O shape	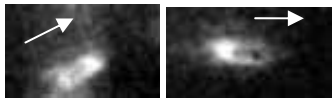	
Triangle shape	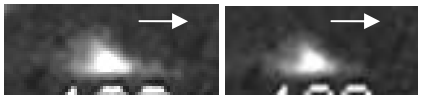	It seems the center of the chain moves ahead first.
Hair pin	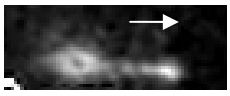	

A-2. The conformation of QD-λ DNA conjugates continue

NAME	EXAMPLE	COMMENTS
E shape	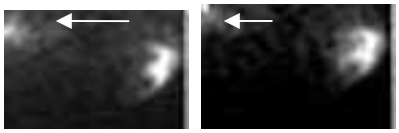	Stocked by two fibers, and the center of the chain moves ahead as well as the two ends.
Necklace	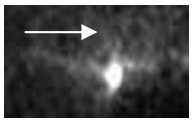	
Line	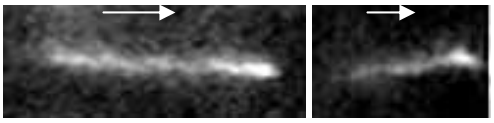	Can be stretched to the full length

A-3. 20bp Cy5-decorated QD-λ DNA conjugates

NAME	EXAMPLE	COMMENTS
U shape	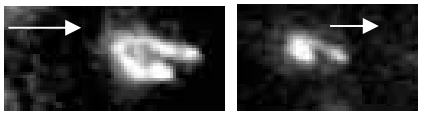	The slowest to release from this shape. Has a lot of U shape.
V shape	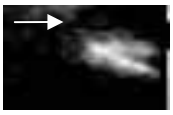	The slowest to release from this shape.
r shape	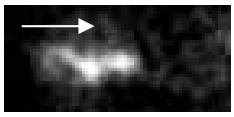	
Half dumbbell	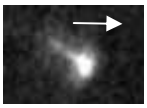	
Triangle shape	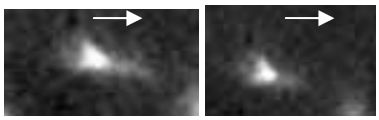	
Line shape	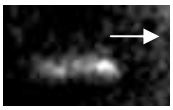	

A-4. 20bp primer-decorated QD-λ DNA conjugates

NAME	EXAMPLE	COMMENTS
U shape	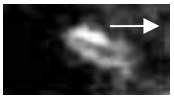	Not as much U shape as the one with cy5 and biotin.
Dumbbell	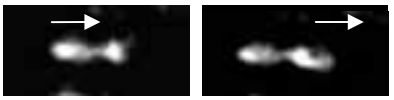	
Half dumbbell	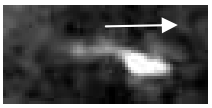	
λ shape	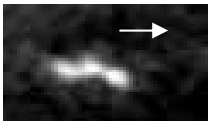	
Line	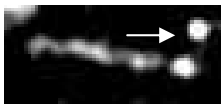	

A-5. 30bp primer decorated QD-λ DNA conjugates

NAME	EXAMPLE	COMMENTS
V shape	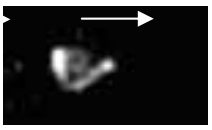	
J shape	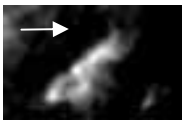	
Dumbbell	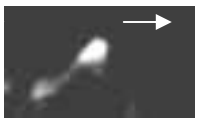	
Half dumbbell	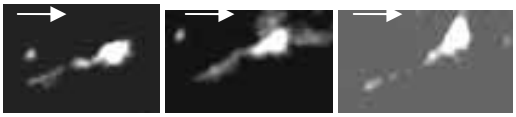	
Necklace	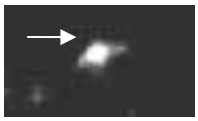	
Line	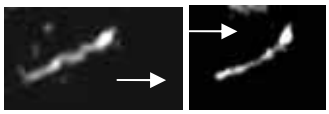	

A-6. 40bp primer decorated QD-λ DNA conjugates

NAME	EXAMPLE	COMMENTS
V shape	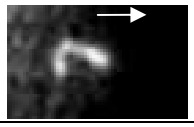	
J shape	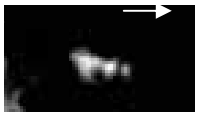	
Line	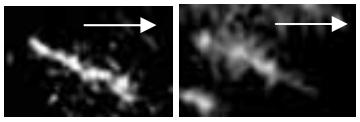	

VITA

Xiaojia Chen received her Bachelor of Science degree in chemical engineering from Sichuan University, China in 2002. She entered the chemical engineering department at Texas A&M University in September 2002. Her research interest is in applying biological concepts to engineering to develop novel technology for medical and biological research purposes.

Ms. Chen may be reached at 3122 TAMU, College Station, TX 77840. Her email is margaret72001@tamu.edu.